Stony Brook University

The Regulatory Potentials of Dynamic Electrical Muscle Stimulation on Preventing Bone Loss and Muscle Atrophy

A Dissertation Presented

by

Hoyan Lam

to

The Graduate School

in Partial fulfillment of the

Requirements

for the Degree of

Doctor of Philosophy

in

Biomedical Engineering

Stony Brook University

August 2008

Stony Brook University

The Graduate School

Hoyan Lam

We, the dissertation committee for the above candidate for the

Doctor of Philosophy degree, hereby recommend

acceptance of this dissertation.

Dr. Yi-Xian Qin – Dissertation Advisor
Professor, Department of Biomedical Engineering

Dr. Stefan Judex – Chairperson of Defense
Associate Professor, Department of Biomedical Engineering

Dr. Peter Brink
Professor and Chairman, Department of Physiology and Biophysics

Dr. Susannah Fritton
Associate Professor, Department of Biomedical Engineering
The City College of New York

This dissertation is accepted by the Graduate School

Lawrence Martin
Dean of the Graduate School

Abstract of the Dissertation

The Regulatory Potentials of Dynamic Electrical Muscle Stimulation on Preventing Bone Loss and Muscle Atrophy

by

Hoyan Lam

Doctor of Philosophy

in

Biomedical Engineering

Stony Brook University

2008

The development of new intervention to prevent osteopenia and muscle atrophy is a critical task as the incidence of osteoporosis continues to rise. The overall objective of this dissertation was to evaluate the role of dynamic muscle stimulation (MS) in preventing trabecular bone loss and muscle atrophy via four studies.

To investigate the importance of optimized stimulation frequency in the loading regimen, animals were divided into seven groups for the 4-week experiment: baseline control, age-matched control, hindlimb suspended (HLS), and HLS with muscle stimulation at 1 Hz, 20 Hz, 50 Hz, and 100 Hz. Quadriceps stimulation was carried out for 10 minutes per day for 5 days per week, for 4 weeks. The distal femurs and proximal tibia were analyzed with microcomputed tomography and histomorphometry methods. Bone quantity and structure were significantly improved by applying MS at mid-frequency (20 Hz & 50 Hz). Similarly, histomorphometric analysis showed slight

enhancement of bone formation indices, such as mineral apposition rate and bone formation rate. However, these values were significantly lower than normal animals, suggesting the prevention of bone loss may be a result of decreasing resorption activity.

To determine whether the contraction-to-rest ratio is an important parameter to affect the skeletal adaptive responses under a functional disuse environment, four contraction-to-rest ratio of 1/4, 2/8, 4/6, and 2/28 were tested. Dynamic MS, applied at 50 Hz frequency, with a 2/8 contraction-to-rest ratio demonstrated significant inhibition of trabecular bone loss against the 4 weeks disuse. The results from this study confirm the potentials of dynamic muscle contraction in regulating skeletal adaptive responses and illustrated the importance of the contraction-to-rest ratio for future study.

To evaluate the potential effects of dynamic MS on muscle atrophy associated with functional disuse, muscle wet weight, fiber cross-sectional area, number of central nuclei, type I, and II fibers were assessed. The results showed that 10 minutes of daily stimulation could maintain muscle fiber types to the level similar to normal muscle. However, the short duration could not compensate for the loss of muscle weight and the reduction of fiber area. These studies suggested that other parameter, i.e., duration of stimulation, may also influence the effect of the stimulation on skeletal muscle, in addition to the selection of stimulation frequency and C-R ratios within the regimen.

To determine the effect of MS on the capillary supply within skeletal muscle, capillary analyses were performed on the quadriceps muscles from the age-matched, HLS, and 50 Hz MS with 2/8 contraction-to-rest ratio. The capillary density and capillary-to-fiber ratio were evaluated. Our results showed that the lack of daily activity significantly decreased the capillary-to-fiber ratio, while daily stimulation could maintain

this ratio similar to the level measured in normal muscle. These results imply that dynamic muscle stimulation has the potential to regulate vascular adaptation, which may further protect the musculoskeletal system under a condition of functional disuse.

Taken together, the overall results suggest that dynamic muscle stimulation, with the optimal stimulation signals, may be used to influence the musculoskeletal and microvascular adaptations concurrently.

Table of Content

List of Figures

List of Tables

Normalized values are mean ± SD. [b] $p < 0.01$ vs. baseline, [#] $p < 0.001$ vs. baseline, [a] $p < 0.01$ vs. age-matched, [*] $p < 0.001$ vs. age-matched.

Values are mean ± SD for averaged fiber cross-sectional area (CSA, μm^2), number of central nuclei (CN, #/fiber), type II and type I muscle fibers (%). [b] $p < 0.01$ vs. baseline; [a] $p < 0.01$ vs. age-matched; [#] $p < 0.001$ vs. age-matched; [*] $p < 0.05$ vs. HLS.

Values are mean ± SD for averaged fiber cross-sectional area (CSA, μm^2), number of central nuclei (CN, #/fiber), type II and type I muscle fibers (%). [b] $p < 0.01$ vs. baseline; [a] $p < 0.01$ vs. age-matched; [#] $p < 0.001$ vs. age-matched; [*] $p < 0.05$ vs. HLS.

Acknowledgments

I would like to take this opportunity to express my sincerest thanks to my advisor, dissertation committee, colleagues, and family. Without them, the successful completion of my dissertation research would be rather difficult.

My advisor, Dr. Yi-Xian Qin, has taken the challenge and allowed me to work in his laboratory in September 2002. Throughout the years, he guided me through numerous projects, which led to the completion of my master and doctoral degrees in biomedical engineering. He provided valuable advices for my hypothesis, *in vivo* models, data analysis, and interpretation. His constant support was the main driving force to the success of my projects. I would like to thank him for his confidence in me, and truly cannot ask for any better advisor.

Next, I have to thank the chair of my committee, Dr. Stefan Judex. He always jokes that I won't be graduating until 2012 and surprises at the amount of food, particularly meats, I can consume. Dr. Judex has given me many important advices (or questions to ponder about) during lab meetings. I often went to him with microCT and statistical questions regarding my projects. I am extremely grateful for his guidance and value the experience very much.

I am thankful to Dr. Peter Brink and Dr. Susannah Fritton, my external members, for their valuable time and constructive comments. Their insights on musculoskeletal physiology and biomechanics at my proposal defense were highly appreciated, and have definitely shaped my final dissertation.

In addition, I would like to extend my appreciation to Dr. Michael Hadjiargyrou and Dr. Clinton Rubin. Dr. Hadjiargyrou has guided me through the

immunohistochemisty procedures. Dr. Rubin has provided numerous ideas and advices for my studies. I most certainly value my experiences in working with these two amazing professors.

Throughout my graduate studies, I have worked with many wonderful colleagues – Dr. Yi Xia, Dr. Anita Saldanha, Dr. David Komatsu, Dr. Russell Garman, Dr. Jonathan Chiu, Dr. Kim Luu, Dr. Liqin Xie, Dr. Yizhi Meng, Dr. Chiung-Yin Chung, Luke Orzechowski, Suzanne Ferreri, Frederick Serra-Hsu, Shiyun Xu, Murtaza Malbari, Engin Ozcivici, and Rob Gersch. I will not go into individual detail because my thanks to them may be longer than my dissertation. Their assistance, discussion, and late night dinners were incredible and have made my graduate school experience impossible to describe. I will always cherish the time we shared.

Most importantly, I would like to thank my parents and my boyfriend for their supports, encouragement, and love. My dad is the most amazing chef in this world and I am blessed with his love and foods (since I don't cook). My mom is always understanding and willing to listen to my problem or complain. She has given me many precious advices. My boyfriend, whom I met in Stony Brook University, is supportive and always knows when I need to concentrate on my work or need some time to relax. With the three of them by my side, I can only say that I am the luckiest girl. My thanks and love to them cannot be described with word.

Lastly, this research is kindly supported by the National Institute of Health (R01 AR52379 and R01 AR49286, Qin), the US Army Medical Research and Materiel Command, the National Space Biomedical Research Institute (TD00405).

I. Background

1. Introduction

The quantity and quality of bone and skeletal muscle are closely interrelated and play important roles in daily physical functions. The deterioration of musculoskeletal tissues, i.e., bone loss and muscle atrophy, are the results associated with osteoporosis. The etiologies of such disease, i.e., lack of weight bearing activity and muscle weakness, are apparent, yet the detailed mechanism leading to the loss and deterioration of bone and muscle are not fully understood. Common countermeasures for osteoporosis include the use of pharmacologic agents, which may have additional side effects toward the body. Exercise can delay the occurrence of bone loss and maintain muscle endurance, but may further generate complications such as microdamage accumulation. Another approach toward such disease is to apply an external mechanical stimulus to initiate and regulate the remodeling processes. Musculoskeletal tissues are responsive to dynamic biomechanical signals. Various biomechanical stimuli, such as vibration, fluid pressure, ultrasound, and electrical stimulation, have been extensively studied as countermeasure for osteoporosis. In particular, this dissertation will focus on using dynamic muscle stimulation as the external stimulus to prevent musculoskeletal tissue loss and deterioration due to disuse.

2. Significance

Osteoporosis is a silent, chronic metabolic bone disease, characterized by low bone mass, deterioration of bone microstructure, loss of muscle volume, decreased bone and muscle strength leading to increased bone fragility and susceptibility to fractures [1-3]. Osteoporosis affects over 200 million people worldwide, including 44 million

Americans, and is expected to increase with the rising aging population [2, 4]. The National Osteoporosis Foundation indicated that osteoporosis is a major public health threat. It is predicted that by 2020, 50% of Americans over 50 would be developing osteoporosis [5].

The increased fracture risk, due to bone and muscle fragility, leads to high morbidity and mortality of the population and imposes a financial burden on the community [1]. According to the National Institutes of Health, osteoporosis is responsible for 1.5 million fractures each year [6, 7]. The most common fracture sites are spine, hip, and wrist, with the estimated incidence of 700,000 at the spine and 250,000 at the hip and wrist [7]. The annual medical expenditures for the management of osteoporosis, such as physician visits and hospitalizations, are estimated at $17 billion and increasing [8].

The etiology of osteoporosis is multi-factorial, including aging, disuse, and hormonal changes. The risk factors involve demographics (age, sex, and ethnicity), genetics (family history), and environmental (nutrients and exercise) aspects of an individual [9, 10]. The standard diagnostic technique for osteoporosis is to measure the bone mineral density (BMD) in the hip, spine, and wrist. Based on epidemiologic studies, the World Health Organization defines osteoporosis on the basis of BMD measurements obtained via dual energy x-ray absorptiometry, as a T-score of greater than 2.5 standard deviations below the mean for young healthy individuals at their peak bone mass [2]. Osteopenia, a condition also characterized by a decrease in bone density, is defined with a T-score between 1 and 2.5 below the reference mean. Studies have shown that osteopenia precedes the development of osteoporosis [11, 12]. Thus, animal models

with osteopenia are often used for determining and improving preventive measures for osteoporosis.

3. Musculoskeletal Physiology

Skeletal Tissue. The principal role of the skeleton is to provide structural support for the body along with important functions of mineral reservoir, hemopoiesis, and protection for internal organs. Given the skeleton's ability to adapt its form to functional demands, it is essential to understand the biology of bone and its processes for structural adaptation.

At the gross morphological level, cortical (compact) bone and trabecular (cancellous) bone have been shown to modify their structure in response to applied mechanical loads, immobilization, hormonal influences, and other factors [13-17]. Cortical bone forms approximately 80% of the skeleton, enclosing the marrow cavity and trabecular bone. In long bones (e.g., femur and tibia), trabecular bone constitutes the metaphyseal and epiphyseal regions, and occupies the marrow cavity [18]. The density and architecture of trabecular bone are important in justifying how applied mechanical forces are distributed to the surrounding cortical bone [19]. Dense cortical bone makes up the diaphyseal region and provides maximum resistance to torsion and bending [19]. Together, long bone can adapt to the additional stresses and strains during weight-bearing activities, such as running.

At the microscopic level, an important structural component of cortical bone is the osteon, or Haversian system. In long bone, osteons are cylindrical structures oriented parallel to its long axis and to the main compression stresses [20]. Structurally, an osteon

is a group of concentric tubes, called lamella, resembling the architecture of plywood [18, 21]. Each lamella is a layer of bone matrix consisting of densely packed collagen fibers running in a single direction. The collagen fibers of adjacent lamellae always run in a different direction, which provides an alternate pattern for withstanding torsion stresses [20].

Blood Supple to Bone. The skeletal vascular system supplies nutrients to and removes wastes from bone tissue, marrow cavity and periosteum. Its organization insures that no cell lies more than 300 μm from a blood vessel [22]. Skeletal injuries can lead to a disruption of blood supply to bone, which can further influence the healing processes of bone tissue [23]. Thus, it is important to understand the distribution of blood supply to bone tissue. In all long bones, there is a similar pattern of blood vessels, consisting of two circulatory systems: the periosteal-diaphyseal-metaphyseal system and the epiphyseal-physeal system [13].

There are three sources of blood supply to the diaphysis and metaphysis of long bones: nutrient arteries, periosteal arteries, and arteries that penetrate the epiphysis and metaphysis. Nutrient arteries pass through the diaphysis and branch proximally and distally within the medullary cavity. These medullary arteries join multiple branches from the periosteal and metaphyseal arteries to form the medullary vascular system [24]. This system feeds the inner two-thirds of the cortex via capillaries, which traverse the bone matrix through anatomical spaces known as Haversian canals [25]. Thus, the primary direction of blood flow through the cortex is centrifugal. As the medullary vascular system supplies the inner two-thirds of the cortex, the outer one-third receives blood from the periosteum [25].

Bone Remodeling. The process of bone remodeling is to remove old bone tissue and replace it with newly formed bone. It occurs throughout one's lifetime and plays a dominant role in maintaining the structure of the skeleton, via the functions of various cell types. The remodeling process is accomplished by osteoblasts and osteoclasts working together as basic multicellular units [26]. Osteoblasts are the bone forming cells that lay down the extracellular matrix and regulate mineralization, while osteoclasts are the multinucleated cells that resorb mineralizing surface [27, 28]. Osteocytes, derived from osteoblasts, are the most abundant in bone and are believed to have a primary role in the detection of mechanical signals [29]. The basic multicellular unit follows well-defined steps; it begins with activation, followed by resorption, and then formation. It is estimated that the total time for one remodeling cycle, from activation to formation is 12 weeks [18].

Muscular Tissue. Skeletal muscular tissues attach to bone, serve to produce movements and maintain posture [30]. Skeletal muscle fibers are multinucleate cells formed by the fusion of myoblasts. The nuclei are arranged around the edge of the fiber and the interior of the fiber consists of protein filaments which are responsible for contraction. Muscles have excellent blood supply with capillaries forming a network between fibers. In mammals, the bulk of muscle fibers are supplied by the alpha motoneurons, innervating a number of muscle fibers [31]. Individual muscle fiber consists of bundles of small myofibrils, where sarcomeres – the repeating striated pattern formed by the thick and thin filaments, are apparent through electron microscopy [32]. The molecular composition of filaments comprises of myosin, actin, troponin, and

tropomyosin. The interactions of these proteins are the basic constituent in skeletal muscle contraction.

Muscle Contraction. Contraction of muscle is initiated by neuromuscular transmission [31]. Calcium ions are released from the sarcoplasmic reticulum and binded to troponin, which in turn allow the binding of myosin and actin to occur. The cross-bridge interaction between myosin and actin is the basis of the sliding filament mechanism, in which contraction occurs due to the sliding motion of the thick and thin filaments, creating an overlapping region [33]. Once contraction is stopped, calcium ions are pumped back out to the sarcoplasmic reticulum, terminating the entire sliding mechanism.

4. Bone Loss as a Characteristic of Osteoporosis

The removal of weight-bearing activity generates skeletal adaptive response, resulting in "disuse osteoporosis". Disuse osteoporosis is mainly experienced by astronauts in long-term space mission and patients with spinal cord injuries (SCI). It has been established that significant and rapid bone loss often occurs in the lower extremities, i.e., femoral neck and pelvic. It is estimated that 1-2% of site specific bone mineral density (BMD) is lost per month due to the exposure to microgravity [34-37]. In 6-months spaceflight, cosmonauts experienced up to 6% and 3% decreases in tibia trabecular and cortical bone mass, respectively, and 13.2% loss of calcaneus broadband ultrasound attenuation [38, 39]. Other demonstrated that trabecular volumetric BMD was lost 2.2 to 2.7% per month at the hip and 0.7% per month at the spine [36]. Similarly, the lack of physical activity following SCI leads to reduction in bone mass is dramatic. In a

study with 41 SCI patients, 61% of the patients were diagnosed with osteoporosis, 20% with osteopenia, and 34% fracture incidences [40]. During chronic immobilization, BMD measurements showed tremendous decrease at both femur (30% at femoral neck, 25% at diaphysis, 48% at distal site) and tibia (45% at proximal site and 25% at diaphysis) [41, 42]. The quantity of bone loss in humans subjected to microgravity and SCI is comparable, yet the mechanisms may not be equivalent. Re-ambulation after unloading allowed some site-specific bone mass to be restored but may not be completely recover back to normal condition [38, 39, 43]. Thus, intervention is continuously being developed through new investigation on the physiological mechanisms underlying disuse osteoporosis.

5. Muscle Atrophy as a Characteristic of Osteoporosis

The interrelationship between muscular and skeletal tissues is an important topic in studying a major skeletal disease like osteoporosis. The structural and functional adaptations of skeletal muscle to microgravity and disuse after SCI have been studied at various levels in link to the reduction of skeletal integrity. In term of lower extremity muscle volume, studies reported a decrease of 10% in the quadriceps, 19% in the gastrocnemius and soleus after a 6-months space mission [44]. Computed tomography measurements of the muscle cross sectional area (CSA) indicated a decrease of 10% in the gastrocnemius and 10-15% in the quadriceps after short-term missions [45, 46]. Similar results were concluded after SCI, where patients suffered significant 21%, 28% and 39% reduction of CSA in the quadriceps femoris, gastrocnemius, and soleus muscles, respectively [47, 48]. In addition to the whole muscle size, muscle fiber characteristics

were also modified due to inactivity. Muscle fiber can mainly classify into two types; slow (type I) fibers play important role in maintaining body posture while fast (type II) fibers response to physical activity. Under disuse condition, all fiber types were decreased in size, 16% for type I and 23-36% for type II [49, 50]. The atrophied soleus muscles were also undergone a shift from type I (-8% in fiber numbers) to type II fibers [50, 51].

The high incidence of falls in elderly women leads to increase fractures is closely associated with muscle weakness and sacropenia, a loss in muscle mass. Approximately 25% of osteopenic and 50% of osteoporotic postmenopausal women also have sacropenia [3]. It was determined that in premenopausal women, the prevalence of sarcopenia was 1.5% but the percentage rose to 19.5% in postmenopausal women [3]. Quadriceps isometric strength was significantly decreased in ten postmenopausal women over a 39-weeks longitudinal study [52]. However, the involvement of hormonal changes on physiological muscle adaptive response is not fully understood. It is clear though, muscular adaptation due to lack or reduction of physical activity has a significant impact on osteoporosis.

6. Musculoskeletal Responses in Functional Disuse Model

Hindlimb suspension (HLS) is a well-developed disuse model, where animal hindlimbs are lifted and suspended for the duration of the study, resulting in the unloading of the hindlimbs that normally have weight-bearing function. There are similarities when comparing musculoskeletal adaptations between animal and humans models. Site specificity is one such feature. Bone loss after space missions was mainly

at the metaphysis and epiphysis regions of the lower extremities [53]. The occurrence of osteopenia subsequent to HLS is also site specific, in which only weight-bearing bone is negatively affected. HLS studies with skeletally mature adult rats have resulted in up to 20% reduction of trabecular BMD at the femoral neck and proximal tibia [54, 55]. Cortical BMD reduction was not effected by the HLS as much as the trabecular bone site [54, 55]. Other studies have shown that HLS reduced calcium content by 7-12% at tibia and 11% at femur [56, 57]. Bone resorption biochemical markers increased after both human and rat HLS disuse models. However, reductions in bone formation were not often mentioned in human spaceflight studies. Histomorphometric analyses in HLS experiments indicated decrease in bone formation rate at various sites, i.e., 34% at the tibio-fibular junction [56], 65-88% at tibia mid-diaphysis periosteal surface [55, 58], and 19% at distal femur metaphyseal trabecular bone surface [54].

Furthermore, hindlimb suspended muscles, i.e., soleus and gastrocnemius, undergo atrophy and slow-to-fast phenotype transition similar to human in spaceflight and after SCI. Soleus atrophy was demonstrated in numerous HLS studies, reducing the soleus to body weight ratio by 30% and individual fiber CSA by 66% [59, 60]. HLS induces muscular adaptation via regulating cellular activities. Satellite cells, myogenic precursor cells, have been shown to serve as a source of new myonuclei during regeneration [61, 62]. 16-days HLS diminished satellite cell mitotic activity yet a period of reloading returned its mitotic activities to normal [60]. Other cellular activities, such as apoptosis, have also activated in response to muscle disuse [63].

7. Fluid Flow as a Mediator for Musculoskeletal Adaptation

Musculoskeletal microvascular circulation provides for the supply of nutrients to and the removal of metabolites from muscle and bone. Incomplete blood flow or discontinuous mechanical-driven fluid flow can reduce the nutrient supply placing the bone cells in a state of stress, initiating remodeling, and thus resulting in osteopenia [23, 64]. Mechanical loading induced intracortical bone fluid flow, via matrix deformation and/or increased intramedullary pressure, has been shown to mediate bone adaptation in normal and disuse conditions [65, 66]. Increased intramedually pressure generates pressure gradients within the marrow cavity which can further induce interstitial fluid flow, initiating metabolic activities at the cellular level [67, 68]. Our previous work using avian model showed that bone subjected to oscillatory fluid flow via increased intramedually pressure resulted in significant new bone formation, which demonstrated anabolic fluid movement play a regulatory role in the remodeling process [23, 65].

Other studies have demonstrated the interactions between blood flow to bone and bone remodeling. One example showed that by ligating the nutrient artery for 5 months can cause removal of cortical bone but formation of periosteal bone [25]. In a goat model, blood was pumped into the marrow cavity to achieve continuous intraosseous pressures of 30-45mmHg for 10 days, and significant increase in BMD was observed [69]. It has been shown that venous occlusion can initiate periosteal bone formation. On the contrary, arterial occlusion can reduce the oxygen pressure within pig femoral condyle from 40mmHg to 15mmHg [70]. The medullary gas composition was linked to osteogenesis, where oxygen consumption was high and is acquired for a specialized transport system to augment diffusion across the cortex [71, 72].

Inducing fluid flow via external mechanical stimuli on muscle adaptation is not well established. Both voluntary and dynamic exercise appears to markedly increase blood flow to musculoskeletal tissue [72]. It is thought that muscle contraction promotes blood flow to bone and muscle based on the muscle pump system. Skeletal muscle contains rich microvasculature, where contraction of the muscle compresses blood vessels. Blood flow in arteries propagates to capillary beds, increasing the intravascular hydraulic pressure [64, 73]. On the other hand, muscle blood flow is promoted by expelling blood out of the venous capacitance vessels, thereby reducing venous pressure and creating a pressure gradient [72-74]. Increased pressure in the nutrient arteries can directly increase the intramedullary pressure and substantially increase the fluid volume in the marrow cavity, which drive fluid flow in bone. Hence, it is thought that dynamic musculo-contraction may follow this mechanism to enhance fluid flow to bone and muscle, and potentially mediate musculoskeletal adaptive responses.

8. Mechanical Loading as a Countermeasure for Osteoporosis

Musculoskeletal tissue is responsive to mechanical stimuli and has the ability to adapt by altering its mass and morphology. In the absence of weight-bearing activity, nutritional and endocrine interventions cannot maintain bone mass [2, 75]. Skeletal muscle contractions via daily activity impose large intrinsic loads on bone, and such loads have been shown to promote osteogenic responses in bone [76, 77]. Reduced muscle contractile activity decreases muscle blood flow, mass, tone, and strength in disuse environment, ultimately reducing postural stability and increasing fracture risk [73].

Mechanical signals are critical in regulating bone and muscle gene expression, cellular activities, tissue morphology, architecture, and function. Evidence has indicated that dynamic low magnitude high frequency signals, such as vibration and muscle-induced contraction, are osteogenic and able to inhibit osteopenia under disuse conditions [78-81]. These adaptive responses are highly dependent of mechanical parameters, i.e., strain rate and magnitude [65, 66, 68, 80]. It is hypothesized that these anabolic low-level mechanical signals generate small mechanical strain information (10-100με), which integrates over time to produce a greater uniform strain stimulus on the skeleton [79, 82]. Muscular adaptations to mechanical signals include muscle fiber size, density and slow-to-fast fiber type transformation [83, 84]. The effects of externally applied mechanical force, i.e., electrical stimulation of muscles, on the musculature have been shown to produce changes not only within the muscle fibers, but also at the muscular microvasculature [85, 86]. The structural and functional remodeling of skeletal muscle microvasculature in respond to mechanical force, suggests that anabolic adaptation may influence fluid flow within the musculoskeletal system and alters blood supply to bone and muscle [64].

9. Musculoskeletal Responses to Electrical Muscle Stimulation

Functional electrical stimulation alters muscle morphology, biochemical, and mechanical properties [83, 87, 88]. However, discrepancies in various results implied the effectiveness of electrical stimulation is highly depended on the regimen. Tissue adaptations are thought to be related to the increased blood flow induced by contraction [73, 89]. Although the underlying mechanism is still unclear, several hypotheses have

been considered. The muscle pump theory, effecting both muscle and bone [64, 74], suggests that the expulsion of blood from the vasculature of skeletal muscle is the result of venous compression. Thus, dynamic contraction repeats this pumping action and potentially increases fluid perfusion to musculoskeletal tissues [89]. Others proposed that skeletal muscle hyperemia is mainly the contribution of vasodilation due to the release of vasoactive substance from contracting muscle [90]. The role of both mechanisms remains controversial, perhaps muscle pump contribute to the immediate response of contraction while vasodilation generates the delayed effect.

Similarly, the influence of electrical muscle stimulation on skeletal adaptive response is also inconclusive. Zerath et. al. reported muscle stimulation partially maintain the anabolic response in unloaded trabecular bone, yet there was no effect in trabecular bone volume and microstructure [91].

To further elucidate the immediate mechanical and fluid responses in bone, we have previously investigated the magnitudes of intramedullary pressure (ImP) and bone stain generated by dynamic el electrical muscle contraction in response to a broad range of stimulation frequencies (1, 2.5, 5, 10, 15 20, 30, 40, 50, 60 and 100 Hz). By applying muscle stimulation, with 1 ms square pulse at 2 V, to quadriceps, our results indicated that the changes in ImP and strain to stimulation frequency were nonlinear at the femur [92]. Normal heart beat generated approximately 4 mmHg of ImP in the femur at a frequency of 5.37 ± 0.35 Hz. The ImP reached a maximum of 45 ± 9.3 mmHg at 20 Hz (Figure 1). The contraction of skeletal muscle generated fluid pressures in the marrow cavity of 17, 24, 37, 26, and 3 mmHg at frequencies of 1, 5, 10, 40, and 100 Hz, respectively (Figure 1). The contraction of skeletal muscle generated femoral matrix

strains of 61, 87, 128, 78, 18, and 10 με at frequencies of 1, 5, 10, 20, 40, and 100 Hz, respectively (Figure 2). The maximum ImP was measured at 20 Hz but the maximum matrix strain was measured at 10 Hz (Figure 2). With the stimulation frequency above 30 Hz, values of matrix strain decreased by more than 75% of the peak strain at 10 Hz. For frequencies from 40 Hz to 100 Hz, values of matrix strain were less than 20 με.

Based on the strain data, we found that the stimulation applied at 1, 2.5, 5, and 10 Hz to the skeletal muscle is equivalent to the loading frequency experienced by the femur (Figure 3). With the stimulation frequency above 10 Hz (20 to 100 Hz), the loading frequency is corresponding to the number of tetanic contraction applied in a given time (Figure 4). For example, stimulation at 20 Hz for 2 seconds followed by 8 seconds rest showed a loading frequency of 0.1 Hz (one contraction every 10 seconds).

10. Summary

Many studies have demonstrated that a change in the mechanical environment, i.e., disuse, can have serious consequences. The development of new intervention to prevent osteopenia and muscle atrophy is a critical task as the incidence of osteoporosis continues to rise. The application of mechanical stimulus to induce adaptations at multiple affected tissues, i.e., muscle and bone, simultaneously is particularly attractive. Although with varied outcomes, the potential of electrical muscle stimulation as a countermeasure for disuse osteoporosis may be uncovered by modifying the stimulation regimen. Hence, it is necessary to determine the mechanical parameters within muscle stimulation regimen that can affect the responsiveness of musculoskeletal tissues.

Figures

Figure 1.1

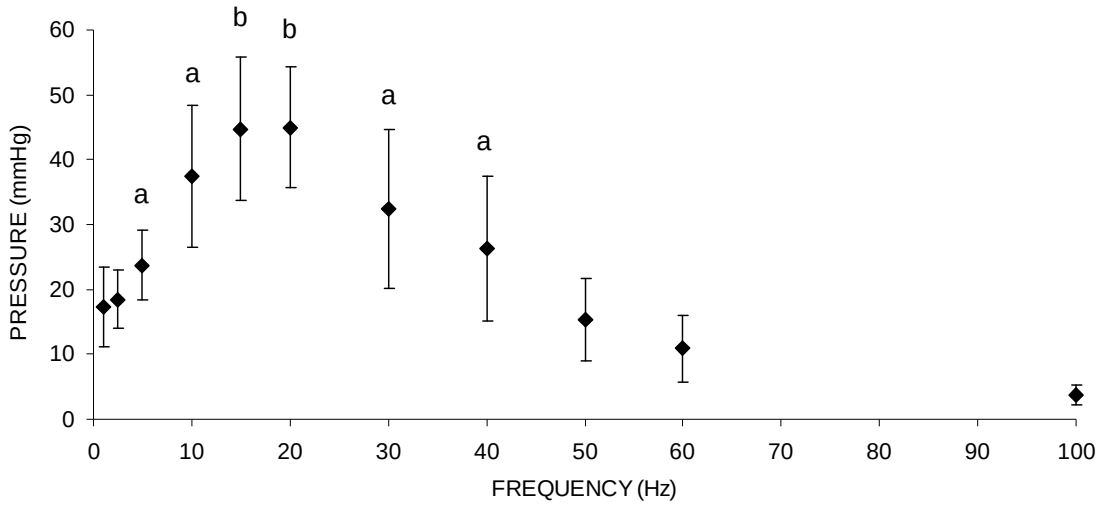

Graphs show mean ± SD values from the ImP measurement. ImP in femur increased significantly with electrical frequency at 5, 10, 15, 20, 30, and 40 Hz. In the loading spectrum from 1 to 100 Hz, stimulation at 1 Hz generated an ImP of 18 mmHg. A maximum ImP of 45 mmHg was measured at 20 Hz, which was 2.5 folds higher than 1 Hz. [a] $p < 0.05$ vs. baseline ImP; [b] $p < 0.01$ vs. baseline ImP.

Figure 1.2

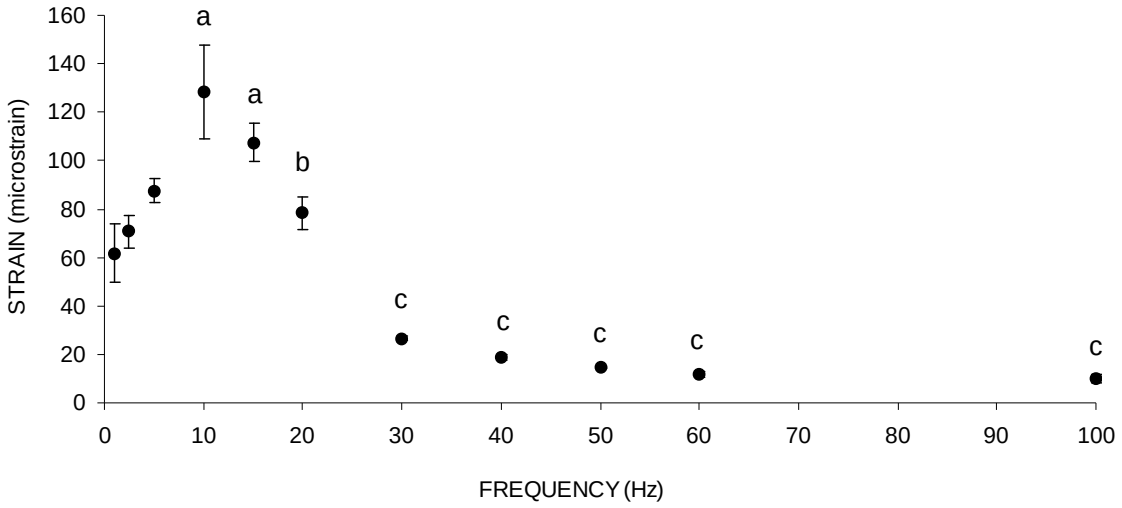

Graphs show mean ± SD values from the bone surface strain measurement. Dynamic muscle stimulation applied at various frequencies significantly increased bone strain. In the loading spectrum from 1 to 100 Hz, stimulation at 1 Hz produced a strain of 62 με. Peak strain of 128 με was recorded at 10 Hz stimulation. The strain magnitude was reduced by >75% of the peak strain for stimulation frequencies greater than 30 Hz. [a] p <0.01 vs. 1, 2.5, and 5 Hz; [b] p <0.01 vs. 10 Hz; [c] p <0.001 vs. stimulation 20 Hz and below.

Figure 1.3

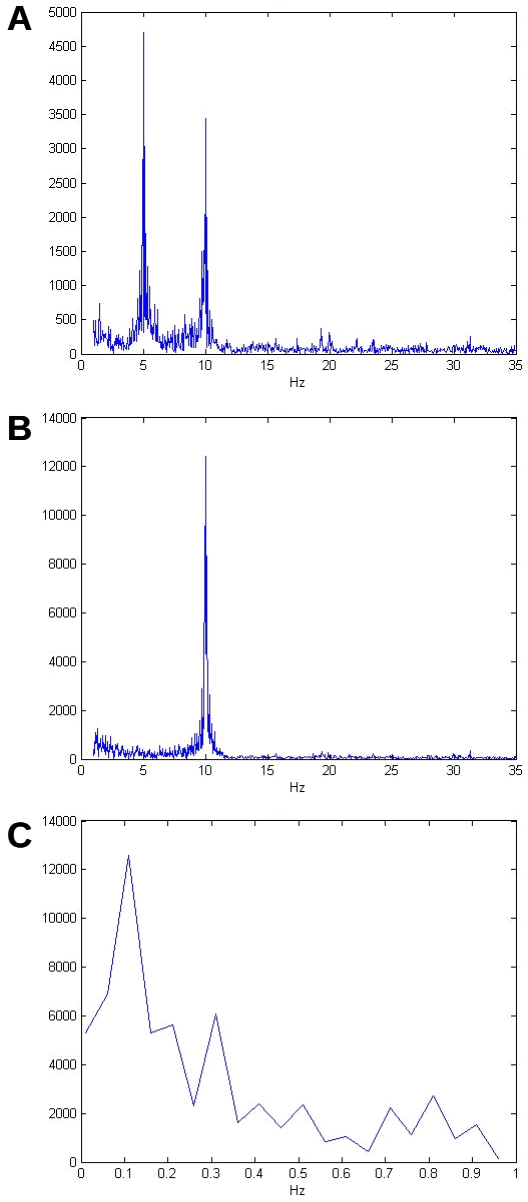

Graphs show the fast fourier transform of the bone strain measurements from stimulation at 5 Hz (A), and 10 Hz (B & C). The stimulation frequencies applied at 5 and 10 Hz is equivalent to the loading frequency experienced by the femur, as shown in A & B. The 0.1 Hz signal, observed in C, was generated by the number of contraction period per cycle (2 seconds contraction per 10 seconds).

Figure 1.4

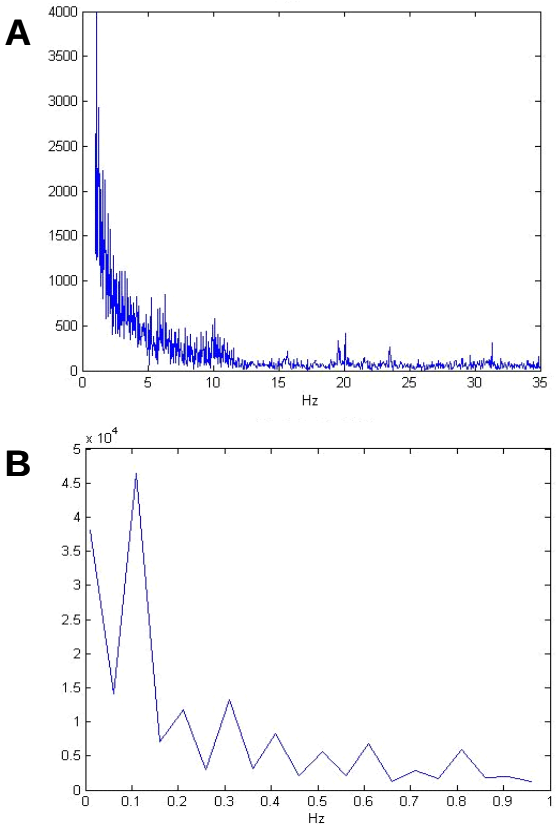

Graphs show the fast fourier transform of the bone strain measurements from stimulation at 20 Hz. (A) The stimulation frequency of a tetanic contraction does not reflect on the bone strain measurement. (B) The loading frequency felt by the femur is corresponding to the number of tetanic contraction applied in a given time (once every 10 seconds).

II. Hypothesis and Specific Aims

Mechanotransduction induced by loading and fluid flow plays a vital role in bone and muscle remodeling processes. Increased fluid perfusion in the musculoskeletal system during physical exercise has the potential to initiate adaptive responses in both tissues and enhance tissue interaction. A change in the physiological and/or pathological environment, i.e., microgravity and functional disuse, can influence skeletal and muscular tissue quantity and quality. These alterations lead to major health concerns, such as osteoporosis and sarcopenia, effecting millions of individuals and posing a significant financial burden. Bone loss and muscle atrophy are often associated with increased fracture risk, critically impact on the individuals' morbidity and mortality. In this study, induced dynamic skeletal muscle contractions will be investigated as a potential prevention and countermeasure for osteoporotic bone loss and muscle atrophy.

The intimate relationship between skeletal muscle and bone mechanic has brought new insights for osteoporosis interventions. Musculoskeletal fluid filtration may serve as a critical mediator for the interactions between muscle and bone, where an external stimulus may enhance such fluid flow and initiate adaptation. Skeletal muscle contraction promotes blood flow within muscular tissue, increasing the intramedullary pressure and generating low-level deformation that further drives fluid flow to bone. The potential of dynamic electrical muscle stimulation (MS) on the musculoskeletal regulatory responses was the main focus of this dissertation. Mechanical components, i.e., stimulation frequency and contraction-to-rest ratio, were varied and used to optimize the adaptive responses in a functional disuse model.

Global Hypothesis: Dynamic MS can regulate osteogenic and muscular adaptations, which alleviates bone deterioration and muscle atrophy under a condition of functional disuse.

The global objective of this dissertation was to evaluate the role of dynamic MS in prevention of bone loss and muscle atrophy, via four specific aims (S.A.) and sub-hypotheses.

S.A.1. Determined the effects of stimulation frequency within the dynamic MS regimen on disused skeletal tissue.

Sub-hypothesis 1. Dynamic MS can prevent bone loss from disuse as a function of stimulation frequency dependant.

- Applied dynamic muscle contraction with stimulation frequency at 1 Hz, 20 Hz, 50 Hz, and 100 Hz, to a 4-week hindlimb suspended rat model.
- Evaluated trabecular bone quantity and its microstructural properties of the femur and tibia using micro-computed tomography (μCT).
- Evaluated the dynamic remodeling processes using fluorescent histomorphometric analysis.

S.A.2. Optimized the skeletal adaptive response by inserting various contraction-to-rest ratios into a frequency-specific MS regimen, result based on S.A.1 (Chapter 2).

Sub-hypothesis 3. Inhibition of bone loss due to disuse can be optimized by inserting a range of rest periods during dynamic MS.

- Applied a frequency-specific MS with various contraction-to-rest ratios of 1 sec-to-4 sec, 2/8, 4/6, and 2/28, to a 4-week hindlimb suspended rat model.

- Examined trabecular bone quantity and its network of the femur and tibia using μCT.
- Evaluated the bone formation activity using histomorphometric analyses.

S.A.3. Investigated the effects of stimulation frequency within the dynamic MS regimen on disused muscular tissues (Chapter 3).

Sub-hypothesis 2. Dynamic MS can reduce muscle atrophy induced by the lack of weight bearing activity and the preventive degree of muscle atrophy is dependent to the stimulation frequency.

- Assessed the cross-sectional area of muscle fibers and the number of fiber with central nuclei via standard H&E method.
- Examined the number and size of type I and type II muscle fibers via ATPase staining.
- Evaluated the regenerative response of muscle fibers using immunohistochemistry technique.

S.A.4. Evaluated the skeletal muscle vasculature adaptation in response to the hindlimb unloading and daily muscle stimulus (Chapter 4).

Sub-hypothesis 5. The skeletal muscles subjected to 4-weeks electro-musculo-contraction can regulate microvasculature adaptive response, i.e., increase the capillary density between muscle fibers.

- Evaluated the capillaries that are embedded between muscle fibers via immunohistochemistry and ATPase staining.

III. The Effects of Frequency-Specific Dynamic Muscle Stimulation on Inhibition of Trabecular Bone Loss in a Disuse Model

Abstract

Clinical electrical stimulation has been shown to alleviate muscle atrophy resulting from functional disuse, yet little is known about its effect on the skeleton. The objective of this study is to evaluate the potential of dynamic electrical muscle stimulation on disused trabecular bone, and to investigate the importance of optimized stimulation frequency in the loading regimen. Fifty-six skeletally matured Sprague-Dawley rats were divided into seven groups for the 4-week experiment: baseline control, age-matched control, hindlimb suspended (HLS), and HLS with muscle stimulation at 1 Hz, 20 Hz, 50 Hz, and 100 Hz. Muscle stimulation was carried out for 10 minutes per day for 5 days per week, for 4 weeks. The metaphyseal and epiphyseal trabecular regions of the distal femurs and proximal tibia were analyzed with microcomputed tomography and histomorphometry methods. HLS alone for 4-week resulted in a significant amount of trabecular bone loss and structural deterioration. Electrical muscle contraction at 1 Hz was not sufficient to inhibit trabecular bone loss and resulted in similar amount of loss to that of HLS alone. However, bone quantity and structure were significantly improved by applying muscle stimulation at mid-frequency (20 Hz & 50 Hz). Dynamic stimulation at 50 Hz demonstrated the greatest preventive effect on the skeleton against functional disused alone animals (up to +147% in bone volume fraction, +38% in trabecular number and -36% in trabecular separation). Similarly, histomorphometric analysis in the femur showed slight enhancement of bone formation indices, such as mineral apposition rate and bone formation rate. These data clearly demonstrated the potentials of frequency-specific dynamic muscle contraction in regulating skeletal adaptive responses under distress conditions. Electrical muscle application, with a specific regimen, may be

beneficial to future orthopedic research in developing a countermeasure for disuse osteoporosis.

Introduction

Disuse osteoporosis is a common skeletal disorder in the elderly, in patients subjected to prolonged immobility or bed-rest, e.g., fracture and spinal injury, and in astronauts who participate in long-duration spaceflight. Conditions associated with disuse osteoporosis are often identified as decreased bone mass and deterioration of the skeletal microarchitecture. These physiological changes generate additional health complications, including increased risk of falls and fracture, and poor long-term recovery. Thus, there is a great need to develop a clinically applicable intervention for the prevention of progressive osteopenia.

Clinical electrical stimulation has been examined extensively in SCI patients to strengthen skeletal muscle and alleviate muscle atrophy with promising outcomes [93, 94]. A few physical training studies further investigated this electrical technique to determine the effect on the skeleton and showed mixed results in bone density data [95-97]. Electrical muscle stimulation (MS) with disuse animal models also demonstrated effectiveness in the musculoskeletal tissues. Several investigators have shown that muscle contraction can prevent muscle atrophy to varying degrees, depending on the experimental regimen [98, 99]. When studying bone adaptive response to electrical stimulus, results were mixed. Zerath et. al. found that electrical stimulation increased osteoblast activity after 3-weeks disuse, while Midura et. al. reported partial preventive

effect on osteopenia [91, 100]. One explanation for these discordant outcomes observed in both clinical and *in vivo* studies might be the selection of the applicable signals.

One potential mechanism for the observed effect of MS in inhibiting skeletal deterioration is through the coupling of muscle and bone mechanotransduction in the skeleton. Bone is more sensitive to dynamic stimulation rather than to static load. Specific mechanical parameters, e.g., frequency, cycle numbers, duration of stimulus, magnitude and rest-insertion, are found to be the key determinants in generating bone strain and bone fluid flow, all of which may be imperative to the mechanotransductive signaling cascade in bone modeling and remodeling [68, 101, 102]. Zhang et. al. showed knee loading at 15 Hz in mice was able to increase cortical cross-sectional area and enhance mineral apposition rate [103], while a preliminary vibration study at 30 Hz with premenopausal women demonstrated a significant increase in BMD [104]. The stimulation frequencies of various types of mechanical loads, e.g., direct compression, vibration, and fluid pressure, determined the outcomes of many *in vivo*, *in vitro*, and clinical trials [65, 103-107].

Our group has demonstrated previously that various stimulation frequencies can generate different level of surface strain and intramedullary pressure in long bone. Here, we hypothesized that daily induced dynamic muscle contraction can inhibit bone loss and maintain the trabecular network during a 4-week study using a functional disuse model, and that the adaptive response is dependent on the stimulation frequency. To further explore the potential of electrical stimulation as a non-invasive approach to the skeletal system, our objective was to investigate the effect of dynamic electrical muscle contraction on disused trabecular bone. In particular, we examined the importance of the

stimulation frequency in the inhibition of osteopenia in a hindlimb suspension (HLS) animal model.

Materials and methods

Experimental Design

All experimental procedures were approved by the Laboratory Animal Use Committee at Stony Brook University. Fifty-six 6-months-old female Sprague-Dawley retired breeder rats (Taconic, NY) were used to investigate the effects of frequency-dependent dynamic muscle stimulation (MS) on skeletal adaptation under disuse environment. They were housed individually in 18”x18”x24” (LxWxH) stainless steel HLS cages in a temperature-controlled room with a 12:12 hour light:dark cycle, and were provided standard rodent chow and water ad libitum. Animals were transferred to these cages one week prior to the experiment start date in order to acclimate them to their environment. Animals were randomly assigned to seven groups with n=8 per group: (1) baseline control, (2) age-matched control, (3) HLS, (4) HLS+1 Hz MS, (5) HLS+20 Hz MS, (6) HLS+50 Hz MS, and (7) HLS+100 Hz MS. Functional disuse was induced by HLS, setup modified from Morey-Holton and Globus [108]. Briefly, animal’s tail was cleaned with 70% alcohol and lightly coated with tincture of benzoin. Once the tail was dried and sticky, a tail harness was attached to the tail with a piece of surgical tape. The tape was secured with two strips of elastic adhesive bandage; one over the end of the tape at the base of the tail and the other about half-way up to the end of the tail. The tail harness was then attached to a swivel apparatus suspended from the top of the cage. An approximately 30° head-down tilt was set to prevent contact of the animal’s hindlimbs

with the cage bottom. The animal's forelimbs were allowed full access to the entire cage bottom. The body weight of each animal was carefully monitored throughout the study.

Electrical MS Protocol

For the four experimental groups, dynamic MS was applied in conjunction with HLS for 4 weeks. Muscle contraction was induced with two needle-size electrodes (L-type gauge #3, Seirin, Weymouth, MA) under isoflurane anesthesia. One electrode was placed at the right lateral proximal quadriceps and the other was placed at the lateral distal quadriceps. The electrodes were then connected to a 100MHz arbitrary waveform generator (Model 395, Wavetek) to transmit a 1ms square pulse with various stimulation frequencies (1 Hz, 20 Hz, 50 Hz and 100 Hz) for 10 minutes per day, 5 days per week, for a total of 4 weeks (Figure 3.1). Control animals (age-matched and HLS) were also subjected to anesthesia for the same amount of time per day as the experimental animals to account for any potential effect due to isoflurane inhalation. A rest-insertion period (2seconds contraction followed by 8seconds rest) was added in the MS regimen to avoid muscle fatigue.

Microcomputed Tomography (μCT)

After 4 weeks of study, animals were euthanized, and the right hindlimbs were harvested and preserved in 70% ethanol. Using a high resolution μCT scanner (μCT-40, SCANCO Medical AG, Bassersdorf, Switzerland), the distal femur and the proximal tibia were scanned with a spatial resolution of 15 μm. All images were evaluated using Gaussian filter, with specific sigma, support and threshold values of 0.5, 1, and 347, respectively. Three consecutive 750 μm regions of trabecular bone (M1, M2 and M3) were analyzed in the distal metaphysis, immediately proximal to the growth plate (Figure

3.2a). M1 is the section closest to the diaphysis, M2 is the middle section between M1 and M3, and M3 is the section closest to the growth plate. One 750 μm region of trabecular bone was also analyzed in the distal epiphysis of each femur (Figure 3.2a). Two regions, 750 μm for metaphysis and 375 μm for epiphysis, were evaluated at the proximal tibia (Figure 3.2b). Values for bone volume fraction (BV/TV, given as %), connectivity density (Conn.D, $1/mm^3$), structural model index (SMI), trabecular number (Tb.N, 1/mm), thickness (Tb.Th, mm) and separation (Tb.Sp, mm) were evaluated for each region [109].

We had also analyzed the contralateral left femurs in the same fashion, as mentioned above. Despite there was a systematic effect of the stimulation to the left limbs, the outcomes of the left femurs were reported but were not used for comparison.

Static and Dynamic Histomorphometry

Two intraperitoneal injections of calcein (10mg/kg) were administered to each animal two and 16 days prior to euthanasia. After scanning with μCT, the distal portions of the femurs (10 mm) were cut and dehydrated with isopropanol. The samples were then infiltrated and embedded with mixture of methyl methacrylate, n-butyl phthalate, and benzoyl peroxide. Longitudinal slices were sectioned to 8 μm using a Leica 2165 microtome (Leica, Wetzlar, Germany). Histomorphometric measurements were made by tracing calcein labels in the trabecular bone at both metaphyseal and epiphyseal regions ($5mm^2$ and $3mm^2$ per section, respectively, 3 sections per bone), using the Osteomeasure software (OsteoMetrics Inc, Decatur, GA). Histomorphometric bone volume fraction (BV/TV – Histo, %), mineralizing surface (MS/BS, %), mineral apposition rate (MAR, μm/day), and bone formation rate (BFR/BS, $\mu m^3/\mu m^2/yr$) were determined [110].

Statistical Analyses

Results are reported as mean ± SD for body weight, μCT, and histomorphometric analyses. We used paired t-test to access the body weight differences at the beginning and the end of the study. For all measurements, significance differences between groups were determined using the SigmaStat 2.03 (Systat Software Inc, San Jose, CA). Analysis of variance (ANOVA) with Tukey's pairwise multiple comparison tests was performed on the μCT data with normal equal variance. For analysis at the distal femoral metaphysis region, two-way ANOVA was used, with the experimental groups and the various metaphyseal regions as the two factors. One-way ANOVA was applied for all other μCT and histomorphometric data. The level of significance was established at $p < 0.05$.

Results

Body weight

Throughout the entire experimental period, the animals' body weight was monitored. The body weights were not significantly different between groups at the beginning of the study, with an average of 320g ± 47g. Age-matched control animals were able to maintain a steady body weight throughout the study, with only a -0.15% difference between the start and end date. Animals subjected to 4-week functional disuse lost a significant amount of body mass. These weight reductions were similar in HLS and HLS+MS groups, with -10% for HLS ($p < 0.05$), -8% for 1 Hz ($p = 0.07$), -9% for 20 Hz ($p < 0.05$), -11% for 50 Hz ($p < 0.01$) and -8% for ($p = 0.09$).

μCT – Femur M1 region

M1 is the distal metaphyseal region 1.5 mm above the growth plate (Figure 3.3). The lack of weight-bearing activity for 4 weeks significantly reduced trabecular bone quantity and quality, demonstrated by a 70% decreases in BV/TV, an 86% decrease in Conn.D, a 28% decrease in Tb.N, a 57% increases in SMI, and a 43% increase in Tb.Sp compared with baseline ($p < 0.001$). Similar results were observed when compared with age-matched control ($p < 0.001$); decreases in BV/TV (66%) , Conn.D (86%) and Tb.N (26%), as well as increases in SMI (39%), and Tb.Sp (39%) were observed. Trabecular BV/TV in electrically stimulated animals was significantly greater than that of disused bone. Animals with MS at 20 Hz and 50 Hz showed an increase in BV/TV by 143% ($p < 0.05$) and 147% ($p < 0.01$), respectively. Stimulation at 100 Hz showed an 86% increase in BV/TV, but this change was not statistically different from the HLS group. The other outcome measures of Conn.D, Tb.N and Tb.Sp were also significantly affected by MS at 20 Hz, 50 Hz and 100 Hz frequencies. There were up to 600% and 38% increases for Conn.D and Tb.N, and up to a 36% decrease for trabecular separation (20 Hz $p < 0.01$, 50 Hz $p < 0.001$ and 100 Hz $p < 0.05$). SMI and Tb.Th were not affected by the stimulus, regardless of its frequency. The animals subjected to 4 weeks of 1 Hz MS showed the same level of bone loss and structural deterioration as did the HLS animals without MS.

As for the contralateral left femur, the values of BV/TV were 0.17 ± 5%, 0.16 ± 4%, 0.05 ± 4%, 0.05 ± 5%, 0.12 ± 7%, 0.13 ± 2%, and 0.09 ± 4% for baseline, age-matched, HLS, 1, 20, 50, and 100 Hz, respectively. Likewise, the values of Tb.N were 3.7 ± 0.5, 3.6 ± 0.5, 2.6 ± 0.4, 2.6 ± 0.4, 3.3 ± 0.6, 3.5 ± 0.3, and 3.1 ± 0.6, respectively. Similar results were observed for Conn.D and Tb.Sp.

μCT – Femur M2 region

M2, the distal metaphyseal region 750 μm above the growth plate, is a region with a moderate amount of trabecular bone under normal condition (Figure 3.4). Four weeks of unloading with no MS and 1 Hz MS demonstrated significant trabecular bone loss. Compared with controls, HLS animals experienced -54% for BV/TV, -77% for Conn.D, -29% for Tb.N and +45% for Tb.Sp (all $p < 0.001$). In this region, 50 Hz MS was the only stimulation that showed positive statistically significant effects in all measured indices against functional disuse, with increased BV/TV (66%; $p < 0.05$), Conn.D (371%; $p < 0.001$), and Tb.N (41%; $p < 0.001$), and reduced Tb.Sp (31%; $p < 0.001$). The changes in trabecular bone parameters observed with 20 Hz and 100 Hz stimulations had a trend similar to those of the 50 Hz MS, but with smaller percentage differences (up to +48% for BV/TV, +241% Conn.D, +29% Tb.N, and -23% Tb.Sp).

As for the contralateral left femur, the values of BV/TV were 0.24 ± 5%, 0.22 ± 4%, 0.11 ± 5%, 0.09 ± 7%, 0.17 ± 8%, 0.18 ± 3%, and 0.12 ± 4% for baseline, age-matched, HLS, 1, 20, 50, and 100 Hz, respectively. Likewise, the values of Tb.N were 4.1 ± 0.5, 4.2 ± 0.5, 2.9 ± 0.4, 3.2 ± 0.4, 3.9 ± 0.7, 4.0 ± 0.3, and 3.6 ± 0.5, respectively.

μCT – Femur M3 region

M3, the distal metaphyseal portion directly above the growth plate, is a region with the most abundant trabecular network with 0.3±0.05 BV/TV and 4.72±0.64 Tb.N (Figure 3.5). Disuse induced a 38% bone loss, 75% decrease in Conn.D, 30% reduction in Tb.N and 43% more spacing within this region. Similar to the results reported for the M2 portion, 50 Hz MS resulted in the greatest preventive effects against disuse osteopenia, with increased BV/TV (40%; $p < 0.05$), Conn.D (305%; $p < 0.001$), and Tb.N (41%; $p < 0.001$), and reduced Tb.Sp (31%; $p < 0.001$). While BV/TV was not

significantly altered by MS at 20 Hz (+26%) and 100 Hz (+20%), trabecular qualities, Conn.D, Tb.N and Tb.Sp, were improved (up to 226%, 28% and 24% respectively, $p < 0.001$). Like the other metaphyseal regions, SMI and Tb.Th were not affected by the stimulation.

Similar to the M1 and M2 regions, the BV/TV values, of the contralateral left femur, were 0.30 ± 5%, 0.27 ± 5%, 0.17 ± 6%, 0.14 ± 8%, 0.22 ± 8%, 0.22 ± 4%, and 0.18 ± 5% for baseline, age-matched, HLS, 1, 20, 50, and 100 Hz, respectively. Likewise, the values for Tb.N were 4.8 ± 0.6, 4.7 ± 0.7, 3.3 ± 0.4, 3.4 ± 0.7, 4.4 ± 0.8, 4.4 ± 0.5, and 3.1 ± 0.6, respectively.

μCT – Differences between metaphyseal regions

Figure 3.6 summarizes the levels of changes in BV/TV and Conn.D in electrically stimulated experimental animals compared with those of disused bone in unstimulated animals at the three metaphyseal regions. With the exception of 1 Hz, stimulation frequencies at 20 Hz, 50 Hz, and 100 Hz had greater effects on the trabecular bone 2.25 cm away from the growth plate, closer to the diaphysis. With MS at 50 Hz, the percent changes at M1 were significantly different from those measured at M2 and M3 for BV/TV (both, $p < 0.001$) and from those measured at M3 for Conn.D only ($p < 0.05$). Also, BV/TV inhibition at M1 was significantly higher ($p < 0.05$) than that of M3 with 20 Hz MS. Although following a trend similar to that of the above indices, at 50 Hz and 20 Hz MS, the percent changes of the μCT measurements were not statistically significant between the three metaphyseal regions.

μCT – Femur E region

The epiphyseal trabecular bone was not significantly affected by the 4-week HLS. The percentage changes were minor versus the metaphyseal regions, with -5% BV/TV, -44% Conn.D, -7% Tb.N, and +4% Tb.Sp. In this region, MS did not induce any measurable effect on bone volume and trabecular integrity at any stimulation frequency. All stimulated values were comparable to age-matched and HLS animals, with up to 10% greater in BV/TV, 8% greater in Tb.N, and a 9% reduction in Tb.Sp. These changes were not statistically significant.

μCT – Tibia M region

Four weeks of functional disuse reduced trabecular BV/TV by 25%, Conn.D by 54% ($p < 0.05$), Tb.N by 9%, and increased Tb.Sp by 107% ($p < 0.05$) (Table 3.1). Trabecular bone loss was inhibited by 24% with MS at 50 Hz. Comparing to the HLS control, the 50 Hz stimulation improved bone quality by maintaining Conn.D by +129% ($p < 0.05$), Tb.N by +30%, and Tb.Sp by -21% ($p < 0.01$). MS at 20 Hz and 100 Hz also showed effects to the trabecular network, but these changes were not statistically different from the HLS group. Similar to the results from the distal femur, MS at 1 Hz was not able to prevent bone loss and maintain the trabecular structure.

μCT – Tibia E region

Comparing to normal animals, HLS significantly lowered BV/TV by up to 18%, Conn.D up to 34%, Tb.N up to 24%, and increased marrow spacing by up to 29% ($p < 0.05$ for all) (Table 3.1). Trabecular BV/TV in electrically stimulated animals was significantly greater than that of disused bone. Animals with MS at 20 Hz, 50 Hz, and 100 Hz showed an increase in BV/TV by 20%, 19%, and 31% ($p < 0.05$), respectively. MS at those frequencies also significantly inhibited trabecular bone deterioration, with

higher values in Conn.D (up to 71%, $p < 0.01$), Tb.N (up to 33%, $p < 0.01$), and a decrease for Tb.Sp (up to 30%, $p < 0.01$) against disuse. Like other regions, 1 Hz MS showed similar degree of bone loss and structural deterioration as did the HLS animals. Furthermore, Tb.N and Tb.Sp measured from stimulated femur at 20 Hz, 50 Hz, and 100 Hz were also significantly different than those measured from 1 Hz.

Static and Dynamic Histomorphometry

In the metaphyseal trabecular bone, BV/TV measured by the 2-D histomorphometric method, was 44% lower in HLS group than in age-matched controls ($p < 0.001$). Using the Pearson Product Moment Correlation (SigmaStat 2.03, CA), this result was correlated with the BV/TV values from the μCT analysis of the M2 region, giving an R^2 value of 0.84 ($p < 0.05$). In other bone formation indices, HLS animals also showed significant decline in MS/BS (76%, $p < 0.001$), MAR (80%, $p < 0.01$) and BFR/BS (88%, $p < 0.01$). As expected, 1 Hz MS showed no ameliorative effect. Electrical stimulation at 20 Hz, 50 Hz and 100 Hz demonstrated slight enhancement on these indices during the 4-week disuse, yet the amount of label in the trabecular bone was still far from that in the aged-matched control. MS at 50 Hz resulted in the greatest percentage increases in bone histomorphometry indices compared with those in unstimulated HLS: 54% for MS/BS, 150% for MAR and 60% for BFR/BS. However, these differences were not statistically significant between the HLS and experimental animals due to the high variability between animals (Table 3.2). Disuse had an insignificant effect on the trabecular BV/TV (-10%), similar to the results of the μCT analysis of the epiphyseal region. Bone formation indices were reduced due to HLS

(54% for MS/BS, 150% for MAR and 60% for BFR/BS), and daily MS failed to prevent such reduction of bone formation activity.

Discussion

The data strongly indicated that dynamic electrical stimulation was able to inhibit bone loss and trabecular architectural deterioration caused by a lack of daily weight-bearing activity. The importance of selecting an effective loading regimen was investigated in this study, in which a wide range of stimulation frequency was tested to determine its effects on skeletal adaptive responses. Throughout this study, we have referred to 1 Hz as low-frequency, 20 Hz and 50 Hz as mid-frequency, and 100 Hz as high-frequency.

From our results, we concluded that the effectiveness of dynamic MS was greatly dependent on the stimulation frequency. In addition, the degree of effectiveness varied in different regions of the distal femur. While low-frequency MS was unsuccessful in preventing osteopenia, mid-frequency MS applied to the quadriceps was able to maintain trabecular bone mass. In this study, 4 weeks of functional disuse significantly reduced the metaphyseal bone volume fraction, mainly via a decrease in trabecular number, thereby reducing its connectivity and augmenting the marrow space. Dynamic MS at the mid-frequency range mediated bone remodeling process to preserve bone mass, trabecular number, and connectivity. Although the changes in bone formation indices were not statistically significant, increases in MAR and BFR were quite promising. The partial enhancement of bone formation may not fully explain our results; bone volume and structures in the metaphyseal regions were maintained at a level similar to that of age-matched controls.

One limitation of our study is that we did not examine bone resorption, which may play a crucial component in regulating skeletal adaptation induced by MS. Our methodology in e*x vivo* processing of the femurs precluded analysis of tartrate-resistant acid phosphatase as a marker of bone resorptive process; hence, resorption analysis will be the focus for future experiments.

The nonlinear relationship between femoral strain measured at the mid-diaphysis, and MS applied at various frequencies was previously examined by our lab. Electrical muscle contraction produced longitudinal surface strain of ~60 με at 1 Hz, ~80 με at 20 Hz, and below 20 με at 50 Hz and 100 Hz. Stimulation frequency at 10 Hz induced peak strain of ~125 με. It has been hypothesized that strain information integrates over time [79], suggesting that low-level mechanical strain induced by mid-frequency electrical MS may dominate in the skeleton, and initiate osteogenic activities. In response to a mechanical stimulus, bone cells have been shown to proliferate and to secrete extracellular matrix. In addition, mechanotransduction induces biochemical signal cascades, including those that produce hormones and growth factors, which in turn affect the coupled processes of formation and resorption [102, 111-113].

Previous experiments, using an 8 weeks disused turkey ulna model, demonstrated that a low strain magnitude (100 με) with high loading cycle number (108,000) was sufficient to maintain cortical bone mass [68]. Here, our 50 Hz and 100 Hz MS, which both induced extremely low-magnitude microstrain and displayed protective effects against disuse osteopenia, delivered only 6,000 and 12,000 daily pulses, respectively, to the skeletal muscle. MS of 50 Hz or100 Hz generates tetanic muscle contraction, in which summation of subsequent stimuli occurs and skeletal muscles are not allowed to relax

during stimulation. During induced tetanic contraction of the quadriceps, the femurs may be subjected to maximal dynamic compressive loading creating the measurable low-magnitude bone strain. Other studies with low-magnitude stimulus, e.g., vibration, have also been shown to enhance bone morphology, promote bone formation, and increase bone strength [107, 114, 115]. An important conclusion from these experiments is that small strain, e.g., induced by muscle contraction, might be one of the key determinants in regulating skeletal adaptation.

Although there were no statistical differences between the 20 Hz, 50 Hz, and 100 Hz experimental groups, our data indicated that mid-frequency MS resulted in greater percentage changes in all bone quantity and quality indices. In addition to bone strain, another factor involved in mediating bone remodeling is bone fluid flow induced by intramedullary pressure (ImP) [116]. Similar to the strain profile, dynamic electrical muscle contraction also yielded a nonlinear ImP distribution. Under normal conditions, a rat's blood pressure produces ImP of up to 5 mmHg. In the presence of MS, femur ImP at the mid-diaphysis was measured to be 18 mmHg at 1 Hz, peak 45 mmHg at 20 Hz, 20 mmHg at 50 Hz and 4 mmHg at 100 Hz. For MS with mid to high stimulation frequencies, the effect on trabecular bone was always greater at M1, closer to the mid-diaphysis. This suggests that there may be an ImP gradient, perhaps generated by the induced muscle contraction, influencing the magnitude of mechanotransductory signals on the trabecular bone at the different regions.

Previous ImP measurement in mice showed a 23% drop in ImP upon HLS, indicate a decrease in interstitial fluid flow via the cortex [117]. On the contrary, increasing the pressure gradient in HLS animals via venous ligation was able to compensate such drop in

ImP [117]. *In vivo* fluid pressure measurements have investigated the close relationship between loading frequency and fluid flow regulation in bone, where 20-50 Hz stimulation could initiate anabolic activities [116, 118]. In the absence of matrix deformation, an increase in ImP induced by direct manipulation of marrow cavity was able to inhibit resorption related to disuse by osteotomy [65]. These observations clearly pointed out that fluid flow can be altered by both ImP and bone strain.

In addition, changes in the fluid environments i.e., pressure gradient and shear stress, have the potential to modulate bone remodeling via autocrine and paracrine signaling cascades, e.g., nitric oxide and prostaglandins [101, 117, 119]. With 50 Hz MS, bone cells on the trabecular surface may sense the 4-fold increase of ImP, accompanying with the low-magnitude strain (< 20 με), thereby activating mechanotransduction and increasing the transport of nutrients and other signaling molecules within the tissues.

Both strain and ImP have the potentials to induce bone fluid flow, thus mediating adaptive responses in the trabecular bone. Another limitation of this presented study was that by using MS, we were unable to isolate the two main fluid flow inducing factors using MS. In order to investigate the influence of MS-induced ImP, a more invasive experimental design is required to eliminate the matrix deformation, in which muscle bundles might be disrupted or damaged in process. In our system to examine the effects of dynamic electrical contraction in a functional disuse model, MS was delivered to the quadriceps muscles in an extremely minimal invasive manner, as the key concept in translational research. The stimulation frequencies were chosen so that different combinations of strain and ImP would be achieved via electrically induced muscle contraction.

The interactive relationships between muscle and bone adaptations are not fully understood. It is clear that MS promotes blood flow, yet the mechanism remains highly controversial. One theory (muscle pump), suggests that at the onset of muscle contraction, veins within skeletal muscle are compressed thus increasing the arteriovenous pressure gradient and promoting blood flow to the vascular bed [74, 120, 121]. The pressure gradient in the muscle vasculature may be relayed to the nutrient vessels in bone and further increasing ImP and inducing fluid flow in bone [64]. Alternatively, vasodilation, with an onset of 5-20 seconds, might also play a role in the rapid release of metabolites, contributing to the initial blood flow response to tetanic MS [73, 90]. Aside from avoiding muscle fatigue, the pattern of 2 seconds stimulation with 8s seconds rest inserted into our loading regimen was designed to address both theories, attempting to maximize the fluid perfusion and nutrient delivery to the musculoskeletal tissues. Further investigations will concentrate on characterizing the effects of frequency-specific MS on muscular morphology and its vasculature, and exploring other mechanical parameters to optimize the dynamic MS regimen.

It is important to note that microgravity and functional disuse affect both muscle and bone. The potential of electrical muscle stimulation in reducing sacropenia and osteopenia would be an ideal clinical intervention. The main objective of this study is to demonstrate that dynamic MS can prevent osteopenia in addition to sacropenia as reported by other investigators. Furthermore, the skeletal adaptive responses induced by MS are highly depended on its stimulation frequency. Although we evaluated only indices of bone formation, it is likely that inhibition of bone resorption activity is also contributory to the observed effects. The findings from this study may assist in

development of future clinical interventions and beneficial to future countermeasure for disuse osteoporosis.

Figures and Tables

Figure 3.1

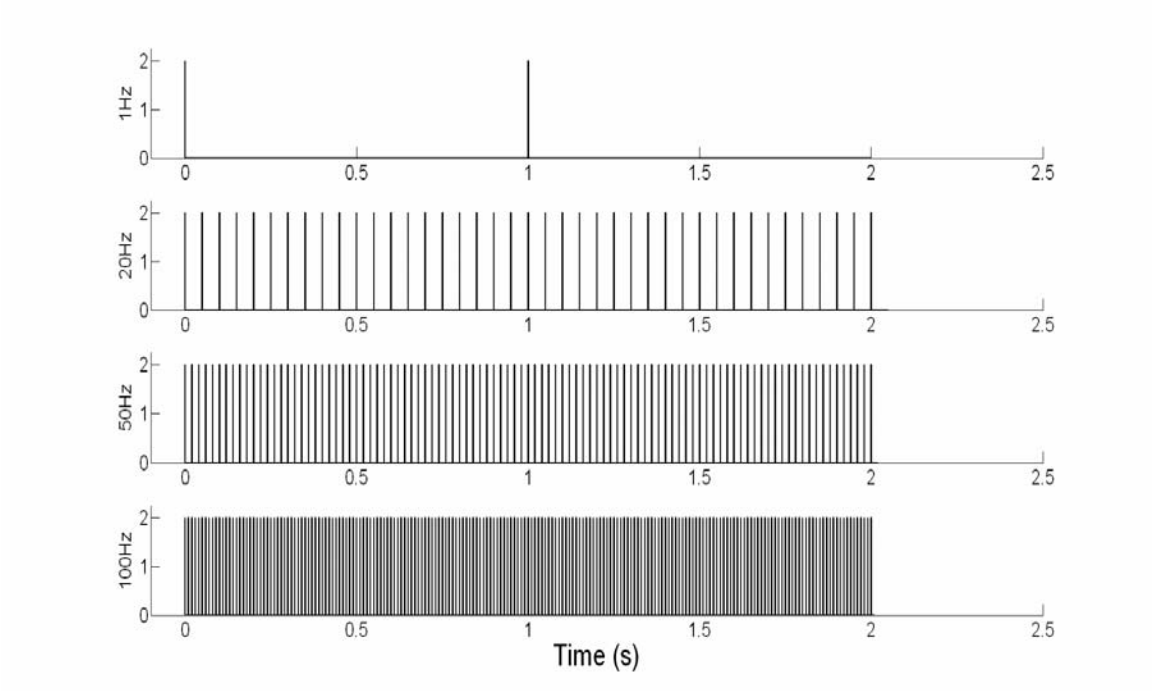

Electrical MS was applied with a 100MHz arbitrary waveform generator to transmit a 1ms square pulse with at stimulation frequency of 1 Hz, 20 Hz, 50 Hz or 100 Hz for 10 minutes/day, 5 days/week, for a total of 4 weeks. Within the daily 10 minutes period, muscle contraction was induced for 2 seconds followed by 8 seconds of relaxation to avoid fatigue.

Figure 3.2

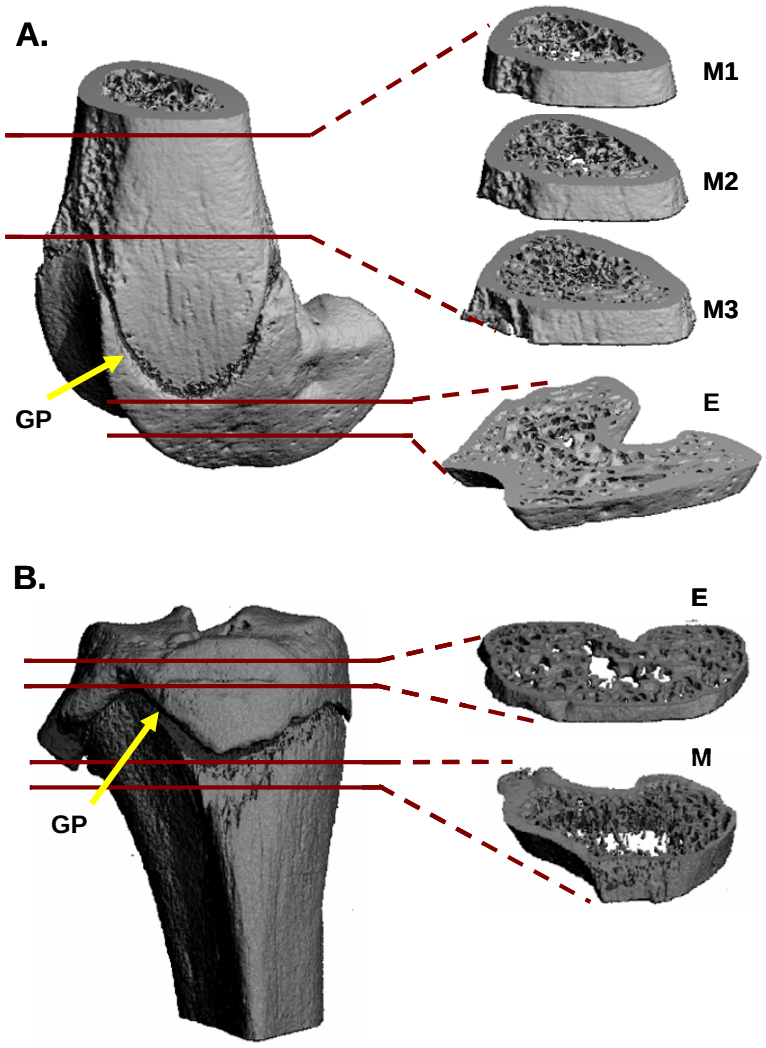

Trabecular bone at three metaphyseal sections and one epiphyseal region of the distal femurs was evaluated using microcomputed tomography. GP = growth plate (arrow) ; M = metaphysis; E = epiphysis.

Figure 3.3

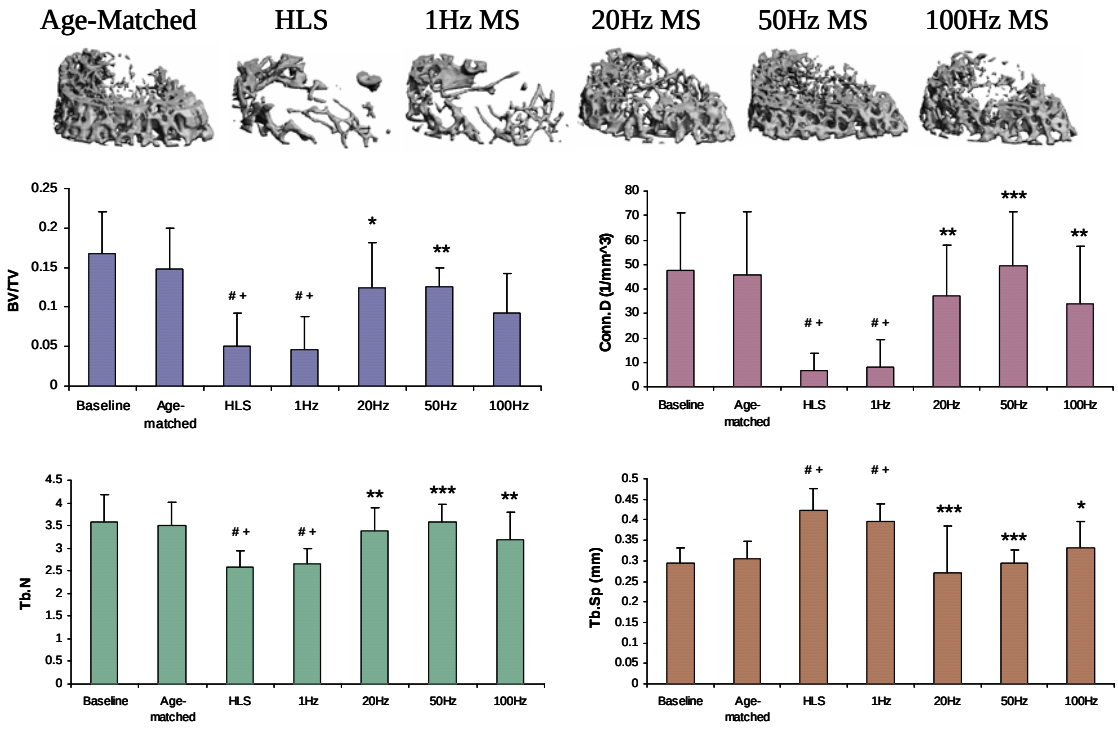

Representative 3D μCT images of trabecular bone in the M1 region (750 μm, closest to femoral diaphysis). Graphs show mean + SD values for bone volume fraction (BV/TV, %), connectivity density (Conn.D, 1/mm^3), trabecular number (Tb.N, 1/mm), and separation (Tb.Sp, mm) at the M1 region. MS at 50 Hz produced a significant change in all indices, compared with values obtained in 4-week HLS. $^{\#}$ p <0.001 vs. baseline; $^{+}$ p <0.001 vs. age-matched; * p <0.05 vs. HLS; ** p <0.01 vs. HLS; *** p <0.001 vs. HLS.

Figure 3.4

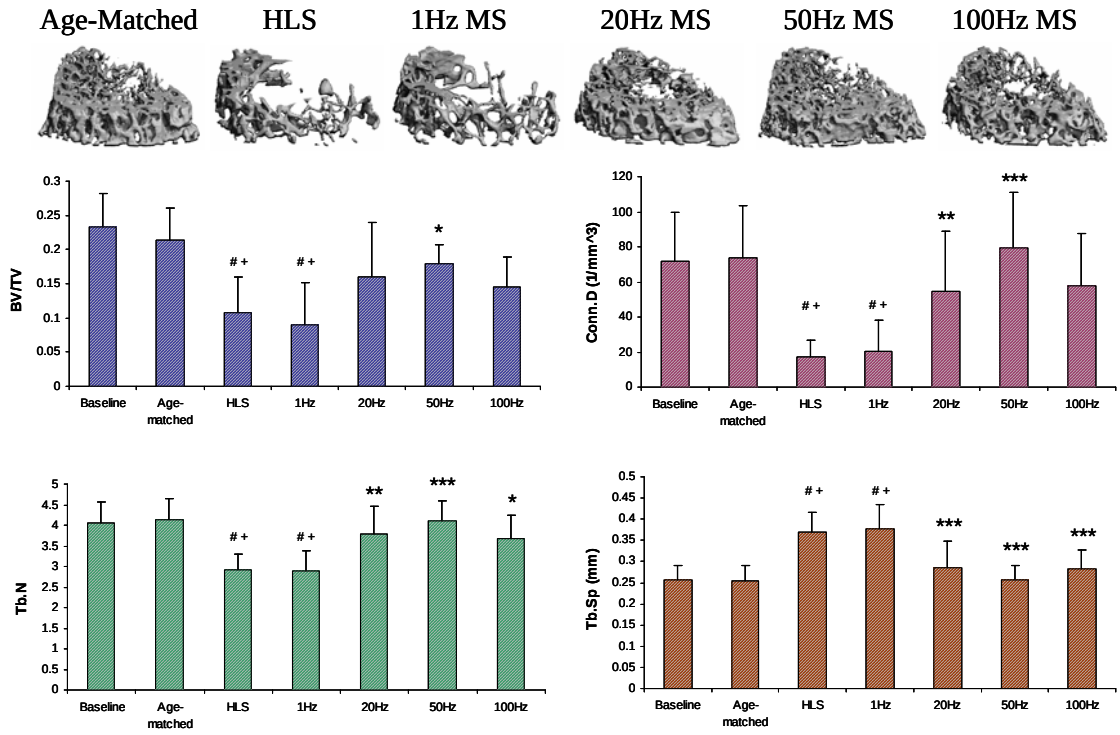

Representative 3D μCT images of trabecular bone in the M2 region (750 μm, in between M1 and M3, 750 μm above the growth plate). Graphs show mean + SD values for bone volume fraction (BV/TV, %), connectivity density (Conn.D, 1/mm^3), trabecular number (Tb.N, 1/mm), and separation (Tb.Sp, mm) at the M2 region. Only 50 Hz MS showed significant effects for all indices against 4-week HLS. $^{\#}$ p <0.001 vs. baseline; $^{+}$ p <0.001 vs. age-matched; * p <0.05 vs. HLS; ** p <0.01 vs. HLS; *** p <0.001 vs. HLS.

Figure 3.5

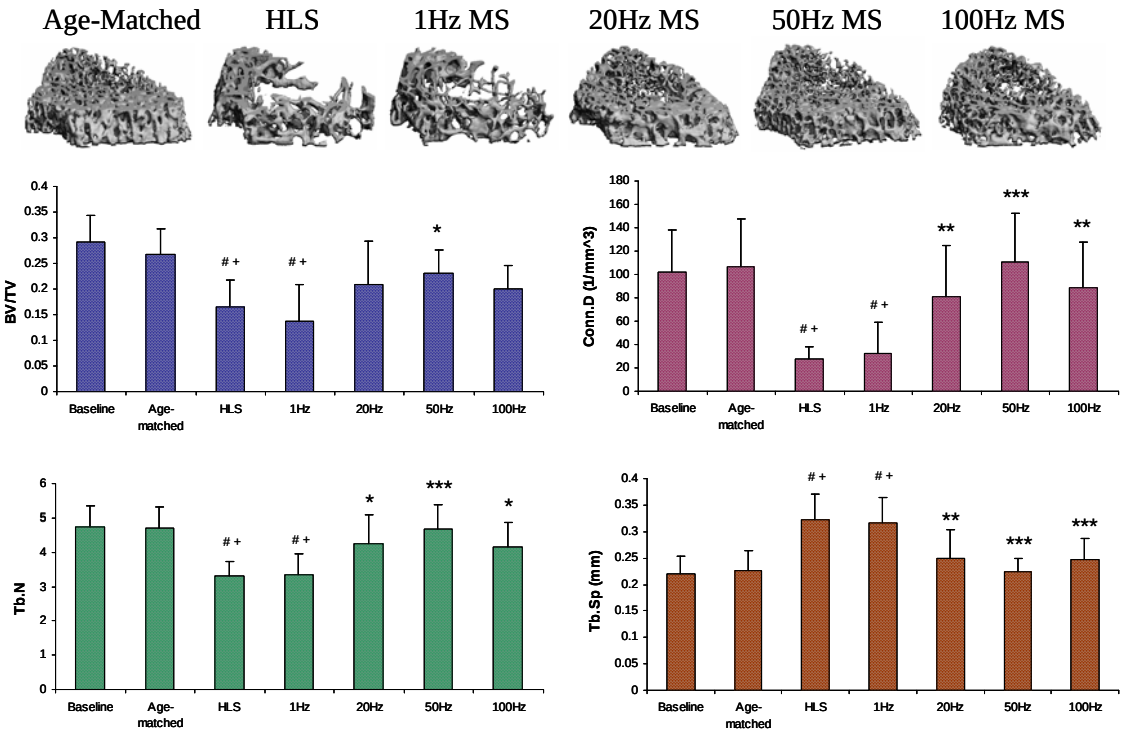

Representative 3D μCT images of trabecular bone in the M3 region (750 μm, immediately above the growth plate). Graphs show mean + SD values for bone volume fraction (BV/TV, %), connectivity density (Conn.D, 1/mm^3), trabecular number (Tb.N, 1/mm), and separation (Tb.Sp, mm) at the M3 region. Only 50 Hz MS demonstrated significant preventive effects for all indices against 4-week HLS. $^{\#}$ p <0.001 vs. baseline; $^{+}$ p <0.001 vs. age-matched; * p <0.05 vs. HLS; ** p <0.01 vs. HLS; *** p <0.001 vs. HLS.

Figure 3.6

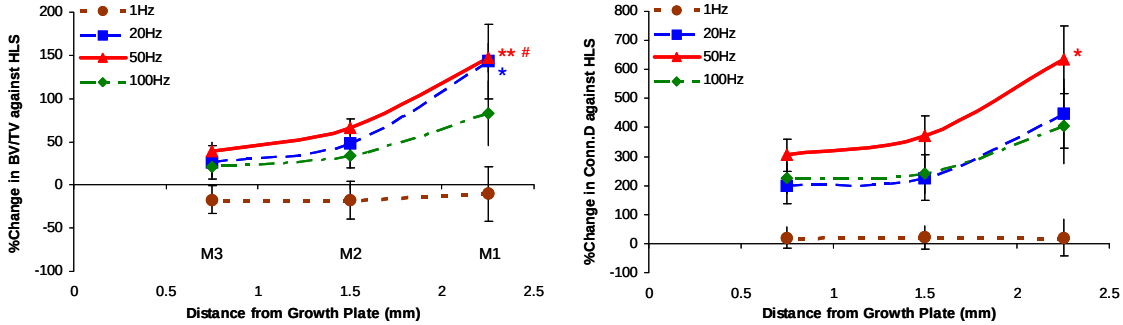

Graphs show the percentage differences between HLS and MS experimental groups ± SD values in all three metaphyseal regions for bone volume fraction (BV/TV) and connectivity density (Conn.D). For MS with mid to high stimulation frequencies, the levels of effectiveness on trabecular bone against functional disuse alone were always greatest at M1 and least at M3. ** p <0.001 vs. M3; * p <0.05 vs. M3; $^{\#}$ p <0.001 vs. M2.

Table 3.1. μCT Analysis of Proximal Tibia.

	Baseline	Age-matched	HLS	1 Hz	20 Hz	50 Hz	100 Hz
Metaphysis							
BV/TV (%)	0.17 ±0.06	0.19 ±0.07	0.14 ±0.07	0.11 ±0.05	0.14 ±0.09	0.17 ±0.06	0.13 ±0.04
Conn.D ($1/mm^3$)	36.9 ±21.2	45.0 ±25.7	20.6 ±16.6 [a]	14.4 ±8.45	41.3 ±33.8	47.4 ±19.1 [* #]	38.3 ±11.8
Tb.N (1/mm)	2.97 ±0.73	2.93 ±0.96	2.67 ±0.35	2.88 ±0.49	3.39 ±0.64	3.46 ±0.60	3.22 ±0.23
Tb.Sp (mm)	0.22 ±0.05	0.19 ±0.08	0.40 ±0.06 [ab]	0.35 ±0.07 [ab]	0.32 ±0.05	0.32 ±0.07 [**]	0.32 ±0.03
Epiphysis							
BV/TV (%)	0.42 ±0.04	0.42 ±0.02	0.34 ±0.03 [ab]	0.35 ±0.09	0.41 ±0.11 [*]	0.40 ±0.04 [*]	0.45 ±0.06 [*]
Conn.D ($1/mm^3$)	47.0 ±7.90	41.4 ±12.9	30.9 ±12.4 [a]	32.1 ±7.99	38.8 ±2.03	52.9 ±11.4 [** # +]	40.8 ±5.50
Tb.N (1/mm)	6.92 ±0.17	6.67 ±0.09	5.24 ±0.21 [ab]	5.15 ±0.33 [ab]	6.99 ±0.22 [** #]	6.83 ±0.15 [** #]	6.87 ±0.29 [** #]
Tb.Sp (mm)	0.17 ±0.01	0.18 ±0.01	0.22 ±0.01 [ab]	0.23 ±0.02 [ab]	0.17 ±0.02 [** #]	0.16 ±0.01 [** #]	0.15 ±0.03 [** #]

Values are mean ± SD for bone volume fraction (BV/TV, %), connectivity density (Conn.D, $1/mm^3$), trabecular number (Tb.N, 1/mm), and separation (Tb.Sp, mm) at the M3 region. Only 50 Hz MS demonstrated significant preventive effects against 4-week HLS at both metaphysis and epiphysis regions of the proximal tibia. [b] p <0.05 vs. baseline; [a] p <0.05 vs. age-matched; [*] p <0.05 vs. HLS; [**] p <0.01 vs. HLS; [#] p <0.05 vs. 1 Hz MS.

Table 3.2. Distal femur metaphysis histomorphometry.

	Control	HLS	1 Hz	20 Hz	50 Hz	100 Hz
BV/TV - Histo (%)	41.1±8.4	22.9±7.6 **	24.2±4.8 *	30.2±13 *	31.0±2.9 *	29.4±7.9 *
MS/BS (%)	8.9±5.3	2.2±2.0 **	1.4±1.7 **	2.3±1.6	3.4±2.3	2.5±1.6
MAR (μm/day)	1.2±0.5	0.2±0.2 *	0.1±0.1 **	0.6±0.3	0.6±0.3	0.5±0.3
BFR/BS ($\mu m^3/\mu m^2/yr$)	41.0±25	0.1±6.9 *	1.7±1.7 *	7.3±5.6	8.2±5.9	8.1±6.8

Values are mean ± SD. BV/TV, bone volume/tissue volume; MS/BS, mineralized surface/bone surface; MAR, mineral apposition rate; BFR/BS, bone formation rate/bone surface. * p <0.05, ** p <0.01 vs. age-matched.

IV. Alteration of Contraction-to-Rest Ratio to Optimize Trabecular Bone Response Induced by Muscle Stimulation

Abstract

Dynamic electrical muscle stimulation as a preventive countermeasure for disuse osteopenia has shown to be successful. The degree of inhibition of trabecular bone loss and deterioration of its microarchitecture depends on the stimulation parameters within the regimen. The objective of this study was to determine whether the contraction-to-rest ratio is an important parameter to affect the skeletal adaptive responses under a functional disuse environment. Fifty-six skeletally matured Sprague-Dawley rats were divided into seven groups for the 4-week experiment: baseline control, age-matched control, hindlimb suspended (HLS), and HLS plus muscle stimulation with a contraction-to-rest ratio of 1/4, 2/8, 4/6, and 2/28. Muscle stimulation was carried out for 10 minutes per day for 5 days per week, for 4 weeks. Trabecular bones at the distal femurs and proximal tibia were analyzed with microcomputed tomography and histomorphometry methods. HLS alone for 4-week resulted in a 25 – 45% trabecular bone loss at the distal femur and 10 – 25% at the proximal tibia. Dynamic muscle stimulation, applied at 50 Hz frequency, with a 2/8 contraction-to-rest ratio demonstrated significant inhibition of trabecular bone loss against the 4 weeks disuse, with up to +74% in bone volume fraction, +164% in connectivity, +20% in trabecular number, and -18% in spacing ($p < 0.05$). Stimulation with 1/4 and 4/6 also showed similar effects but with a lesser percentage differences when comparing to the HLS animals. Similarly, histomorphometric analysis showed partial enhancement in mineralizing surface and mineral apposition rate. The results from this study confirm the potentials of dynamic muscle contraction in regulating skeletal adaptive responses and illustrated the importance of the contraction-to-rest ratio for future study.

Introduction

Musculoskeletal traumas, i.e., spinal cord injury and fracture, can impose short- and long-term consequences to bone. Significant amount of bone mineral density (BMD) reduction at the lower extremities has been reported in numerous studies [41, 42, 122]. Following acute spinal cord injury (< 6 months), BMD was reduced by 17 to 25% at various sites. In addition to bone loss, such injuries can alter bone microarchitecture and increase lower extremity fracture incidence by 1 to 34% [16, 40-42, 122-124]. Therefore, successful interventions are necessary to prevent osteopenia and subsequent complications.

With the exposure to daily activities, bone experiences repetitive bouts of mechanical loading. Under disuse condition, due to injury or paralysis, external mechanical stimulus applied to bone has the potential to induce remodeling [77, 125, 126]. Many in vivo studies have determined parameters, such as frequency, strain magnitude, strain history, and fluid pressure, within stimulation regimens to be influential to bone adaptation [79, 127-129]. The concept of inserting rest period has recently shown to enhance osteogenesis. Short rest duration, e.g., 10 seconds, inserted into a low frequency loading regime augmented anabolic response at the periosteal surfaces of isolated avian ulnae [130]. Even with a 10-fold decreased in cycle numbers, rest period implemented into a high frequency signal significantly increased the bone formation rate of immobilized tibia [131]. These stimuli applied direct loading to the skeleton, generating bone strain on the order of 1000με. It is thought that insertion of rest period

improves osteogenic responses by avoiding mechanosensitivity saturation in bone tissue [132].

We have previously demonstrated that dynamic electrical muscle contraction has anti-catabolic effect on disused skeleton [133]. In particular, the level of osteopenic inhibition is depended on the stimulation frequency. Whether inserting rest period into muscle stimulation (MS) regimen, with a specific frequency, can optimize bone's adaptive response remains uncertain. Another factor to be considered is the fluid flow induced by MS [73, 134, 135]. The contraction of skeletal muscle generates an intramuscular pressure gradient and increases venous circulation. Once relax, intramuscular flows restore. The duration of the contraction and relaxation may partially regulate the mean muscle flow rate and subsequently affects the fluid flow to the skeleton [89]. It has been shown that hindlimb suspension in rodents significantly reduced the intramedullary pressure (ImP) gradient and implied the decrease of interstitial fluid flow in bone [117]. On the contrary, dynamic MS, applied at mid-stimulation frequency, significantly increased the ImP [92].

Given that dynamic MS can prevent osteopenia and the promising results from various rest insertion studies, altering the contraction-to-rest (C-R) ratio may enhance fluid perfusion in skeletal muscle and further drive fluid flow to bone. Here, we hypothesized that the C-R ratio is a critical parameter within the MS regimen. Its alteration can optimize the inhibition of trabecular bone loss and deterioration induced by the lack of weight bearing activity.

Materials and methods

Experimental Design

All experimental procedures were approved by the Laboratory Animal Use Committee at Stony Brook University. Fifty-six 6-months-old female Sprague-Dawley retired breeder rats (Taconic, NY) were used to investigate the effects in varying the C-R ratio of dynamic muscle stimulation (MS) on skeletal adaptation under disuse environment. They were housed individually in 18”x18”x24” (LxWxH) stainless steel HLS cages in a temperature-controlled room with a 12:12 hour light:dark cycle, and were provided standard rodent chow and water ad libitum. Animals were transferred to these cages one week prior to the experiment start date in order to acclimate them to their environment. Animals were randomly assigned to seven groups with n=8 per group: (1) baseline control, (2) age-matched control, (3) HLS, (4) HLS+1/4 (1 sec contraction-to-4 sec rest) MS, (5) HLS+2/8 MS, (6) HLS+4/6 MS, and (7) HLS+2/28 MS. Functional disuse was induced by HLS. The description of the HLS setup was previously discussed in Chapter 1. The body weight of each animal was carefully monitored throughout the study.

Electrical MS Protocol

For the four experimental groups, dynamic MS was applied in conjunction with HLS for 4 weeks. Muscle contraction was induced with two needle-size electrodes (L-type gauge #3, Seirin, Weymouth, MA) under isoflurane anesthesia. One electrode was placed at the right lateral proximal quadriceps and the other was placed at the lateral distal quadriceps. The electrodes were then connected to a 100MHz arbitrary waveform generator (Model 395, Wavetek) to transmit a 1ms square pulse at a stimulation

frequency of 50 Hz for 10 minutes per day, 5 days per week, for a total of 4 weeks. The contraction was applied for either 1 sec with 4 sec rest, 2 sec with 8 sec rest, 4 sec with 6 sec rest, and 2 sec with 28 sec rest. All animals, including the control groups, were subjected to anesthesia for the same amount of time per day to account for any potential effect due to isoflurane inhalation.

Microcomputed Tomography (μCT)

After 4 weeks of study, animals were euthanized, and the right femurs were harvested and preserved in 70% ethanol. Using a high resolution μCT scanner (μCT-40, SCANCO Medical AG, Bassersdorf, Switzerland), the distal femur was scanned with a spatial resolution of 15 μm and the proximal tibia was scanned with a resolution of 30 μm. All images were evaluated using Gaussian filter, with specific sigma, support and threshold values of 0.5, 1, and 347, respectively. Three consecutive 750 μm regions of trabecular bone (M1, M2 and M3) were analyzed in the distal metaphysis, immediately proximal to the growth plate. M1 is the section closest to the diaphysis, M2 is the middle section between M1 and M3, and M3 is the section closest to the growth plate. One 750 μm region of trabecular bone was also analyzed in the distal epiphysis of each femur. Two regions, 1.5 mm for metaphysis and 450 μm for epiphysis, were evaluated at the proximal tibia. Values for bone volume fraction (BV/TV, given as %), connectivity density (Conn.D, $1/mm^3$), structural model index (SMI), trabecular number (Tb.N, 1/mm), thickness (Tb.Th, mm) and separation (Tb.Sp, mm) were evaluated for each region [109].

Static and Dynamic Histomorphometry

Two intraperitoneal injections of calcein (10mg/kg) were administered to each animal two and 16 days prior to euthanasia. After scanning with μCT, the distal portions of the femurs and the proximal tibia (10 mm) were cut and dehydrated with isopropanol. The samples were then infiltrated and embedded with mixture of methyl methacrylate, n-butyl phthalate, and benzoyl peroxide. Longitudinal slices were sectioned to 8 μm using a Leica 2165 microtome (Leica, Wetzlar, Germany). Histomorphometric measurements were made by tracing calcein labels in the trabecular bone at the metaphyseal region (3 sections per bone, $3mm^2$ per section), using the Osteomeasure software (OsteoMetrics Inc, Decatur, GA). Histomorphometric bone volume fraction (BV/TV – Histo, %), mineralizing surface (MS/BS, %), mineral apposition rate (MAR, μm/day), and bone formation rate (BFR/BS, $\mu m^3/\mu m^2/yr$) were determined [110].

Statistical Analyses

Results are reported as mean ± SD for body weight, μCT, and histomorphometric analyses. Paired t-test was used to evaluate the body weight changes at the beginning and the end of the study. For all measurements, significance differences between groups were determined using the SigmaStat 2.03 (Systat Software Inc, San Jose, CA). Analysis of variance (ANOVA) with Tukey's pairwise multiple comparison tests was performed on the μCT data with normal equal variance. For analysis at the distal femoral metaphysis region, two-way ANOVA was used, with the experimental groups and the various metaphyseal regions as the two factors. One-way ANOVA was applied for all other μCT and histomorphometric data. The level of significance was established at $p < 0.05$.

Results

Body weight

Animals' body weight was carefully monitored via the course of the 4 weeks study. The body weights were not significantly different between groups at the beginning of the study, with an average of 302g ± 30g. Age-matched control animals maintained a steady body weight throughout the experiment, with a -0.46% difference between the start and end date. Animals subjected to 4-week functional disuse experienced a significant body weight loss and that MS did not have an effect on the overall body mass. The weight reductions over the 4 weeks were 7% for the HLS control ($p < 0.05$), 1/4 MS ($p < 0.01$), and 2/8 MS ($p < 0.001$), 4/6 MS ($p < 0.001$), and 2/28 MS ($p < 0.001$).

μCT – Femur M1 region

M1 is the distal metaphyseal region 1.5 mm above the growth plate. Four weeks functional disuse significantly reduced demonstrated by a 46% decreases in BV/TV, a 51% decrease in Conn.D, a 12% decrease in Tb.N, a 23% increases in SMI, and a 13% increase in Tb.Sp compared with age-matched control ($p < 0.01$) (Figure 4.1). Similar results were observed when compared with baseline control ($p < 0.01$). MS with 2/8 C-R ratio showed the greatest prevention against disuse, with a 74% higher BV/TV ($p < 0.05$), 164% in Conn.D ($p < 0.01$), 20% in Tb.N ($p < 0.01$), and a reduction of 18% in Tb.Sp ($p < 0.01$). Statistically significance was also observed for the bone quality parameters between HLS and MS with 4/6 ratio, with +106% in Conn.D ($p < 0.01$), +17% in Tb.N ($p < 0.01$), and -14% in Tb.Sp ($p < 0.05$). Stimulation with 1/4 and 2/28 ratios displayed similar preventive trend for trabecular deterioration but the percentage changes compared to disuse were not as astounding as the effects seen with 2/8 C-R ratio.

μCT – Femur M2 region

M2 is the distal metaphyseal region 750 μm above the growth plate. The removal of daily activity to the hindlimbs generated a significant 35% of trabecular bone loss and compromised the structural network by decreasing the Conn.D by 43% and Tb.N by 17%, increasing SMI by 22% and Tb.Sp by 21%, $p < 0.01$ for all (Figure 4.2). Like other regions, Tb.Th was not altered by 4 weeks disuse or MS. Similar to M1, 50 Hz MS with 2/8 ratio was the only stimulation that demonstrated positive significant effects in all measured indices against functional disuse, with increased BV/TV (39%; $p < 0.05$), Conn.D (109%; $p < 0.01$), and Tb.N (23%; $p < 0.01$), and reduced Tb.Sp (20%; $p < 0.01$). The changes in trabecular bone parameters observed with 1/4 and 4/6 C-R ratios had a trend similar to those of the 2/8 ratio, but with smaller percentage differences, up to +28% for BV/TV, +78% Conn.D ($p < 0.01$), +20% Tb.N ($p < 0.05$), and -17% Tb.Sp ($p < 0.05$). MS with 2/28 ratio produced only minimal, not significant, effects to the trabecular bone in this region. Furthermore, the inhibition responses evaluated at M1 and M2 regions were compared and did not illustrate any significance differences for all the parameters.

μCT – Femur M3 region

M3 is the distal metaphyseal portion directly above the growth plate. This region had the most abundant trabecular network and the loss of bone due to disuse was significantly less than the loss measured in the M1 region ($p < 0.05$). In contrast to the M1 and M2 regions, MS also induced the least amount of changes on the trabecular bone in the region. Animals subjected to disuse alone experienced a 25% bone loss, 41% decrease in Conn.D, 15% reduction in Tb.N and 18% more spacing within this region (*p*

< 0.01) (Figure 4.3). Trabecular BV/TV was not significantly affected by the stimulation. However, 50 Hz MS with 1/4 and 2/8 C-R ratios maintained the trabecular structure, with as high as 64% and 19% enhancement in Conn.D and Tb.N, respectively, and 15% decline in the spacing ($p < 0.05$). Like the other metaphyseal regions, SMI and Tb.Th were not affected by the stimulation. The changes in BV/TV and Conn.D induced by MS in this metaphyseal region were significance difference than the effects observed in M1 ($p < 0.05$) but not in M2.

μCT – Femur E region

The epiphyseal trabecular bone was not affected by the 4-week HLS or MS, with BV/TV of 0.35 ± 0.06% for HLS and 0.32 ± 0.05% for MS groups. The percentage changes were minor versus the metaphyseal regions, with -1.2% BV/TV, -11% Conn.D, -4% Tb.N, and +6% Tb.Sp. MS did not induce any positive effect, regardless of the C-R ratio. All stimulated values were not significant and comparable to age-matched and HLS animals, with approximately 9% lower in BV/TV, 7% greater in Tb.N, and a 7% reduction in Tb.Sp.

μCT – Tibia M region

Four weeks of functional disuse reduced trabecular BV/TV by 25% ($p < 0.05$), Conn.D by 33% ($p < 0.05$), Tb.N by 7%, and increased Tb.Sp by 19% ($p < 0.05$) (Table 4.1). Trabecular bone loss was inhibited by 27%, 39% ($p < 0.05$), and 33% with MS with C-R ratio of 1/4, 2/8, and 4/6, respectively. Although most of the preventive outcomes induced by MS were not significantly difference, due to the high variability between animals, MS with the 1/4, 2/8, and 4/6 ratios still demonstrated improvement in bone quality by maintaining Conn.D by +24 to 44%, Tb.N by +13 to 18%, and Tb.Sp by -13 to

28%. The group subjected to 2/28 ratio MS was not able to prevent bone loss and maintain the trabecular structure in this region.

μCT – Tibia E region

HLS significantly reduced BV/TV by 10%, Conn.D by 14%, and Tb.N by 6% ($p < 0.05$ for all) (Table 4.1). Trabecular BV/TV was significantly greater in stimulated animals than that of the disused bone. Animals with the ratio of 2/8 and 4/6 MS showed an increase in BV/TV by 22% and 23% ($p < 0.05$), respectively. In this region, the changes for bone quality parameters were not statistically significance and were comparable to both HLS and age-matched controls.

Static and Dynamic Histomorphometry

Trabecular BV/TV-Histo, measured by the 2-D histomorphometric method, was 33% and 48% lower in HLS group than in age-matched controls ($p < 0.001$) at the metaphysis regions of femur and tibia, respectively (Table 4.2). For the other bone formation indices, HLS animals also showed significant decline in MS/BS (68 - 74%, $p < 0.01$), MAR (68 -71%, $p < 0.01$) and BFR/BS (83%, $p < 0.01$) in both areas. Similar to the μCT results, MS with 2/8 C-R ratio demonstrated positive protection on the histomorphometric indices during the 4-week disuse with an increase of 26% in BV/TV-Histo ($p < 0.05$), 142% in MS/BS ($p < 0.05$), 140% in MAR ($p < 0.05$) and 65% in BFR/BS. The tibia metaphyseal region also showed an increase of 77% in BV/TV-Histo ($p < 0.05$), 170% in MS/BS ($p < 0.05$), 43% in MAR and 61% in BFR/BS. In addition, MS with 1/4 and 4/6 ratios resulted in up to +130% for MS/BS, +88% for MAR, and 28% for BFR/BS at femur, and up to +115% for MS/BS, 33% for MAR and 21% for BFR/BS at tibia. The C-R ratio of 2/28 had the least effect in maintaining bone

formation. Comparing to the age-matched control, the histomorphometric values measured from the stimulated groups were still lower by 13 – 72% in MS/BS, 29 – 70% in MAR, and 70 – 87% in BFR/BS.

Discussion

The data from this study once again strongly signified that dynamic muscle stimulation has the potential to inhibit trabecular bone loss and architectural deterioration induced 4 weeks functional disuse. Previously in chapter 1, we demonstrated the importance in selecting the stimulation frequency within the regimen to affect the skeletal adaptive responses [133]. Here, we investigated another critical parameter, C-R ratio, in a frequency-specific MS regimen to potentially optimize the preventive measure against disuse. Our selection of the C-R ratios was based mainly on the number of individual 1 ms stimulation pulse applied to the muscle and the number of daily cycle number to bone.

As 50 Hz MS showed the greatest percentage of inhibition of bone loss and deterioration against disuse, we applied this mid-frequency for all of the experimental groups in this study. One characteristic in applying MS greater than 20 Hz is the type of muscle contraction it produces – tetanic contraction. The stimulation cycle number generated by the tetanic contraction (MS at > 20 Hz), that is sensed by the skeleton, is depended on the C-R ratio. For example, 50 Hz stimulation with 2/8 C-R ratio (2 sec contraction followed by 8 sec rest period), delivered 100 stimulation pulse and a tetanic contraction once every 10 sec. In a daily 10 minutes of stimulation, 50 Hz MS with 2/8 C-R ratio delivered 6000 stimulation pulse to the quadriceps and a cycle number of 0.1 Hz to the femur. Likewise, MS with 1/4 C-R ratio delivered also 6000 stimulation pulse but a

cycle number of 0.2Hz. 4/6 C-R ratio doubled the stimulation pulse to 12,000 with a cycle number of 0.1 Hz. Lastly, 2/28 C-R ratio only delivered 2000 stimulation pulse and 20 cycles daily.

Although the cycle number varied between groups, several implications can be drawn from this study. First, doubling the cycle number from 1,200 to 2,400 applied to the femur during the entire study, by altering the C-R ratio from 2/8 to 1/4, did not enhance osteogenesis. Given the equation derived by Qin et al., stimulation generated such small cycle number would need to compensate with higher strain level in order to maintain cortical bone mass [68]. Direct mechanical loading at 1 Hz generated greater than 1000 με and significantly increased cortical bone formation rate [136, 137]. However, MS at 50 Hz generated extremely low-level bone strain, which is below 10 με [92]. This discrepancy may be explained by the differences in stimulation and its frequency. It has been shown that the strain magnitude decreases in an inverse relation with the induced loading frequency [138]. Extremely low-magnitude strain (< 10 με), perhaps arise through muscle activity, was measured thousands of times a day and may be a key determinant to maintain bone's form and function [78, 118]. In addition, induced low-magnitude mechanical signal has the ability to be produced osteogenic responses on both cortical and trabecular levels if the stimulation is applied at high frequency (> 30 Hz) [78, 115, 118, 139]. Consistent with the observations from this study, MS at 50 Hz with 2/8 C-R ratio for 10 minutes per day was sufficient to inhibit trabecular bone loss and maintain its structure against 4 weeks of hindlimb suspension, partially by retaining the amount of mineralizing surface and the mineral apposition rate. Even though 1/4 C-R ratio doubled the cycle number, the percentage of inhibition was not as great as the 2/8 C-R ratio, which implied that cycle

number may not be an important factor in dynamic MS and that other mechanisms, such as fluid perfusion in relation to the rest period, may be involved.

Second, increasing the stimulation pulse from 120,000 to 240,000 deliver to the quadriceps, by changing the C-R ratio from 2/8 to 4/6, also did not augment the inhibition responses at the disuse femur and tibia. It was stated that contraction period compressed the vasculature within the skeletal muscle, diminishing arterial blood inflow and that blood is rapidly expelled into the extramuscular venous circulation [74, 140, 141]. Muscle perfusion is recovered during the rest period [74]. Studies have confirmed that venous blood flow increased by 61 ml/min·100g during isometric tetanic contraction of canine sciatic nerve [89]. This augmentation in flow subsequently increased the oxygen uptake and the work performed by the muscle [89]. By examining the ratio of 2/8 and 4/6, we would like to maximize the contraction period yet avoiding muscle fatigue and reducing the contractility. Despite there is no statistically significant between the two groups, our analyses showed that the adaptive responses from MS with 4/6 C-R ratio were comparable to the 2/8 C-R ratio, but the percentage changes comparing to the HLS were still lower for all the parameters. Although no detrimental outcome was observed at the tissue level with the 4 sec of continuous tetanic contraction, vascular perfusion and the exchange of nutrient and waste in the vessels may be disrupted by the combination of longer contractile duration with the shorter rest period [135, 142]. Taken both implications into account, a more in depth experimental design for future study should investigate the true consequences of the various contractile and non-contractile periods. Perhaps by extending the daily duration of the stimulation group, this way the same number of stimulation pulse and cycle number would be applied to the musculoskeletal tissues.

An alteration in the musculoskeletal fluid flow environment may also contribute to the osteogenic effects observed in this study. The close relationship between muscle and bone hypothesizes that a change in vascular perfusion within skeletal muscle can indeed cascade to a change in fluid pressure in bone [92]. The decline in femoral ImP due to hindlimb suspension and the increase in femoral ImP induced by MS firmly demonstrated the importance of fluid flow in medicating bone physiological processes [92, 117]. Bone fluid flow can enhance mechanosensitivity at the cellular level has been illustrated via various studies [143-146]. Mechanical loading accentuates fluid shear stress on bone cells, thus releasing signaling molecules, e.g., nitric oxide, to further medicate bone remodeling [145, 146]. In addition to circumvent muscle fatigue, the rest period inserted into the MS regimen may potentially heighten the mechanotransductive responses by allowing flow within the small fluid channel in bone to recover from the damping effects after each stimulation, increasing the convective transport of nutrient and signaling molecules, and medicating bone adaptation [67, 147, 148].

In conclusion, the devastation of bone loss associated with disuse osteopenia can lead to serious medical complications. The application of dynamic MS has showed to be beneficial as a preventive intervention for such disease, and its effectiveness is highly depended on the stimulation parameter, i.e., frequency. This study attempted to optimize the skeletal adaptive responses by varying the C-R ratio and to further alleviate trabecular bone deterioration due to the lack of daily weight bearing activity. We showed that C-R ratio does play an important role in stimulating trabecular bone responses in both disused limbs. Although a more in depth study is probably needed to determine the true effects of cycle number and the duration of rest insertion, the implications from this study presented

the significance of the C-R ratio with this non-invasive stimulation and the preliminary layout of future investigations.

Figures and Tables

Figure 4.1

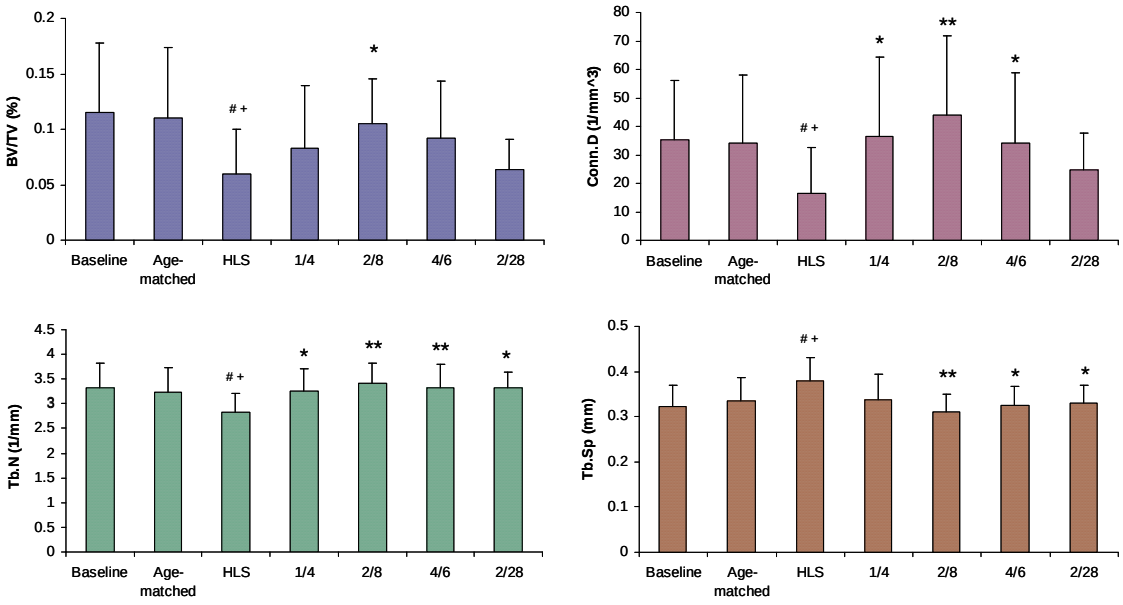

μCT analysis of the trabecular bone in the distal femoral M1 region (750 μm, closest to femoral diaphysis). Graphs show mean + SD values for bone volume fraction (BV/TV, %), connectivity density (Conn.D, $1/mm^3$), trabecular number (Tb.N, 1/mm), and separation (Tb.Sp, mm) at the M1 region. MS at 50 Hz with 2/8 C-R ratio produced significant changes in all indices, compared with values obtained from 4-week HLS. MS with 4/6 C-R ratio also demonstrated significant higher values for the bone quality parameters. $^{\#}$ p <0.01 vs. baseline; $^{+}$ p <0.01 vs. age-matched; * p <0.05 vs. HLS; ** p <0.01 vs. HLS.

Figure 4.2

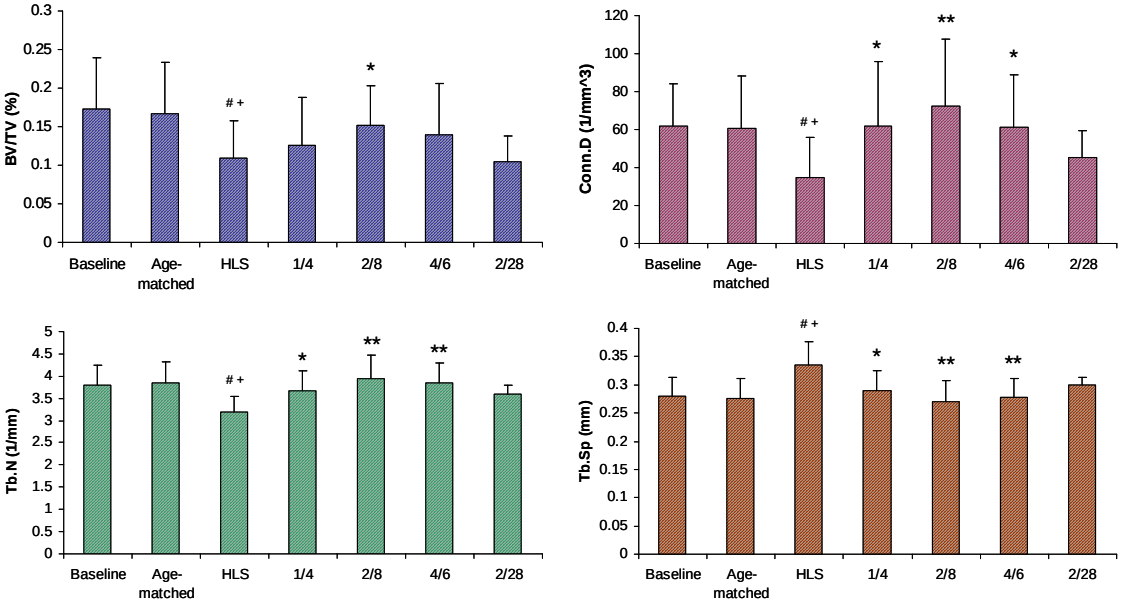

μCT measurement of the trabecular bone in the distal femoral M2 region (750 μm, in between M1 and M3, 750 μm above the growth plate). Graphs show mean + SD values for bone volume fraction (BV/TV, %), connectivity density (Conn.D, 1/mm^3), trabecular number (Tb.N, 1/mm), and separation (Tb.Sp, mm) at the M2 region. 50 Hz MS with 2/8 C-R ratio showed significant effects for all indices against 4-week HLS. MS with 1/4 and 4/6 C-R ratios also provided significant protection on the trabecular bone structure. $^{\#}$ p <0.01 vs. baseline; $^{+}$ p <0.01 vs. age-matched; * p <0.05 vs. HLS; ** p <0.01 vs. HLS.

Figure 4.3

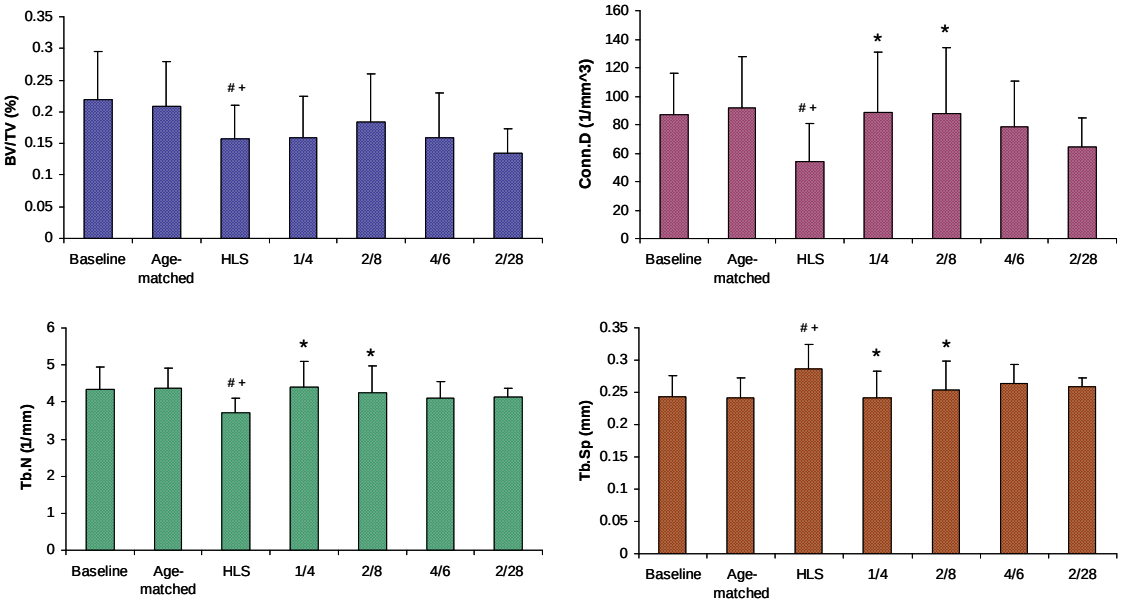

μCT evaluation of the trabecular bone in the distal femoral M3 region (750 μm, immediately above the growth plate). Graphs show mean + SD values for bone volume fraction (BV/TV, %), connectivity density (Conn.D, 1/mm^3), trabecular number (Tb.N, 1/mm), and separation (Tb.Sp, mm) at the M3 region. 50 Hz MS with 1/4 and 2/8 C-R ratios were able to maintain trabecular bone network during 4 weeks of the lack of weight bearing activity. $^{\#}$ p <0.01 vs. baseline; $^{+}$ p <0.01 vs. age-matched; * p <0.05 vs. HLS; ** p <0.01 vs. HLS.

Table 4.1. μCT Analysis of Proximal Tibia.

	Baseline	Age-matched	HLS	1/4	2/8	4/6	2/28
Metaphysis							
BV/TV (%)	0.19 ±0.07	0.21 ±0.09	0.16 ±0.07 [a]	0.19 ±0.10	0.21 ±0.11 [*]	0.21 ±0.10 [*]	0.16 ±0.08
Conn.D ($1/mm^3$)	28.5 ±13.3	36.8 ±20.2	24.6 ±14.1 [a]	34.0 ±20.8	35.4 ±25.1	30.6 ±18.2	23.6 ±13.6
Tb.N (1/mm)	1.81 ±0.47	2.16 ±0.98	2.00 ±0.95	2.27 ±0.98	2.25 ±0.95	2.35 ±0.85	2.21 ±0.89
Tb.Sp (mm)	0.60 ±0.13	0.56 ±0.23	0.67 ±0.35 [a]	0.52 ±0.31	0.58 ±0.28	0.49 ±0.16 [*]	0.55 ±0.29
Epiphysis							
BV/TV (%)	0.50 ±0.08	0.54 ±0.09	0.48 ±0.12 [a]	0.56 ±0.04	0.59 ±0.06 [*]	0.60 ±0.07 [*]	0.56 ±0.06
Conn.D ($1/mm^3$)	39.2 ±3.71	38.4 ±4.65	33.0 ±6.25 [ab]	37.4 ±4.15	36.1 ±4.83	33.5 ±4.51	35.8 ±3.42
Tb.N (1/mm)	7.34 ±0.35	7.32 ±0.38	6.86 ±0.32 [ab]	7.55 ±0.23	7.58 ±0.20	7.66 ±0.75	7.38 ±0.18
Tb.Sp (mm)	0.15 ±0.01	0.16 ±0.01	0.17 ±0.02	0.15 ±0.02	0.14 ±0.03	0.15 ±0.02	0.16 ±0.01

Values are mean ± SD for bone volume fraction (BV/TV, %), connectivity density (Conn.D, $1/mm^3$), trabecular number (Tb.N, 1/mm), and separation (Tb.Sp, mm) at the M3 region. There was significant reduction of trabecular bone induced by HLS. Stimulation with 2/8 and 4/6 ratio significantly inhibit bone against 4-week HLS at both metaphysis and epiphysis regions of the proximal tibia. MS was not able to maintain the trabecular microarchitecture in the proximal tibia [b] $p < 0.05$ vs. baseline; [a] $p < 0.05$ vs. age-matched; [*] $p < 0.05$ vs. HLS.

Table 4.2. Distal femur and proximal tibia metaphysis histomorphometry.

	Control	HLS	1/4 MS	2/8 MS	4/6 MS	2/28 MS
Femur Metaphysis						
BV/TV - Histo (%)	36.1±7.2	24.3±5.3 **	27.1±8.2	30.7±5.3 #	29.0±9.2 #	24.3±8.6
MS/BS (%)	9.11±3.6	2.37±1.1 *	5.45±3.3	5.74±3.3 #	4.70±2.0	2.58±1.4
MAR (μm/day)	1.18±0.3	0.34±0.3 *	0.65±0.5	0.83±0.5 #	0.58±0.5	0.49±0.5
BFR/BS ($\mu m^3/\mu m^2/yr$)	35.9±17	6.03±5.4 *	7.75±6.3	9.95±7.5	5.88±5.0	4.58±5.8
Tibia Metaphysis						
BV/TV - Histo (%)	32.5±10	19.2±3.4 **	26.3±3.9	34.0±4.7 #	24.0±9.5	21.9±14
MS/BS (%)	8.92±2.8	2.88±0.5 *	6.20±2.8	7.78±2.8 #	5.20±2.2	3.76±2.2
MAR (μm/day)	1.65±0.3	0.54±0.5 *	0.71±0.5	0.77±0.3	0.63±0.5	0.37±0.5 *
BFR/BS ($\mu m^3/\mu m^2/yr$)	39.8±17	7.35±6.3 *	8.93±9.1	11.8±4.5	7.76±6.1	5.63±4.2

Values are mean ± SD. BV/TV, bone volume/tissue volume; MS/BS, mineralized surface/bone surface; MAR, mineral apposition rate; BFR/BS, bone formation rate/bone surface. * p <0.05 vs. age-matched, $^{\#}$ p <0.05 vs. HLS.

V. The Effects of Dynamic Muscle Stimulation on Preventing Skeletal Muscle Atrophy in a Disuse Model

Abstract

The potential effects of dynamic electrical muscle stimulation on muscle atrophy, associated with functional disuse, were the focus of the two present studies. The stimulation regimens were to vary the stimulation frequency and the contraction-to-rest (C-R) period. Skeletally matured Sprague-Dawley rats were divided into seven groups for the each study. For the frequency study, the groups were baseline control, age-matched control, hindlimb suspended (HLS), and HLS with muscle stimulation at 1 Hz, 20 Hz, 50 Hz, and 100 Hz. For the C-R study, the groups were baseline control, age-matched control, HLS, and HLS with 1/4, 2/8, 4/6, and 2/28 C-R ratios. Muscle wet weight, fiber cross-sectional area, number of central nuclei, type I and II fiber were evaluated. The results showed that 10 minutes of daily stimulation could maintain muscle fiber types to the level similar to normal muscle. However, the short duration could not compensate for the loss of muscle weight and the reduction of fiber area. Overall, the findings of these studies suggested that other parameter, i.e., duration of stimulation, may also influence the effect of dynamic muscle stimulation in addition to the selection of stimulation frequency and C-R ratios within the regimen.

Introduction

Decreases in muscle activity lead to muscle atrophy has been reported following space mission, spinal cord injury, bed rest, and aging. The alteration in mechanical environment rapidly induces muscular adaptation in fiber size and metabolic properties [44, 49, 51, 149-151]. Short-term spaceflight caused significant losses in muscle volume by 5 to 17%, fiber cross-sectional area by 11 to 24%, and type I fiber by 6 to 8% [44, 49].

Likewise, 6 week post spinal cord injury caused a 15% lean muscle mass loss at the lower extremities and an averaged muscle cross-sectional areas reduction by 18 to 46% [152, 153]. These changes are often associated with increased muscle weakness and fracture risk [154].

As an intervention, functional electrical stimulation produces isometric contractions in replacement for the lack of muscle activity [155]. The induced contractions have been shown to increase muscle volume, muscle cross-sectional area, and improve fatigue resistance in human [156, 157]. However, the effects of this external stimulus were highly depended on the variability in the duration and frequency of the stimulation [93].

Small animal models have been extensively studied to mimic the condition of disuse [54, 108, 158, 159]. Similar to human, rodent studies displayed a loss of skeletal muscle mass, greatest in the postural muscles, and decreased in muscle force [160-163]. Chemical-induced paralyzed limb in rat showed the highest decline (~40%) in muscle weight and fiber cross-sectional area in the soleus muscle [98]. The degree of muscle atrophy was not as profound in the tibialis anterior and gastrocnemius, ~20%. Rat hindlimb unloading also supported these findings, where there was significantly reduction in both type I and type II muscle fibers area for the soleus and plantaris muscles [88]. In additional, hindlimb suspension decreased the percentage of type I muscle fibers by an approximately 40% while the number of type II fibers augmented by ~20% [88].

Electrical stimulation applied to animals has reported various effects on the skeletal muscle morphology and biochemistry. Numerous stimulation paradigms has been tested and generated mixed conclusion on the benefit of such stimulations. The

discrepancies were mainly contributed by the applied stimulation frequency, the duration of the stimulation, and the type of muscle analyzed [83, 87, 164, 165]. Stimulation at 10 Hz for 24 hours per day increased fatigue resistance yet decreased the size of the tibialis anterior muscles [166]. Lower frequency, such as 2 Hz, applied for 10 hours per day demonstrated a marked reduction in paralyzed soleus atrophy [98]. Most studies that showed positive effects of electrical muscle contraction at the tissue level have used extremely long stimulation protocols, from 2 to 24 hours. In addition, the application of the stimulation frequency ranged from 1 to 100 Hz.

The possibility in applying electrical muscle stimulation as a countermeasure for skeletal muscle atrophy against functional disuse was clearly illustrated by current clinical data and in vivo studies. However, without an optimized protocol and with the long hours of stimulation, the application of electrical muscle stimulation for clinical use remains impractical. Thus, we were interested in investigating the possibility to shorten the stimulation duration and optimizing our dynamic muscle stimulation protocol. The optimization was evaluated in two separate studies: (1) by varying the stimulation frequency and (2) by altering the contraction-to-rest ratio. The degree of muscle weight loss, fiber cross-sectional area decrease, the number of centralized nuclei, type I, and type II fibers were analyzed in these studies.

Materials and methods

Experimental Design

The two experimental protocols were taken from Chapter 1 and 2. The effect of dynamic muscle stimulation (MS) on preventing skeletal muscle atrophy induced by the

lack of daily activity was investigated. The first study (n = 56) focused on the importance of stimulation frequency and the second (n = 56) targeted on the alteration of the contraction-to-rest (C-R) ratio. Animals were randomly assigned to seven groups for each study with n=8 per group. For study 1: (1) baseline control, (2) age-matched control, (3) HLS, (4) HLS+1 Hz MS, (5) HLS+20 Hz MS, (6) HLS+50 Hz MS, and (7) HLS+100 Hz MS. For study 2: (1) baseline control, (2) age-matched control, (3) HLS, (4) HLS+1/4 (1 sec contraction-to-4 sec rest) MS, (5) HLS+2/8 MS, (6) HLS+4/6 MS, and (7) HLS+2/28 MS. Functional disuse was induced by HLS, setup modified from Morey-Holton and Globus [108]. The body weight of each animal was carefully monitored throughout the study.

Electrical MS Protocol

As stated in previous chapters, dynamic MS was applied via two needle-size electrodes (L-type gauge #3, Seirin, Weymouth, MA) under isoflurane anesthesia, for 10 minutes per day, 5 days per week, for a total of 4 weeks. One electrode was placed at the right lateral proximal quadriceps and the other was placed at the lateral distal quadriceps. The electrodes were then connected to a 100MHz arbitrary waveform generator (Model 395, Wavetek) to transmit a 1ms square pulse with the appropriate application signal, either with various stimulation frequency (1 Hz, 20 Hz, 50 Hz and 100 Hz) or C-R ratio (1/4, 2/8, 4/6, 2/28). Control animals (age-matched and HLS) were also subjected to anesthesia for the same amount of time per day as the experimental animals to account for any potential effect due to isoflurane inhalation. After 4 weeks of study, the quadriceps (Quad), gastrocnemius (Gas), and soleus (Sol) of the stimulated limb were harvested immediately after sacrifice and their wet weights were recorded.

Histochemical Analysis

After the weight measurements, the tissues were cut to an approximate length of 10 mm with a cross-sectional area of 25 mm^2. The samples were embedded with OCT compound (Tissue Tek), frozen in liquid nitrogen-chilled isopentane, and stored at -80°C until analysis. Multiple 8 μm cross sections were cut with a cryostat (Lecia) at -18°C. Three sections were then stained with hematoxylin and eosin (H&E, Polyscience) for muscle fiber cross-sectional area (CSA, μm^2) and central nuclei (CN, number per fiber) evaluation (Figure 5.1). Three other sections were used for myofibrillar ATPase staining to characterize myosin isoforms. For the ATPase staining, the Quad and Gas sections were immersed into alkaline preincubation solution at a pH value of 10.4 and the Sol sections were submerged into acid preincubation solution at a pH value of 4.6. All sections were then incubated with ATP solution at a pH value of 9.4. The fibers were classified as either type I or type II. Two cross-sectional bright field images (670 μm x 530 μm) were captured from each muscle section with a Zeiss microscope (AxioVision 4.5, Germany) at 200X magnification. All evaluations were performed with the ImageJ software, downloaded from the NIH, website. For each analysis, 150 – 350 fibers were assessed per muscle section.

Immunohistochemistry

Additional 8 μm cross-sections were cut from the Quad muscles for Pax7 immuno-staining. The primary antibodies anti-Pax7 (Developmental Studies Hybridoma Bank, Iowa City, IA) and anti-laminin (Sigma, St. Louis, MO) were used. Pax7 is a transcription factor that expresses in satellite cells, and is thought to play critical roles in skeletal muscle development and regeneration. Laminin is a marker for basement

membranes. Two secondary antibodies were applied (Vector Laboratories, Burlingame, CA); the rat adsorbed fluorescein anti-mouse IgG was used to detect for Pax7 while texas red anti-rabbit IgG for laminin. Working dilutions of these antibodies were 1:200 for Pax7 and the secondary antibodies and 1:500 for laminin in 1% bovine serum albumin (BSA), diluted with 1X phosphate-buffered saline (PBS). The immuno-staining of Pax7 and laminin was performed simultaneously. Tissue sections were first fixed with 4% paraformaldehye in PBS, permeabilized with 0.5% of Triton X-100 diluted in PBS, and blocked with 1% BSA. Primary antibodies were incubated with the sections overnight at 4°C. The secondary antibodies were incubated for one hour at room temperature. Lastly, the sections were dehydrated with a series of ethanol (70%, 95%, and 100%), cleared with xylene, and mounted with Vectashield with DAPI (Vector Laboratories, Burlingame, CA). Muscle fibers and satellite cells were visualized with a Zeiss microscope (AxioVision 4.5, Germany) with the FITC (Pax7), TRITC (Laminin), and DAPI (myonuclei) filters at 630X magnification.

Statistical Analyses

All of the histochemical results are reported as mean ± SD. For each analysis, significance differences between groups were determined using the SigmaStat 2.03 program (Systat Software Inc, San Jose, CA). Analysis of variance (ANOVA) with Tukey's pairwise multiple comparison tests was performed on the CSA, CN, type I and II muscle fibers data. The level of significance was considered at $p < 0.05$.

Results

Muscle wet weight

The Quad, Gas, and Sol wet weight of the stimulated limbs were recorded after harvesting of study 2. Individual muscle weight was normalized to the animal's final body weight (Table 5.1). HLS alone led to muscle weight loss of 22% in Quad ($p < 0.01$), 17% in Gas ($p < 0.01$), and 43% in Sol ($p < 0.001$). 50 Hz MS with various C-R ratios had no influence on the hindlimb muscle weight and the average weight loss was similar to the one from HLS control. Comparing to the age-matched control, the muscle weight loss was 21% in Quad ($p < 0.01$), 10 – 19% in Gas ($p < 0.01$), and 39 – 44% in Sol ($p < 0.001$).

Histochemistry

Multiple representative H&E and ATPase images of the Quad, Gas, and Sol muscles cross-sectional were presented in Figure 5.2 – 5.4. The morphological (CSA) and histochemical (fiber type) changes between the age-matched, HLS, and MS at 50 Hz could be visualized.

Muscle Fiber Cross-Sectional Area (CSA)

In addition to the wet weight loss, 4 weeks of HLS induced quadriceps muscle atrophy by decreasing the muscle fiber CSA, 26% in study 1 and 29% in study 2 ($p < 0.01$). Electrical stimulation was directly applied to the quadriceps muscle. Surprisingly, 10 minutes of MS, regardless of the stimulation frequency or C-R ratios, was not sufficient to prevent muscle atrophy. Comparing to the age-matched control, the degree of CSA decline varied with the stimulation frequency, -31% for 1 Hz, -27% for 20 Hz, -19% for 50 Hz, and -42% for 100 Hz ($p < 0.01$ for all) (Figure 5.5). The fiber CSA

subjected to stimulation at 50 Hz was 9% higher than the HLS ($p < 0.05$). When we altered the C-R ratio within the 50 Hz MS, similar findings were observed (Figure 5.6). The percent decline in CSA versus the age-matched group was 29%, 23%, 31%, and 32% for 1/4, 2/8, 4/6, and 2/28 C-R ratios, respectively ($p < 0.01$). Overall, 50 Hz stimulation with 2/8 as the C-R ratio showed a slight positive change (7 – 9%), not statistically significance ($p = 0.2$), against 4 weeks of disuse.

Although the Gas and Sol were not stimulated, we were interested to determine whether the movement induced by the quadriceps contraction has an effect on neighboring tissues and their morphologies. The disused muscle CSA was significantly decreased by 18% in Gas ($p < 0.01$) and 49 – 59% in Sol ($p < 0.001$) (Table 5.2 & 5.3). The contraction at the Quad did not affect the CSA in these two muscle groups. Comparing to the age-matched animals, the CSA decline in the stimulation frequency study was 11 – 33% in Gas ($p < 0.01$) and 43 – 75% in Sol ($p < 0.001$), where 100 Hz MS had the highest decrease. Similarly, the CSA in the C-R ratio study was reduced by 11 - 27% in Gas ($p < 0.01$) and 53 – 59% in Sol ($p < 0.001$).

Central Nuclei (CN) within Fibers

Although the difference in the number of CN per fiber between age-matched and disused was not statistically significance, the disused quadriceps increased the number of CN by 48% in the frequency study and 24% in the C-R ratio study. These increases were prevented by the dynamic electrical stimulation with a specific regimen. While 1 Hz MS showed an 82% increase in CN versus normal animals ($p < 0.05$), 50 Hz MS showed a 37% and 57% reduction in CN per muscle fiber versus age-matched ($p < 0.05$) and HLS ($p < 0.01$), respectively (Figure 5.5). MS at 20 Hz and 100 Hz also prevented the

occurrence of CN by 20% and 30% against disuse, respectively (Figure 5.5). Furthermore, changes in the C-R ratios within the 50 Hz stimulation regimen demonstrated significant decline of CN, with -38%, -41%, -35%, and -25% versus HLS for 1/4, 2/8, 4/6, and 2/28 C-R ratios ($p < 0.05$ for all), and -24%, -27%, -20%, and -7% versus age-matched for 1/4, 2/8, 4/6, and 2/28 C-R ratios, respectively (Figure 5.6).

Disused Gas and Sol also showed an increase in the number of CN per fiber, with 28% and 29% in the frequency study and 34% and 13% in the C-R study, respectively (Table 5.2 & 5.3). The number of CN per fiber was lower after daily MS was applied. Stimulation at 50 Hz with 2/8 C-R ratio demonstrated significant 30 – 42% decrease in the number of CN per fiber from both studies. Likewise, comparing to HLS, the number of CN was 30 – 38% lower in the Sol from the stimulated animals.

Muscle Fiber Characteristics

The numbers of type I and II muscle fibers are normalized to the total fibers analyzed. Quad mostly contains type II fibers, the normalized fiber ratios of type I and II were 0.02 and 0.98, respectively. Quad subjected to 4 weeks disuse alone and 1 Hz MS showed a decrease in type II fibers (up to 4%, $p < 0.05$) and an increase in type I fibers (up to 158%, $p < 0.05$). Stimulation at 20 Hz was able to either maintain the fibers ratios to those of the age-matched control (Figure 5.5). MS at 50 Hz and 100 Hz lower the type I fiber ratio, 72% and 87% versus normal animals (not significance), and 86% and 94% against HLS $p < 0.01$, respectively (Figure 5.5). For the C-R ratio study, HLS and MS with 2/28 C-R ratio significantly increased the type I fiber ratio and decreased the type II ratio, as expected ($p < 0.05$). Comparing to HLS the number of type I and II fibers were

significantly changed with 1/4 ($p < 0.05$), 2/8 ($p < 0.01$), and 4/6 C-R ($p < 0.01$) ratios (Figure 5.6).

In the Gas, no significance change in fiber type was observed between age-matched, HLS, and experimental group. Surprisingly, the Sol muscle seems to response to both disuse and MS to the Quad (Table 5.2 & 5.3). This muscle group is dominantly occupied by type I fiber, the normalized fiber ratios of type I and II were 0.86 and 0.14, respectively. Four weeks disuse significantly decreased the type I fiber ratio (20%) and subsequently increased type II ratio (121%) ($p < 0.01$). MS at mid to high frequency partially counteract the alterations seen in HLS, by increasing type I fiber ratio by 15% ($p < 0.05$). Within the 50 Hz MS regimen, C-R ratios of 2/8 and 4/6 were also able to maintain the fiber ratio similar to those of the age-matched control.

Immunohistochemistry

Satellite cells and basement membrane of the muscle were successfully visualized by Pax7 (Green) and laminin (Red) staining (Figure 5.7). Pax7 is a transcription factor thus only expressed in the nucleus, as matched by the DAPI staining (Blue). The Quad cross-sections from normal animals, and animals subjected to HLS, and HLS + 50 Hz MS all shown to have satellite cells. However, the numbers of satellite cells within each sample were extremely small and difficult to locate, thus not suitable for quantification.

Discussion

In this study, the 10 minutes daily dynamic MS partially induced conversion between myosin heavy chain isoforms but was inadequate to prevent the loss of muscle weight and fiber cross-sectional area due to functional disuse. We have also explored the

efficacy of MS with different stimulation frequencies and C-R ratios on muscular adaptation induced by 4 weeks of HLS. Taken together the results from chapter 1 and 2, the present data confirmed that the effectiveness of dynamic MS is highly dependent of the stimulation frequency and the C-R ratio but to a lesser degree.

Mechanical stimulations have been researched to alleviate muscle atrophy. Long duration (10 – 24 hours) electrical stimulations at low frequency significantly prevented weight loss in soleus and tibialis anterior [98, 166]. However, others found that stimulation with higher frequency can maintain muscle mechanical properties, i.e. twitch and tetanic force, as well as reduce muscle weight loss and fiber CSA [83, 167]. Surprisingly, our dynamic MS, regardless of stimulation and C-R ratio, was unable to inhibit hindlimb muscle atrophy. We have previously showed that dynamic MS, applied 10 minutes per day, can partially prevent trabecular bone loss in disused femur. To our knowledge, this study was the first to examine the effect of such short-term duration (10 minutes) on disuse muscle. Daily 30 minutes of electrical stimulation at 45 – 60 Hz was previously studied with healthy individuals [93]. Since the subjects did not experience any disuse-related muscle loss, the stimulation served as an enhancement and showed an increased in averaged CSA by 14% and in the number of type II fibers. Taken other studies into consideration, longer daily stimulation (30 minutes to 1 hour) may be required to counteract the loss of function to the skeletal muscle and to induced changes at the tissue level.

The Quad and Gas muscles are examples of fast-twitch muscles, which is highly responsive to contraction with abundant of type II muscle fibers [51, 93, 168]. In contrast, the soleus is considered as a posture muscle (slow-twitch) with abundant of type I fibers

[51, 93, 168]. For our study, the percentages of type II and type I muscle fibers were 98% and 2% in normal Quad, 70% and 30% in Gas, and 14% and 86% in Sol, respectively. Other studies on fast-twitch muscle groups, i.e., extensor digitorum longus (EDL), also detected ~95% of type II fibers via histochemical analysis and myosin heavy chain (MHC) II isoform via protein analysis [87, 168, 169]. Soleus expressed ~85% of MHC II and 15% of MHC I [170]. It has been reported that slow-twitch fibers are more sensitive to HLS than fast muscle fibers, and that disuse induces slow-to-fast transformation [171, 172]. We found that to be partly true, in which the fiber type conversion was different based on muscle groups. Inactivity decreased type II fibers and proportionally increased type I fibers in disused Quad, demonstrating a fast-to-slow transformation. However, the changes were reversed for disused Gas and Sol [170]. Our stimulation at 1 Hz showed the similar muscle type transformation as HLS. Chronic continuous stimulation at 10 Hz for 10 to 24 hours per day converted EDL and tibialis anterior muscle from fast to slow [87, 169]. Yet, MS at 50 Hz and 100 Hz increased the number of type II fibers to almost 100% in the Quad in response to the contraction. This discrepancy with previous results was possibly due to the type of MS, where we applied an intermittent signal with high stimulation frequency.

The occurrence of centralized nuclei is a hallmark for regenerating skeletal muscle. An increase in the number of central nucleus within the muscle fibers is a characteristic in many muscular diseases [173]. In normal muscle, less than 3% of fibers should have internal nuclei as observed in our analysis. MS at mid to high frequencies reduced the numbers of CN to normal level, suggesting the skeletal muscle was not damage due to disuse or the stimulation. Another indication for muscle development and/or regeneration is the detection of satellite cells. Satellite cells, lie quiescent in the

basement membrane, are responsible for the generation of new myonuclei [174-176]. It has been hypothesized that impaired skeletal muscle has a lower number of satellite cells, thus fail to maintain muscle mass [62, 174]. However, the link between sarcopenia and satellite cell content has been inconclusive. One study showed suppression of satellite cell mitotic activity occurs immediately upon unloading but histochemical analysis was not specific toward any satellite cell marker [62]. In a more detailed study with the elderly, the number of satellite cells decreased was in conjunction with the type II fiber atrophy [177]. The success of Pax7 immuno-staining demonstrated the existence of satellite cells in our study. However, the changes in type II fibers were somewhat ambiguous and the detection for satellite cell was relatively low in all groups. Thus, future study may consider other analysis to detect Pax7 expression in a more accurate manner.

The variation of stimulation frequencies within the dynamic MS regimen generated two types of isometric contraction at the quadriceps. MS at low frequency, such as 1 Hz, produced isometric twitch, in which there is a rapid increase in muscle tension and then gradually return to normal [178]. MS at mid to high frequency, such as 50 Hz, generated isometric tetanus, where a peak muscle tension is achieved by a summation effect [83]. For our studies, we concentrated in determining the morphological and biochemical consequences of dynamic MS and did not focus on the functionality properties of the muscles. Stimulation at 1 Hz induced twitch contractions, which fail to prevent muscle atrophy but was able to maintain maximum twitch tension [178]. Previous studies by Gorza et. al. measured the maximum tetanic tension of an innervated soleus to be 1.9 N and a denervated soleus to be 0.046 N. The tension of the denervated muscle rose to 0.68 N

with stimulation at 15 Hz and 1.1 N with stimulation at 100 Hz [83]. Similar results were found with HLS rats subjected to isometric exercise, the tetanic force of the soleus was increased by 30% [162]. The degree of protection with the stimulation was less when measured in a fast-twitch muscle, such as extensor digitorum longus. Nevertheless, the tension – frequency relation could potentially be one of the key elements in selecting the optimal stimulation frequency within the MS paradigm.

Another consideration in the design of MS regimen is the elevation of fluid flow induced by contraction. Muscular contraction can raise intramuscular pressure and blood flow [179]. It is thought that rhythmical contractions increase venous outflow by compressing the arteries and veins, the vessels are refilled during relaxation [73]. This concept of muscle pump is well appreciated and may be a potentially mechanism in the effects of dynamic MS. Treadmill exercise and 1 second of tetanic stimulation at 30 Hz both decreased arterial blood flow and increased venous blood flow at the onset of contraction [180]. Blood flow then returned to normal level during rest period. In addition, blood expelled from the venous system increased as function of increased stimulation frequency [89]. Extensive researches also suggested other mechanisms, i.e., vasodilation, to explain the rapid increase in blood flow during the first few second of contraction [181, 182]. Regardless of the possible mechanism, MS increased microvasucular fluid perfusion is undeniable. Although 10 minutes daily MS failed to distinguish the significance between C-R ratios, the combination of the contraction and relaxation period should continue to be considered for future design of experiment. Prolonged stimulation may enhance perfusion, augment oxygen and other metabolites delivery, and further protect the muscular tissues against the lack of functional activity.

In conclusion, 10 minutes daily dynamic MS to the quadriceps may be too short to be effective in prevent skeletal muscle atrophy, induced by 4 weeks of HLS. The variation of stimulation frequency has promising impacted on the histochemical and metabolic properties of the muscle fibers. The shift in fiber types suggested the initiation of muscular responsiveness. Although the mechanism between stimulation and tissue adaptation remain unclear, these studies demonstrated the importance in considering the type of contraction that is being applied and the changes in fluid perfusion that is being generated by the stimulation. Future investigation may target on the duration of the stimulation, supplement with the appropriate stimulation frequency and C-R ratios within the dynamic MS regimen.

Figures and Tables

Figure 5.1

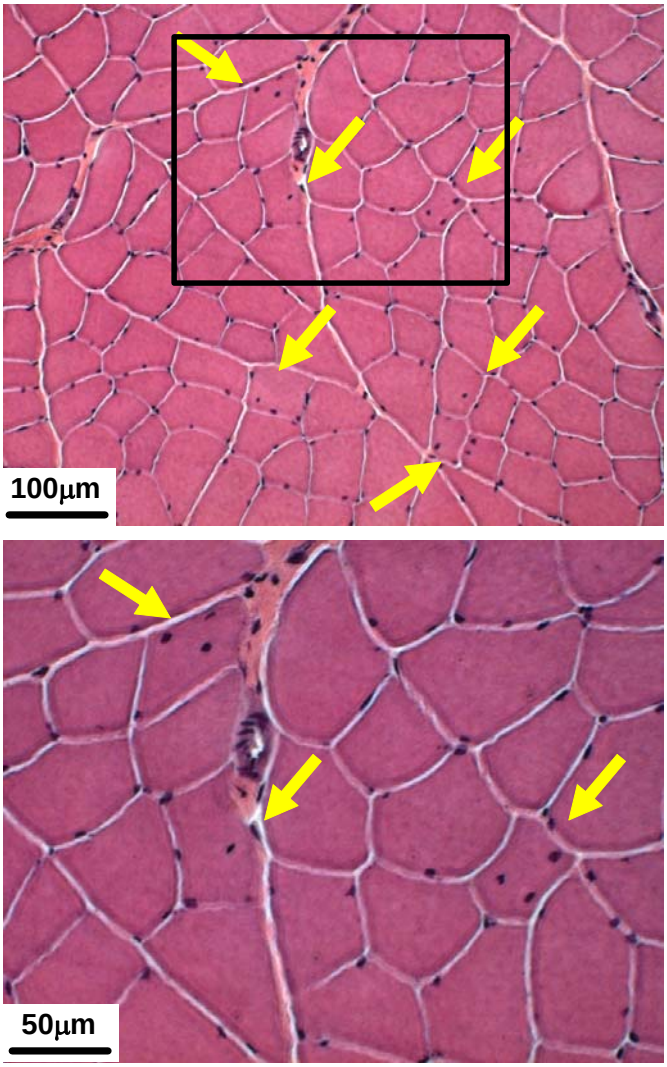

Representative H&E images of disused quadriceps taken at 200X (Top) and 400X (Bottom) magnification. The bottom image was taken at the same region as the box shown in the top image. Arrows indicate central nuclei.

Table 5.1. Skeletal Muscle Wet Weight Normalized to Individual Body Weight

	Baseline	Age-matched	HLS	1/4 C-R	2/8 C-R	4/6 C-R	2/28 C-R
Quadriceps (mg/g)	8.47 ±0.40	9.67 ±1.33	7.52 ±0.34 ab	7.75 ±0.73 ab	7.78 ±0.61 ab	7.67 ±1.04 ab	7.59 ±1.01 ab
Gastrocnemius (mg/g)	5.35 ±0.31	5.22 ±0.32	4.36 ±0.22 ab	4.58 ±0.31 ab	4.71 ±0.20 ab	4.25 ±0.26 ab	4.35 ±0.76 ab
Soleus (mg/g)	0.45 ±0.03	0.45 ±0.04	0.25 ±0.03 #*	0.26 ±0.02 #*	0.27 ±0.04 #*	0.26 ±0.03 #*	0.25 ±0.02 #*

Normalized values are mean ± SD. [b] $p < 0.01$ vs. baseline, [#] $p < 0.001$ vs. baseline, [a] $p < 0.01$ vs. age-matched, [*] $p < 0.001$ vs. age-matched.

Figure 5.2

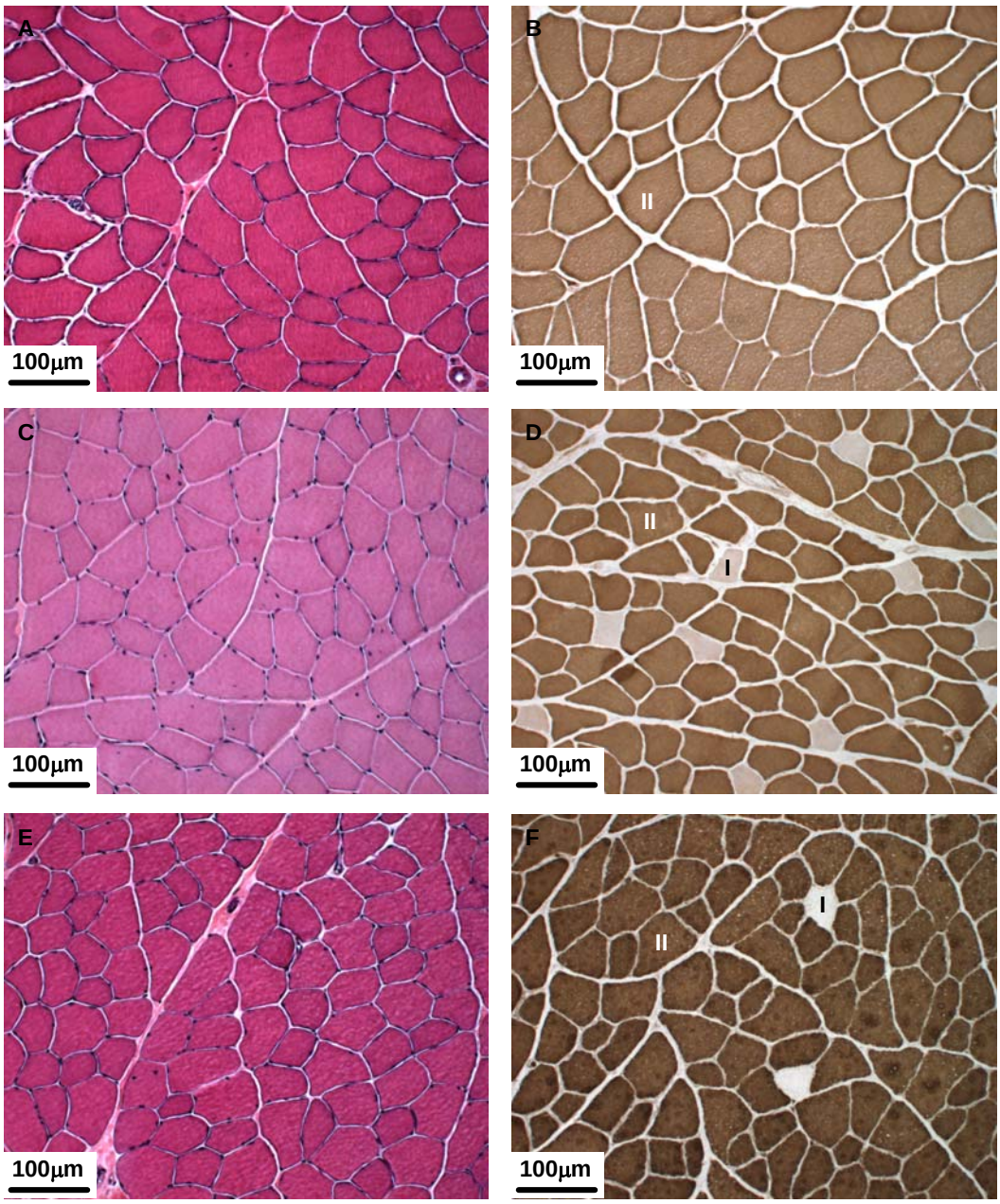

Representative H&E (A, C, E) and ATPase (B, D, F) stained images of the quadriceps, taken at 200X magnification. Age-matched (A & B); HLS (C & D); HLS + 50 Hz with 2/8 C-R ratio (E & F). Quadriceps sections were stained with alkaline solution (pH 10.4). Type I muscle fibers are shown in light color and type II fibers are shown in dark.

Figure 5.3

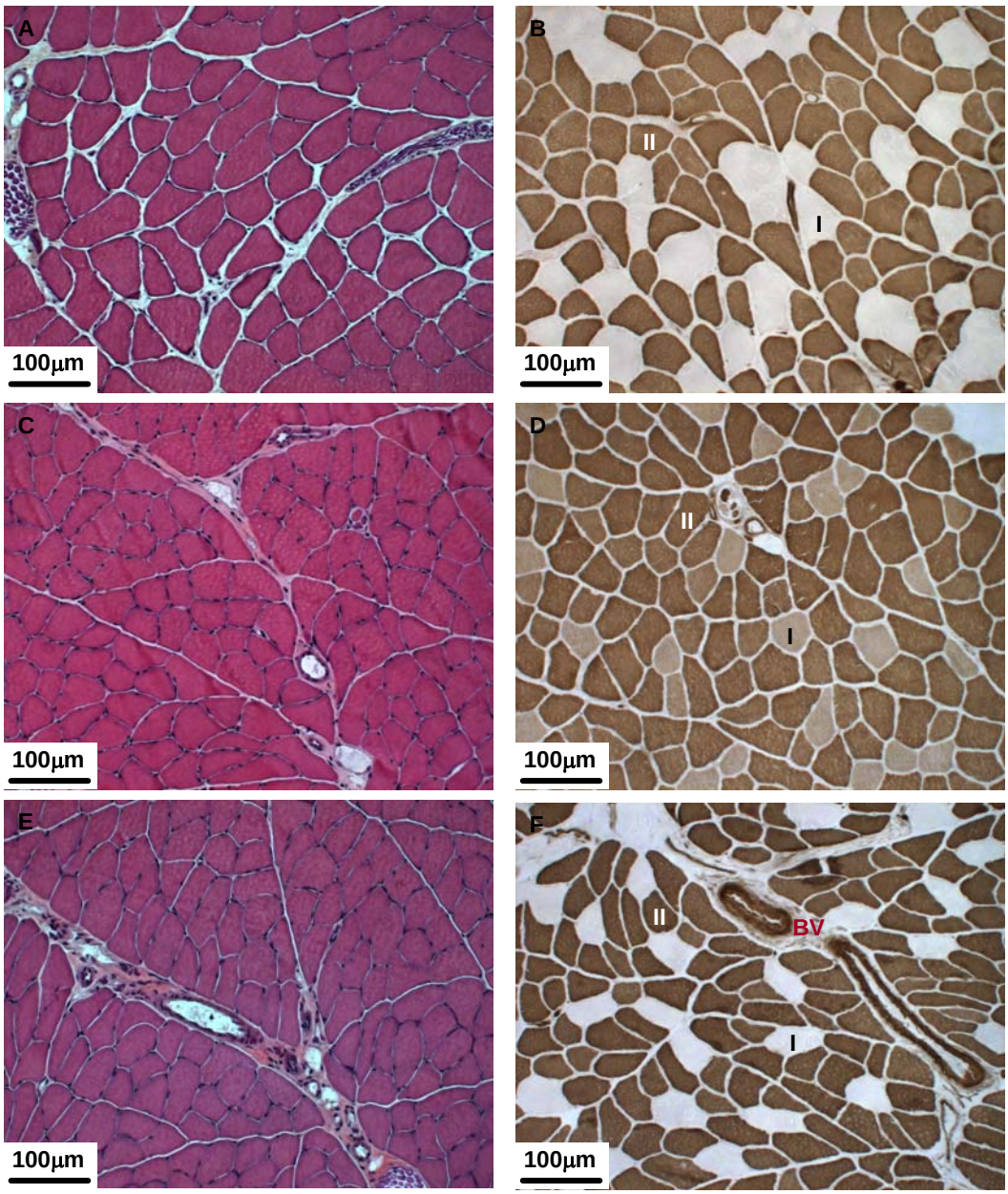

Representative H&E (A, C, E) and ATPase (B, D, F) stained images of the gastrocnemius, taken at 200X magnification. Age-matched (A & B); HLS (C & D); HLS + 50 Hz with 2/8 C-R ratio (E & F). Gastrocnemius sections were stained with alkaline solution (pH 10.4). Type I muscle fibers are shown in light color and type II fibers are shown in dark. BV = Blood vessel.

Figure 5.4

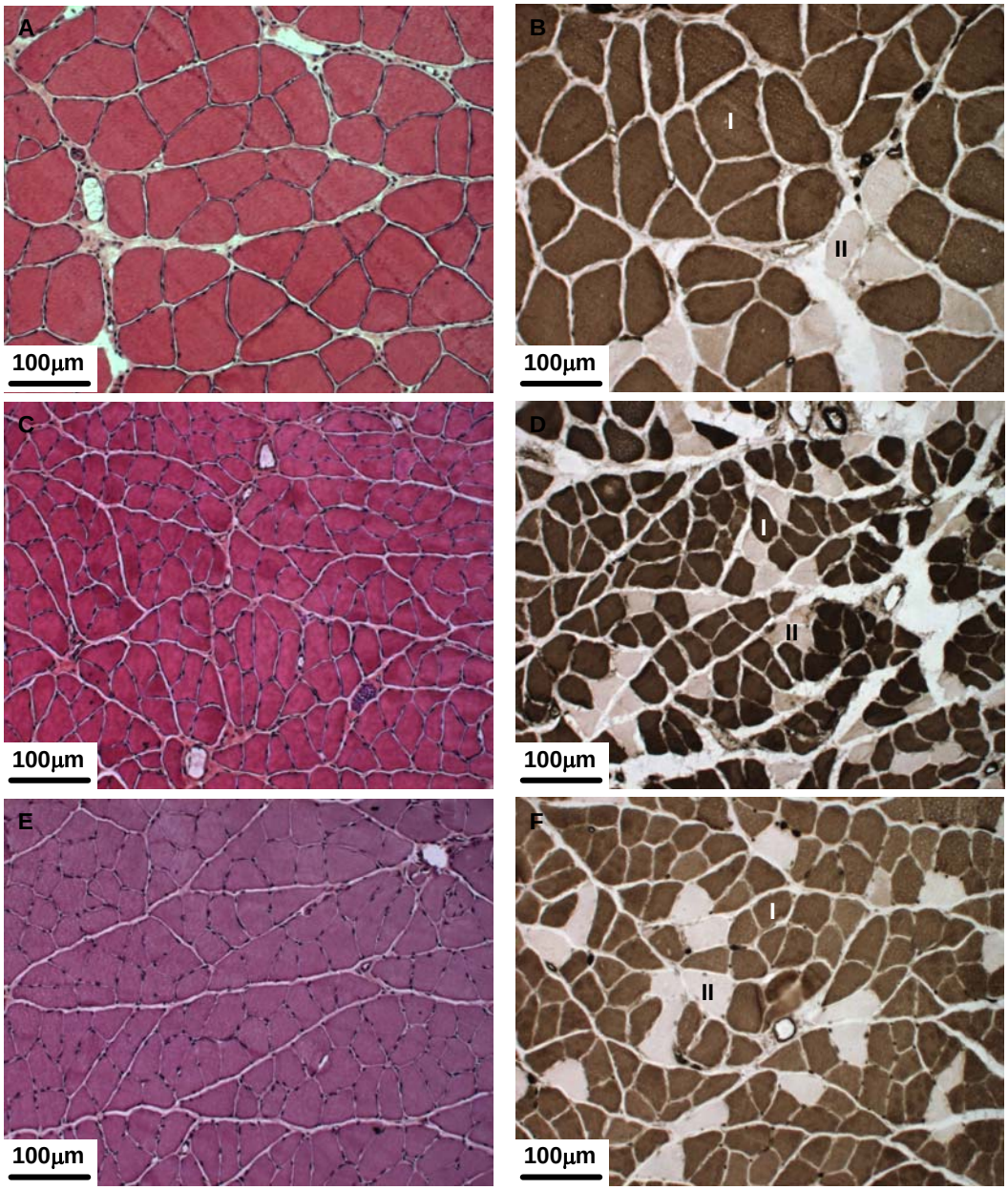

Representative H&E (A, C, E) and ATPase (B, D, F) stained images of the soleus, taken at 200X magnification. Age-matched (A & B); HLS (C & D); HLS + 50 Hz with 2/8 C-R ratio (E & F). Soleus sections were stained with acid solution (pH 4.6). Type I muscle fibers are shown in dark color and type II fibers are shown in light.

Figure 5.5

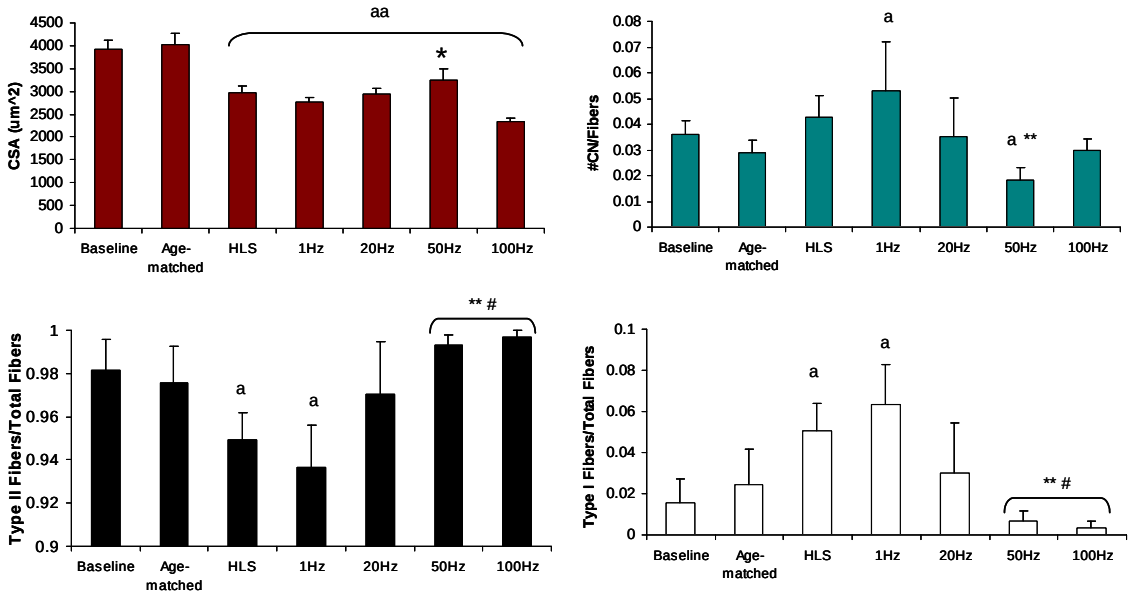

Graphs show mean + SD values for fiber cross-sectional area (CSA, μm^2), number of central nuclei per fiber (#CN/Fiber), type II fiber per total fiber, and type I fiber per total fiber. Compared to HLS, MS at 50 Hz produced a significant change in all indices. ^{a} p <0.05 vs. baseline and age-matched; ^{aa} p <0.01 vs. baseline and age-matched; * p <0.05 vs. HLS; ** p <0.01 vs. HLS; $^{\#}$ p <0.01 vs. 1 Hz.

Figure 5.6

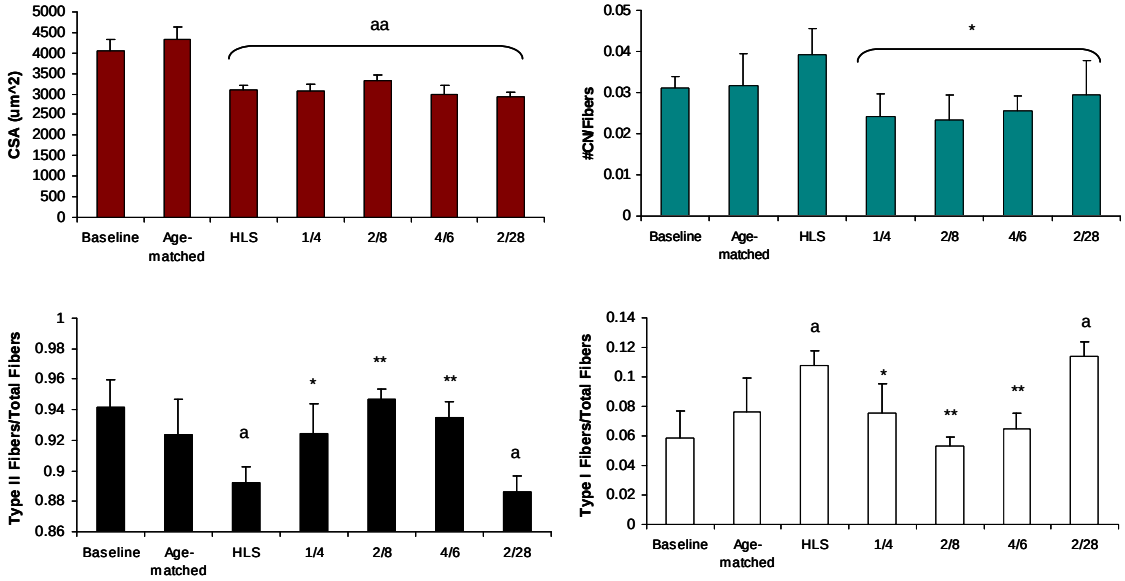

Graphs show mean + SD values for fiber cross-sectional area (CSA, μm^2), number of central nuclei per fiber (#CN/Fiber), type II fiber per total fiber, and type I fiber per total fiber. [a] $p < 0.05$ vs. baseline and age-matched; [aa] $p < 0.01$ vs. baseline and age-matched; [*] $p < 0.05$ vs. HLS; [**] $p < 0.01$ vs. HLS.

Table 5.2. Effects of Stimulation Frequency on Properties of Gastrocnemius & Soleus

	Baseline	Age-matched	HLS	1 Hz	20 Hz	50 Hz	100 Hz
Gastrocnemius							
CSA (μm^2)	2704 ±442	2923 ±795	2401 ±260 [a]	2587 ±341 [a]	2126 ±417 [a]	2584 ±344 [a]	1953 ±994 [a]
CN (#/Fiber)	0.010 ±0.005	0.017 ±0.011	0.023 ±0.017	0.023 ±0.005	0.017 ±0.009	0.013 ±0.008	0.018 ±0.008
Type II Fibers (%)	68.1 ±17	70.0 ±14	71.7 ±2.8	72.9 ±9.8	79.0 ±12	74.8 ±8.4	74.0 ±3.6
Type I Fibers (%)	31.9 ±17	30.0 ±14	28.3 ±2.8	27.1 ±9.5	21.0 ±12	25.2 ±8.4	26.0 ±3.6
Soleus							
CSA (μm^2)	3994 ±916	3468 ±576	1771 ±366 [#]	1946 ±383 [#]	1647 ±826 [#]	1605 ±599 [#]	855 ±106 [#]
CN (#/Fiber)	0.035 ±0.053	0.038 ±0.016	0.049 ±0.019	0.044 ±0.025	0.049 ±0.027	0.030 ±0.015	0.013 ±0.005
Type II Fibers (%)	17.7 ±8.6	14.2 ±5.6	31.3 ±7.0 [ab]	27.7 ±5.0 [ab]	21.0 ±14 [*]	20.8 ±4.7 [*]	21.4 ±4.7 [*]
Type I Fibers (%)	82.3 ±8.6	85.8 ±5.6	68.7 ±7.0 [ab]	72.3 ±5.0 [ab]	79.0 ±14 [*]	79.2 ±4.7 [*]	78.6 ±4.7 [*]

Values are mean ± SD for averaged fiber cross-sectional area (CSA, μm^2), number of central nuclei (CN, #/fiber), type II and type I muscle fibers (%). [b] $p < 0.01$ vs. baseline; [a] $p < 0.01$ vs. age-matched; [#] $p < 0.001$ vs. age-matched; [*] $p < 0.05$ vs. HLS.

Table 5.3. Effects of C-R Ratio on Properties of Gastrocnemius & Soleus

	Baseline	Age-matched	HLS	1/4 C-R	2/8 C-R	4/6 C-R	2/28 C-R
Gastrocnemius							
CSA (μm^2)	2859 ±495	2688 ±554	2217 ±239 [a]	2233 ±397 [a]	2385 ±856 [a]	1956 ±262 [a]	2097 ±291 [a]
CN (#/Fiber)	0.009 ±0.005	0.015 ±0.014	0.020 ±0.011	0.017 ±0.014	0.014 ±0.011	0.017 ±0.005	0.018 ±0.011
Type II Fibers (%)	67.9 ±14	71.0 ±3.3	75.8 ±8.1	77.9 ±3.4	74.3 ±4.4	73.4 ±5.0	74.0 ±6.4
Type I Fibers (%)	32.1 ±14	29.0 ±3.3	21.5 ±8.1	22.1 ±3.4	25.7 ±4.4	26.6 ±5.0	26.0 ±6.4
Soleus							
CSA (μm^2)	3968 ±873	3819 ±722	1661 ±299 [#]	1731 ±319 [#]	1607 ±324 [#]	1632 ±202 [#]	1637 ±481 [#]
CN (#/Fiber)	0.034 ±0.005	0.043 ±0.014	0.048 ±0.017	0.032 ±0.017	0.035 ±0.025	0.037 ±0.031	0.051 ±0.025
Type II Fibers (%)	18.8 ±21	12.9 ±6.7	26.9 ±5.8 [ab]	20.1 ±7.8	15.2 ±8.9 [*]	16.9 ±3.9 [*]	23.7 ±8.4 [ab]
Type I Fibers (%)	81.2 ±21	87.1 ±6.7	73.1 ±5.8 [ab]	79.9 ±7.8	84.8 ±8.9 [*]	83.1 ±3.9 [*]	76.3 ±8.4 [ab]

Values are mean ± SD for averaged fiber cross-sectional area (CSA, μm^2), number of central nuclei (CN, #/fiber), type II and type I muscle fibers (%). [b] $p < 0.01$ vs. baseline; [a] $p < 0.01$ vs. age-matched; [#] $p < 0.001$ vs. age-matched; [*] $p < 0.05$ vs. HLS.

Figure 5.7

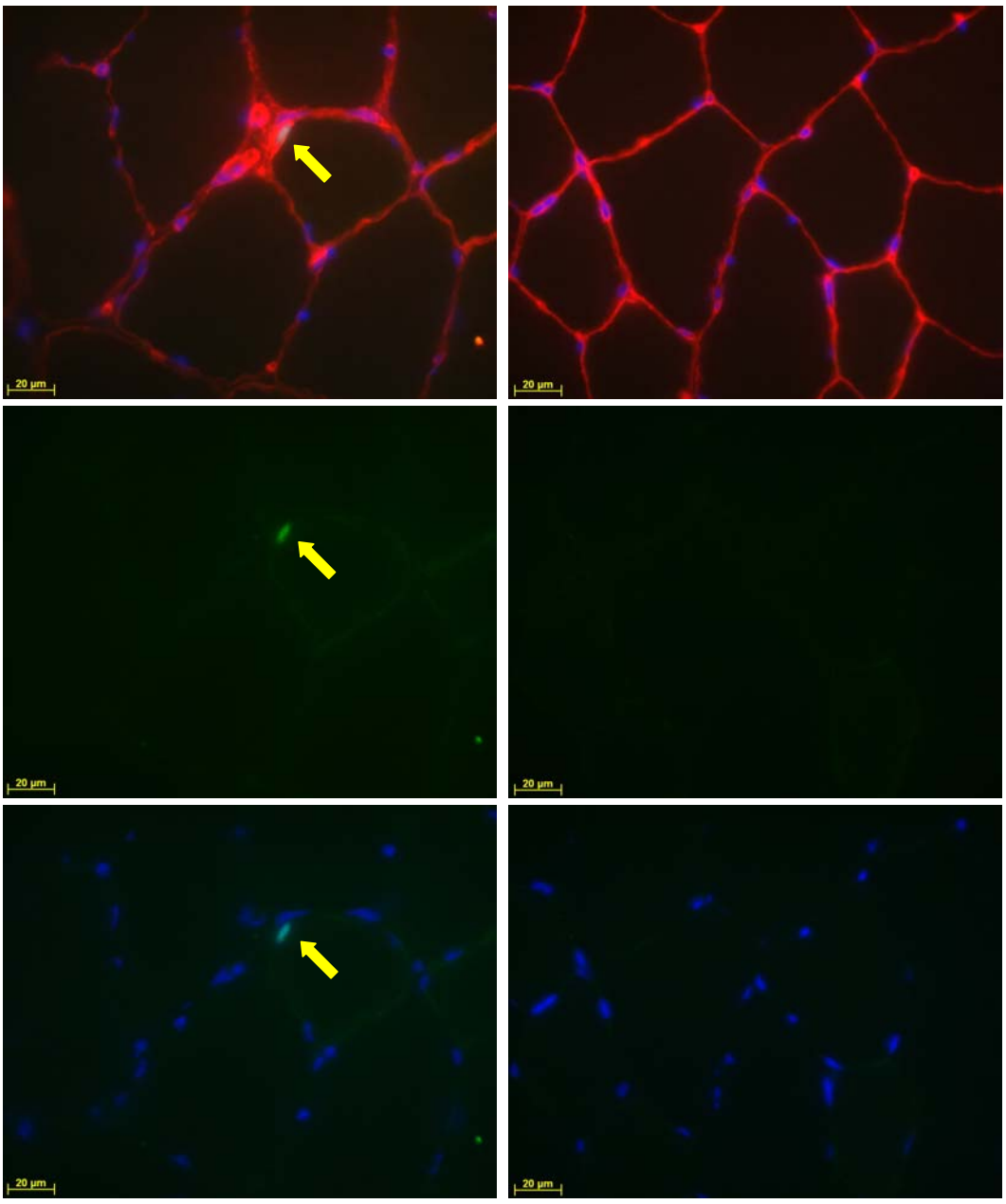

Representative immuno-stained images of the quadriceps, taken at 630X magnification. Anti-laminin staining of basement membrane is shown in red; Anti-Pax staining for satellite cell (arrow) is shown in green. Myonuclei are stained in blue with DAPI. Scale bar = 20 µm.

VI. The Effects of Dynamic Muscle Stimulation on Skeletal Muscle Microvasculature in a Disuse Model

Abstract

Alteration in the microvascular system may affect musculoskeletal tissues adaptation. The objective of this study is to determine the effect of dynamic muscle stimulation on the capillary supply within skeletal muscle. The capillary analyses were performed on the quadriceps muscles that were from the age-matched control, hindlimb suspended (HLS), and HLS with 50 Hz muscle stimulation with 2/8 contraction-to-rest ratio. Capillary were visualized via immunohistochemical and ATPase stainings. The capillary density and capillary-to-fiber ratio were evaluated. Our results showed that there was no difference in capillary between the three groups. However, the lack of daily activity significantly decreased the capillary-to-fiber ratio, while daily stimulation could maintain this ratio similar to the level measured in normal muscle. Overall, capillary quantification suggests that dynamic muscle stimulation has the potential to regulate vascular adaptation which may further protect the musculoskeletal system under a condition of functional disuse.

Introduction

Skeletal muscle blood flow increases during contraction and restore to normal level during relaxation [89]. Capillary supply of muscle is important for delivery of oxygen and other nutrients to muscle cells [183, 184]. The relationship between the microvasculature and functional demand, whether it is decreased during disuse or increased during exercise, is unclear. Many contradicted results have been reported for the change in the number of capillaries [185-187].

Parameters that are frequently evaluated include the number of capillary per area and capillary-to-fiber (C/F) ratio. Studies have shown that decreased muscle use led to muscle atrophy, capillary number reduction, and increased damage to the capillary endothelium [187-189]. In contrast, other studies that had undergone various forms of disuse, i.e., chemical-induced, denervation, hindlimb suspension, induced significant muscle loss but maintained microvascular network [189-191]. When taken the number of fibers into account, the C/F ratio demonstrated an increase by the augmentation of muscle activity and a decrease by disuse [86, 192]. The inconsistency in acquiring the effect of capillary in response to various functional demands remains uncertain. The different in experimental designs, duration of study, types of stimuli, and muscle examined may contribute to the inconsistency.

Exercise and electrical stimulation can induce adaptations in both skeletal and muscular tissues, by altering their morphologies and biochemical properties [133]. Increased capillary supply has been observed in hypertrophic muscles in chickens, mice, and rats [193-195]. Although the mechanism for capillary growth is not know, it has been postulated that fluid flow-induced mechanical factors, such as shear stress and tension, are responsible to the microvascular adaptation [141]. Results proven that electrical stimulation with a specific stimulation frequency can augment intramuscular and intramedullary pressure, increased blood flow in muscle and perhaps to bone [64, 141].

We have previously showed that dynamic muscle stimulation (MS) at 50 Hz with a contraction-to-rest (C-R) ratio of 2 to 8 seconds can prevent bone loss and induce muscle fiber transformation. Thus, the objective of this study is to determine in effect of

this optimized MS signal on the skeletal muscle microvasculature. In addition to musculoskeletal adaptation, we hypothesized that the optimal signal of MS can also generate changes to the microvasculature.

Materials and methods

All experimental procedures were approved by the Laboratory Animal Use Committee at Stony Brook University. Details on the experimental design were previously described. Animals were either allowed normal activities, subjected to 4 weeks of hindlimb suspension (HLS) or HLS with MS at 50 Hz with 2/8 C-R ratio. Stimulation was applied at 2 V with 1 ms square pulse for 10 minutes per day, 5 days per week, for a total of 4 weeks. The vasculatures of the quadriceps muscle were assessed. The tissues were embedded with OCT compound (Tissue Tek), frozen in liquid nitrogen-chilled isopentane, and stored at -80°C until analysis.

Immunohistochemistry

Multiple 8 μm cross-sections were cut from the Quad muscles for laminin, von Willebrand factor (vWF), and CD31 immuno-staining. The primary antibodies anti-laminin (anti-rabbit from Sigma, St. Louis, MO, anti-mouse from Developmental Studies Hybridoma Bank, Iowa City, IA), anti-vWF (anti-rabbit from Sigma, St. Louis, MO), and anti-CD31 (anti-mouse from Millipore, Bedford, MA) were used. Laminin is a marker for basement membranes. vWF is a blood glycoprotein, that is required for normal homeostasis, and reacts specifically with the cytoplasm of endothelial cells. CD31, also called platelet-endothelial cell adhesion molecule-1, is a transmembrane glycoprotein and a surface marker for endothelial cells. Two secondary antibodies were applied (Vector

Laboratories, Burlingame, CA); the rat adsorbed fluorescein anti-mouse IgG was used to detect for laminin purchased from DSHB and CD31, while texas red anti-rabbit IgG for laminin purchased from Sigma and vWF. Working dilutions of these antibodies were 1:500 for laminin (Sigma) and 1:200 for all other primary and secondary antibodies in 1% bovine serum albumin (BSA), diluted with 1X phosphate-buffered saline (PBS). The immuno-staining of vWF or CD31 and laminin was performed simultaneously. Tissue sections were first fixed with acetone for 15 minutes, air dried, and blocked with 1% BSA for 1 hour. Primary antibodies were incubated with the sections overnight at 4°C. The secondary antibodies were incubated for one hour at room temperature. Lastly, the sections were dehydrated with a series of ethanol (70%, 95%, and 100%), cleared with xylene, and mounted with Vectashield with DAPI (Vector Laboratories, Burlingame, CA). Muscle fibers and blood vessels were visualized with a Zeiss microscope (AxioVision 4.5, Germany) with the FITC (laminin from DSHB and CD31), TRITC (laminin from Sigma and vWF), and DAPI (myonuclei) filters.

Histochemical Analysis

Additional 8 μm cross-sections were cut for demonstration of the muscle capillary network using hischemical ATPase method. A modified ATPase protocol has been developed to simultaneously stain for capillaries and fiber types [196, 197]. However, we further modified the protocol to clearly visualize capillary only. The sections were immersed into acid preincubation solution at a pH value of 4.2. All sections were then incubated with ATP solution at a pH value of 9.4. Twenty cross-sectional bright field images (150 μm x 120 μm) were captured from each muscle section with a Zeiss microscope (AxioVision 4.5, Germany) at 630X magnification. All evaluations were

performed with the ImageJ software, downloaded from the NIH, website. For each analysis, 75 – 100 fibers were assessed per muscle section.

Statistical Analyses

All of the histochemical results are reported as mean ± SD. For each analysis, significance differences between groups were determined using the SigmaStat 2.03 program (Systat Software Inc, San Jose, CA). Analysis of variance (ANOVA) with Tukey's pairwise multiple comparison tests was performed. The level of significance was considered at $p < 0.05$.

Results

Immunohistochemistry

Blood vessels and basement membrane of the quadriceps muscles were visualized by vWF (Red) and laminin (Green) staining (Figure 6.1), and CD31 (Green) and laminin (Red) staining (Figure 6.2). Both vWF and CD31 successfully stained larger vessels. However, capillaries were difficult to capture. Thus, quantification of capillary density and C/F ratio were not performed based on these fluorescent sections.

Capillary Density

From the modified ATPase staining, capillaries were clearly observed in black and counted (Figure 6.3). Figure 3 shows representative cross-sectional images of the quadriceps from HLS and HLS with MS. The capillary density was not statistically different between age-matched, HLS, and stimulated groups. However, the capillary density was decreased by 9% due to 4 weeks of disuse, and only 3% with the stimulation (Figure 6.4).

Capillary to Fiber Ratio (C/F)

Taking into consideration that the numbers of muscle fibers, in a given region, were different between the age-matched control, HLS, and stimulated animals, the C/F ratios were evaluated (Figure 6.4). The CF ratio of the HLS group was significantly lower than the normal control ($p < 0.01$) by 19%. Although the C/F ratio was not fully maintain by MS at 50 Hz, it showed a 16% higher C/F ratio comparing to the HLS animals ($p < 0.05$).

Discussion

The present data indicated that dynamic electrical stimulation was able to preserve the skeletal muscle microvasculature even with the occurrence of muscle atrophy induced by disuse. MS at 50 Hz with 2/8 C-R ratio, for 10 minutes per day, was unable to prevent the reduction in muscle weight and fiber size. Yet, the stimulation can maintain the fiber type I and type II ratio, and partially inhibited the decrease in capillary supply.

For this study, we chose three different staining methods to visualize the capillaries. vWF has been a well known endothelial cells and often used to stain human skeletal muscle biopsies [198, 199]. Although it has been widely used, some studies claimed that vWF could not capture some endothelial cell under certain conditions and only larger blood vessels were successfully stained [200]. Similar to our results, vWF clearly stained vessels of approximately 50 to 100 μm. The detection of capillary was questionable. The antibody incubation time with the sections was suggested to alter the staining quality, but was not confirmed. CD31 has also been widely studied and shown to express strongly at endothelial cell-cell junction, on platelets and leukocytes [201]. To our surprise, the quality

of CD31 immuno-staining was the lowest and only large vessels were stained. Perhaps further optimization of the protocol may provide better insight in capillary detection with CD31. The use of histochemical ATPase method evidently demonstrated the capillaries surround the muscle fiber via endothelial ATPase enzyme activity. ATPase method is often employed to differentiate muscle fiber type via the change of pH values. It has been found that this method, with some modification, is capable to stain blood vessels as well [196, 197]. Since quadriceps contained abundant of type II fiber, alkaline ATPase method (pH of 9.4) would not be suitable since both fibers and vessels would stain black. Here, we used a pH value of 4.2, which eliminate any enzyme activity of the fiber thus only blood vessels, including capillary were visualized.

The two parameter, capillary density and C/F ratio, have been accepted for general capillary quantification [202]. However, the change in capillary density may not truly reflect the change in capillary number in a given region, especially if there is an alteration in fiber size. Many studies on the effects of aging and disuse have reported no change in capillary density while there was a significant decrease in C/F ratio [86, 203, 204]. Others have measured the capillary luminal diameter and demonstrated that average capillary diameter in rat soleus was 5.5 μm [203, 205]. Two weeks HLS was significantly reduced the capillary diameter to approximately 3 μm [204]. It was reported that the critical diameter is 2.45 μm for rat red blood cell to pass through and suggested that reduction in capillary luminal diameter would decrease oxygen delivery [206]. Unfortunately, the capillary luminal diameter could not be evaluated from our experiment due to the lack of perfusion, thus occlusion of vessels might occur.

In healthy adult, 30 minutes daily electrical stimulation at 45 to 60 Hz increased quadriceps muscle fiber area and type II fibers [93]. The study also confirmed an augment in C/F ratio. More interestingly the increase in C/F ratio was specific to type II muscle fiber. Isometric stimulation at 4 Hz increased C/F ratio but did not affect the muscle mechanical properties [193]. It was concluded that mechanical stimulus induce capillary growth by regulating signaling molecules, i.e., fibroblast growth fact. It is evident that mechanical stimuli applied to skeletal muscle can produce changes in the vasculature [85, 207, 208]. The effects were highly depended on the type and magnitude of the stimulus [207, 208]. High-frequency, low-magnitude mechanical signals, such as vibration, has been shown to be anabolic to bone [115, 139]. However, 45 Hz whole body vibration decreased the number of capillary per fiber and the degree of suppression was varied at the different region of the soleus muscle [209]. This observation suggested that there might be local hemodynamic effect within the muscular tissue thus regional changes of vasculature may be different. We have also demonstrated that 50 Hz MS signals increased intramedullary pressure and induced anti-catabolic effect in disused trabecular bone. Although our short duration stimulus did not have significant effect in protecting skeletal morphology, the stimulation increased type II fibers. Most importantly, the augmentation of capillary supply suggests enhancement of fluid flow in the muscular tissues and perhaps to bone.

In conclusion, this study established the effect of dynamic muscle contraction on skeletal muscle microvasculature. The various analyses also demonstrated the relevant technique in performing capillary quantification. Although the mechanism in which mechanical stimuli alter skeletal, muscular, and vascular adaptations is not clearly defined,

our findings indicate the possibility in using dynamic MS to maintain physiological functions for this complex system.

Figures

Figure 6.1

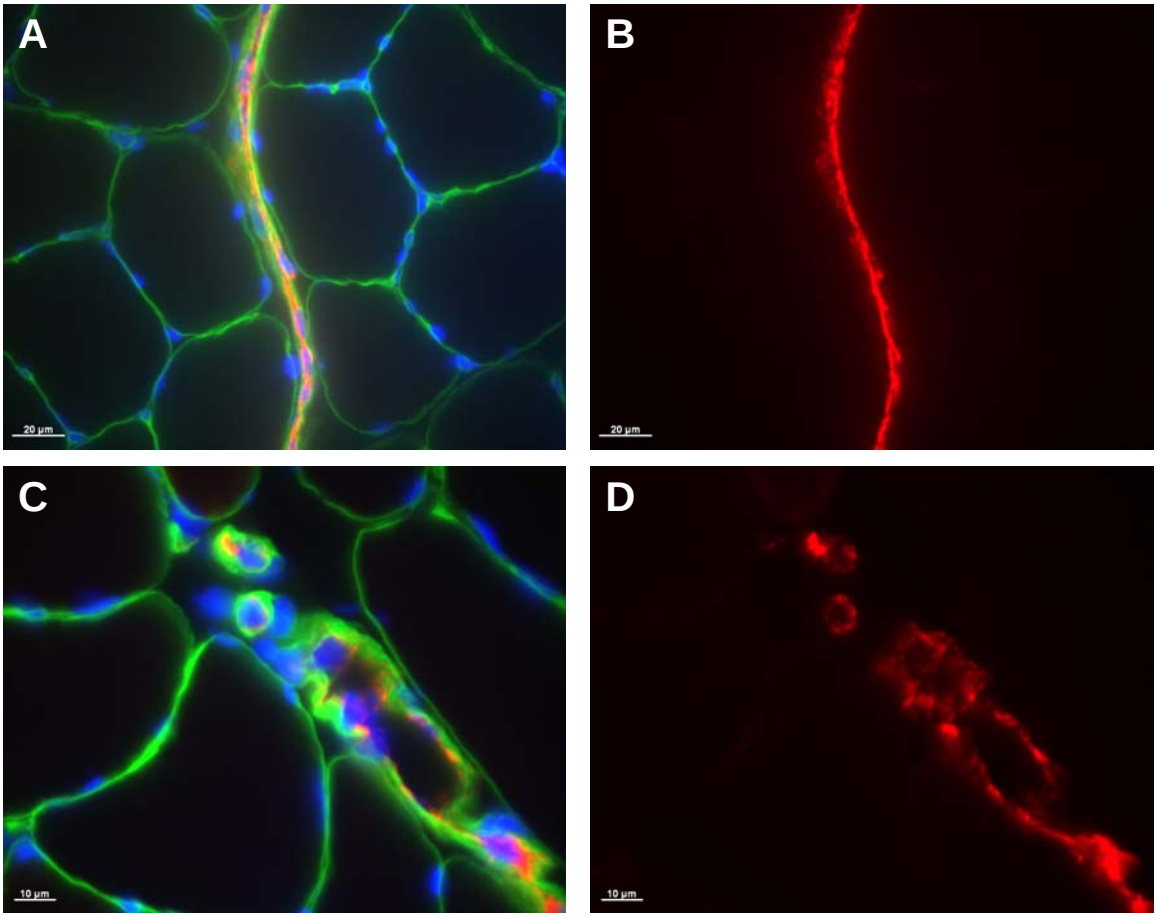

Representative immuno-stained images of the quadriceps, taken at 630X (A & B) and 1000X (C & D) magnification. Anti-laminin staining of basement membrane is shown in green; Anti-vWF staining for blood vessel is shown in red. Myonuclei are stained in blue with DAPI. Scale bar = 20 µm for A & B and 10 µm for C & D.

Figure 6.2

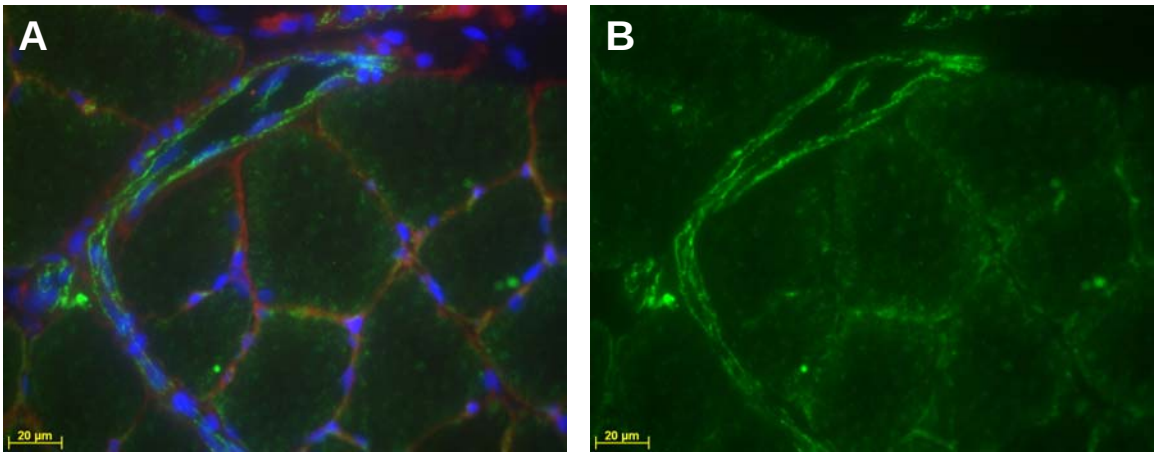

Representative immuno-stained images of the quadriceps, taken at 630X magnification. Anti-laminin staining of basement membrane is shown in red; Anti-CD31 staining for blood vessel is shown in green. Myonuclei are stained in blue with DAPI. Scale bar = 20 µm.

Figure 6.3

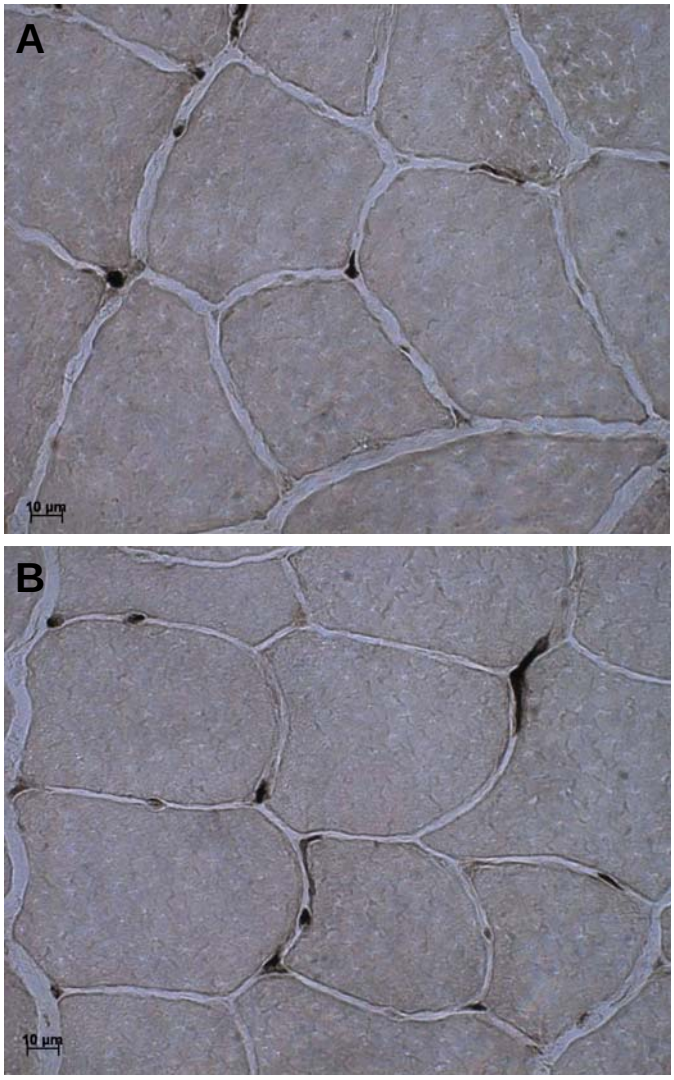

Representative ATPase stained capillary images of the quadriceps, taken at 1000X magnification. HLS (A) and HLS + 50 Hz with 2/8 C-R ratio (B). Sections were stained with acid solution (pH 4.2). Capillaries are shown in black. Scale bar = 10 μm.

Figure 6.4

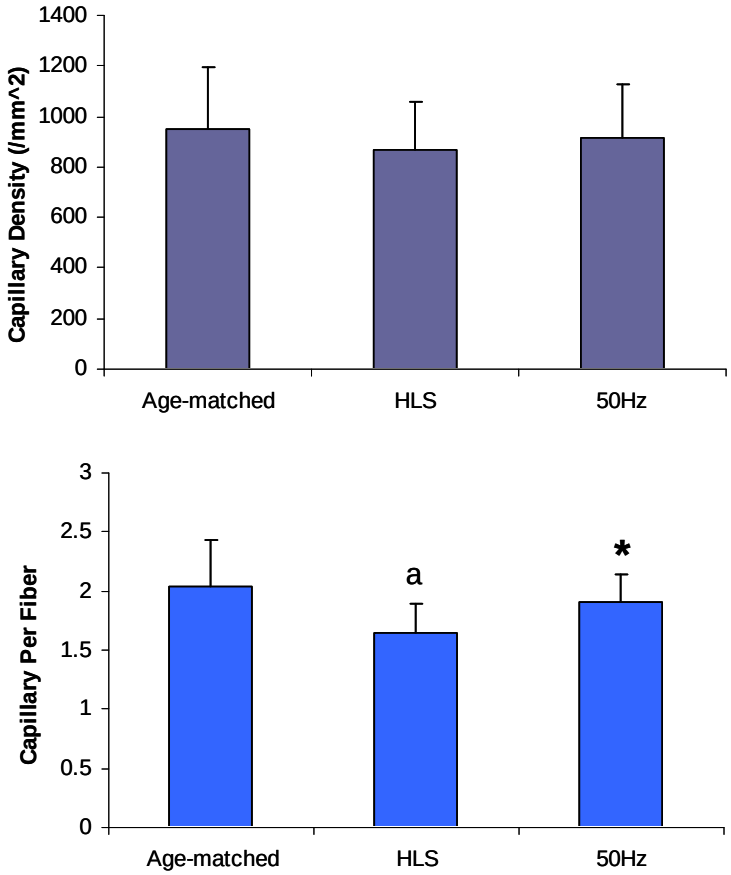

Graphs show mean + SD values for capillary density (/mm^2) and the number of capillary per fiber (C/F ratio). [a] p <0.01 vs. age-matched; [*] p <0.05 vs. HLS.

VII. Global Discussion

The regulatory potentials of dynamic electrical muscle stimulation (MS) on musculoskeletal adaptation in a disuse environment were investigated in this dissertation. In order to optimize the effectiveness of the stimulus, we designed two *in vivo* experiments which were to vary the stimulation frequency and the contraction-to-rest ratio (C-R) ratio. The skeletal, muscular, and vascular tissues of the lower extremities were evaluated and presented via the four specific aims. Our results indicated that dynamic MS can indeed positively induce adaptive responses in these tissues. In particular, the degree of responsiveness was differed depended on the applied stimulation frequency and C-R ratio. Four major conclusions can be drawn from these studies:

1. Stimulation at mid frequencies, i.e., 20 Hz and 50 Hz, inhibited trabecular bone loss and deterioration that would otherwise devastated by 4 weeks of functional disuse. The inhibition was demonstrated by the increases in bone volume fraction, connectivity, trabecular number, and the decrease in trabecular spacing. Yet, stimulation at low frequency, such as 1 Hz, had no protective effect against disuse.
2. 50 Hz stimulation with 2 seconds contraction followed by 8 seconds rest insertion showed the greatest percentage of prevention on the unloaded trabecular bone. On the other hands, tetanic contraction applied with a C-R ratio of 2/28 showed the smallest percentage changes against disuse.
3. The 10 minutes daily stimulation did not ease skeletal muscle atrophy. The fiber size of the stimulated muscle was similar to the one subjected to disuse. However, the stimulations at mid to high frequencies increased fast-twitch fibers in the quadriceps and soleus.

4. Compared to the hindlimb suspended animals, MS at 50 Hz with 2 seconds contraction followed by 8 seconds augmented the number of capillary per fiber in the quadriceps, but showed no difference in capillary density.

These conclusions clearly illustrated the possibility of this non-invasive mechanical intervention to maintain morphological and functional modifications in multiple tissues, i.e., bone, muscle, and vessels, which were affected by the lack of weight bearing activity. Our results implied an intimate relationship between the musculoskeletal and vascular systems. Dynamic stimulation applied to the skeletal muscle may initiate a cascade of events that lead to changes observed in the four studies.

It is well known that rhythmic exercise leads to skeletal muscle hyperemia [140, 210-213]. The mechanism relates to the increase in blood flow due to the onset of exercise has been researched extensively but remain elusive. Some said contraction generates a pressure gradient within the microvasculature thus enhancing fluid perfusion [214]. Yet some showed the increased blood flow is independent of venous pressure and that rapid vasodilation was measured using Doppler ultrasound [212]. Perhaps, both mechanisms are involved, where the mechanical activity of muscle contraction and relaxation contribute to the pressure change and vasodilatory signals determine vascular conductance [213]. Regardless of the mechanism, the increase in blood flow is indisputable. Whether it is the increase in shear stress or the existence of vasodilatory agents, such as nitric oxide, prostaglandins, contraction as a function of frequency and duration initiates microvasculature adaptation [93, 202]. The augment in the capillary number per fiber and capillary luminal diameter are two examples [193, 215, 216]. In

addition, enhancements of both convective and diffusive transports within the microvascular bed have been exhibited in stimulated muscle [217].

Increased capillary supply improves oxygen delivery, which in turn induce adaptation to the neighboring muscular tissue. Although muscle atrophy due to inactivity was not inhibited in our study, the biochemical transformation suggests the short term stimulation can regulate muscle properties. Other studies with longer duration of stimulation prevented weight loss in soleus and tibialis anterior [98, 166]. Stimulation with higher frequency (45 – 100 Hz) can maintain muscle mechanical properties, i.e. twitch and tetanic force, as well as reduce muscle weight loss and fiber CSA [83, 167]. Thus, it is reasonable to assume that stimulation duration is another crucial factor, in addition to frequency and C-R ratio, within the protocol to induce muscle morphological alteration. Perhaps, increasing the contraction from 10 minutes to 30 minutes may prevent the atrophy produced by the four weeks hindlimb suspension [93].

We have previously measured the increased intramedullary pressure within the femur as a function of the stimulation frequency. Our results showed that mid-frequency stimulation augmented the ImP by 2 to 4 folds. Concurrently, low-level bone strain was recorded, where mid-frequency stimulation generated physiological strain of below 100 με. The fluid and mechanical responses induced by dynamic MS may lead to an initiation of mechanotranductive reactions.

Earlier strain data demonstrated animal's daily activity comprises of few high-magnitude strain events and thousand of low-magnitude (< 10 με) strain events [78]. The data implied that the main contribution to strain history of a bone arises from muscle posture activity. It is possible that by providing an external stimulus to deliver low-level

bone strain may compensate for the posture muscle activity in a functional disuse environment. Speculation on how bone cells sense extremely small deformation has been proposed, in which signals are being amplified in the lacunar-canalicular porosity and sensed by osteocyte cell processes [218]. Osteocyte may then transduces the amplified signals to influence expression at the molecular level, i.e., growth factor, hormone [219].

Another mechanotransduction pathway, bone fluid flow, has also been discussed. Hindlimb suspension caused a reduction in femoral ImP [117]. It is hypothesized that interstitial bone fluid flow is required for cellular perfusion. Both blood flow and mechanically induced fluid flow are needed for normal metabolic activity. Stimulation enhances bone fluid flow, which may influence bone remodeling. The increased ImP measured induced by dynamic MS amplified the interstitial fluid flow through the trabecular bone. Subsequently, bone cells responses to the change in shear force, activating a series of aurtocrine/paracrine signaling cascade to modulate the remodeling processes [119, 220, 221]. Likewise, bone perfusion may also initiate bone remodeling via vascular mechanism. Endothelium releases agents that further affect fluid flow to bone. Blood vessels locate close to the basic multicelluar units, where remodeling activity takes place [222]. In our experiments, MS may ultimately inhibit the osteoclast activity since 50 Hz signal partially maintain bone loss against disuse but not through increasing bone formation.

We emphasized that the studies presented in this dissertation provide fundamental understanding of the effects of dynamic MS on skeletal, muscular, and vascular tissues. However, there are a number of limitations that need to be addresses and considered for future studies. First is to access the capillary luminal diameter. The capillary luminal

diameter may clarify the vascular perfusion in relation to MS-altered blood flow and nutrient exchanges. To access the luminal diameter, a perfusion fixation method should be use at the end of the study to avoid the occlusion of vessels after euthanasia. The perfusion fixation method may also be the solution for our second limitation. The potential anti-catabolic response in the trabecular bone needs to be evaluated. The existence of osteoclast on bone surface may be counted with the use of goldner trichrome stain to differentiate the osteoclast by their multinucleated morphology. The golden standard to analyze resorption activity is to stain for tartrate-resistant acid phosphatase (TRAP), which is highly expressed in osteoclast. The perfusion fixation may aid to preserve the enzymatic activity. Lastly, previous studies clearly demonstrate that electrical stimulation has the capacity to reduce skeletal muscle atrophy due to disuse. This was not evident in our analyses, in which the short duration stimulation was not sufficient to maintain the significant declined in fiber area, due to the 4 weeks hindlimb suspension. However, the effective threshold of the stimulation duration may be elucidated by an additional experiment to vary the duration and determine its effect on the skeletal, muscular, and vascular tissues.

Disuse osteoporosis associates with the alternations in musculoskeletal and, perhaps, vascular systems. It is important to develop a non-invasive intervention that has the ability to counteract tissues loss and deteriorations in multiple physiologic systems. Given the results provided, dynamic MS may be such intervention. It has the capability to inhibit trabecular bone loss and maintain its microstructure, initiate protein level changes to retain muscle fiber types, and induce microvascular adaptation by increasing the capillary-to-fiber ratio. Future studies should examine additional parameters that may optimize the protocol to intensify the adaptive responses.

VIII. References

[1] NIH Consensus Development Panel on Osteoporosis Prevention, Diagnosis, and Therapy, March 7-29, 2000: highlights of the conference. South Med J 2001;94: 569-73.
[2] Lin JT, Lane JM. Osteoporosis: a review. Clin Orthop Relat Res 2004;126-34.
[3] Walsh MC, Hunter GR, Livingstone MB. Sarcopenia in premenopausal and postmenopausal women with osteopenia, osteoporosis and normal bone mineral density. Osteoporos Int 2006;17: 61-7.
[4] Reginster JY, Burlet N. Osteoporosis: a still increasing prevalence. Bone 2006;38: S4-9.
[5] National Osteoporosis Foundation. In; 2006.
[6] FDA. Boning up on osteoporosis. In: FDA Consumer Magazine; 1996.
[7] Riggs BL, Melton LJ, 3rd. The worldwide problem of osteoporosis: insights afforded by epidemiology. Bone 1995;17: 505S-511S.
[8] Ray NF, Chan JK, Thamer M, Melton LJ, 3rd. Medical expenditures for the treatment of osteoporotic fractures in the United States in 1995: report from the National Osteoporosis Foundation. J Bone Miner Res 1997;12: 24-35.
[9] Melton LJ, 3rd. The prevalence of osteoporosis: gender and racial comparison. Calcif Tissue Int 2001;69: 179-81.
[10] Tracy JK, Meyer WA, Flores RH, Wilson PD, Hochberg MC. Racial differences in rate of decline in bone mass in older men: the Baltimore men's osteoporosis study. J Bone Miner Res 2005;20: 1228-34.
[11] Seeman E, Eisman JA. 7: Treatment of osteoporosis: why, whom, when and how to treat. The single most important consideration is the individual's absolute risk of fracture. Med J Aust 2004;180: 298-303.
[12] Ullom-Minnich P. Prevention of osteoporosis and fractures. Am Fam Physician 1999;60: 194-202.
[13] Buckwalter J, Cooper R. Bone structure and function: American Academy of Orthopedic Surgeons; 1987.
[14] Duan Y, Beck TJ, Wang XF, Seeman E. Structural and biomechanical basis of sexual dimorphism in femoral neck fragility has its origins in growth and aging. J Bone Miner Res 2003;18: 1766-74.
[15] Khosla S, Melton LJ, 3rd, Atkinson EJ, O'Fallon WM. Relationship of serum sex steroid levels to longitudinal changes in bone density in young versus elderly men. J Clin Endocrinol Metab 2001;86: 3555-61.
[16] Modlesky CM, Majumdar S, Narasimhan A, Dudley GA. Trabecular bone microarchitecture is deteriorated in men with spinal cord injury. J Bone Miner Res 2004;19: 48-55.
[17] Riggs BL, Khosla S, Melton LJ, 3rd. A unitary model for involutional osteoporosis: estrogen deficiency causes both type I and type II osteoporosis in postmenopausal women and contributes to bone loss in aging men. J Bone Miner Res 1998;13: 763-73.
[18] Martin R, Burr D, Sharkey M. Skeletal tissue mechanics. New York: Springer-Verlag; 1998.
[19] Buckwalter J, Glimcher M, Cooper R, Recker R. Bone biology I: Structure, blood supply, cells, matrix, and mineralization; 1996.

[20] Bostrom M, Boskey A, Kaufman J, Einhorn T. Form and Function of Bone: Orthopaedic Basic Science; 2001.
[21] Nordin M, Frankel V. Biomechanics of bone; 1989.
[22] Whiteside L. Circulation in bone. In: Evarts C, editor. Surgery of the musculoskeletal system. New York: Churchill Livingstone; 1983.
[23] Otter MW, Qin YX, Rubin CT, McLeod KJ. Does bone perfusion/reperfusion initiate bone remodeling and the stress fracture syndrome? Med Hypotheses 1999;53: 363-8.
[24] Oni OO, Gregg PJ. The relative contribution of individual osseous circulations to diaphyseal cortical blood supply. J Orthop Trauma 1990;4: 441-8.
[25] Brookes M. The blood supply of bone: an approach to bone biology. London: Butterworth; 1998.
[26] Parfitt AM. Osteonal and hemi-osteonal remodeling: the spatial and temporal framework for signal traffic in adult human bone. J Cell Biochem 1994;55: 273-86.
[27] Lian J, Stein G. Osteoblast Biology; 2001.
[28] Vaananen HK, Zhao H, Mulari M, Halleen JM. The cell biology of osteoclast function. J Cell Sci 2000;113 (Pt 3): 377-81.
[29] Aarden EM, Burger EH, Nijweide PJ. Function of osteocytes in bone. J Cell Biochem 1994;55: 287-99.
[30] Frost H. Introduction to a new skeletal physiology. Pueblo: Pajaro Group; 1995.
[31] Keynes R. Nerve and muscle. New York: Cambridge University Press; 1991.
[32] Matthews G. Neurobiology: molecules, cells, and systems. Malden: Blackwell Science, Inc; 2001.
[33] Herzog W, Leonard TR, Joumaa V, Mehta A. Mysteries of muscle contraction. J Appl Biomech 2008;24: 1-13.
[34] Giangregorio L, Blimkie CJ. Skeletal adaptations to alterations in weight-bearing activity: a comparison of models of disuse osteoporosis. Sports Med 2002;32: 459-76.
[35] Iwamoto J, Takeda T, Sato Y. Interventions to prevent bone loss in astronauts during space flight. Keio J Med 2005;54: 55-9.
[36] Lang T, LeBlanc A, Evans H, Lu Y, Genant H, Yu A. Cortical and trabecular bone mineral loss from the spine and hip in long-duration spaceflight. J Bone Miner Res 2004;19: 1006-12.
[37] LeBlanc A. Summary of research issues in human studies. Bone 1998;22: 117S-118S.
[38] Collet P, Uebelhart D, Vico L, Moro L, Hartmann D, Roth M, Alexandre C. Effects of 1- and 6-month spaceflight on bone mass and biochemistry in two humans. Bone 1997;20: 547-51.
[39] Vico L, Collet P, Guignandon A, Lafage-Proust MH, Thomas T, Rehaillia M, Alexandre C. Effects of long-term microgravity exposure on cancellous and cortical weight-bearing bones of cosmonauts. Lancet 2000;355: 1607-11.
[40] Lazo MG, Shirazi P, Sam M, Giobbie-Hurder A, Blacconiere MJ, Muppidi M. Osteoporosis and risk of fracture in men with spinal cord injury. Spinal Cord 2001;39: 208-14.
[41] Dauty M, Perrouin Verbe B, Maugars Y, Dubois C, Mathe JF. Supralesional and sublesional bone mineral density in spinal cord-injured patients. Bone 2000;27: 305-9.

[42] Kiratli BJ, Smith AE, Nauenberg T, Kallfelz CF, Perkash I. Bone mineral and geometric changes through the femur with immobilization due to spinal cord injury. J Rehabil Res Dev 2000;37: 225-33.
[43] Wilmet E, Ismail AA, Heilporn A, Welraeds D, Bergmann P. Longitudinal study of the bone mineral content and of soft tissue composition after spinal cord section. Paraplegia 1995;33: 674-7.
[44] LeBlanc A, Lin C, Shackelford L, Sinitsyn V, Evans H, Belichenko O, Schenkman B, Kozlovskaya I, Oganov V, Bakulin A, Hedrick T, Feeback D. Muscle volume, MRI relaxation times (T2), and body composition after spaceflight. J Appl Physiol 2000;89: 2158-64.
[45] LeBlanc A, Rowe R, Schneider V, Evans H, Hedrick T. Regional muscle loss after short duration spaceflight. Aviat Space Environ Med 1995;66: 1151-4.
[46] Narici MV, Kayser B, Barattini P, Cerretelli P. Changes in electrically evoked skeletal muscle contractions during 17-day spaceflight and bed rest. Int J Sports Med 1997;18 Suppl 4: S290-2.
[47] Gorgey AS, Dudley GA. Skeletal muscle atrophy and increased intramuscular fat after incomplete spinal cord injury. Spinal Cord 2006;
[48] Shah PK, Stevens JE, Gregory CM, Pathare NC, Jayaraman A, Bickel SC, Bowden M, Behrman AL, Walter GA, Dudley GA, Vandenborne K. Lower-extremity muscle cross-sectional area after incomplete spinal cord injury. Arch Phys Med Rehabil 2006;87: 772-8.
[49] Edgerton VR, Zhou MY, Ohira Y, Klitgaard H, Jiang B, Bell G, Harris B, Saltin B, Gollnick PD, Roy RR, et al. Human fiber size and enzymatic properties after 5 and 11 days of spaceflight. J Appl Physiol 1995;78: 1733-9.
[50] Stewart BG, Tarnopolsky MA, Hicks AL, McCartney N, Mahoney DJ, Staron RS, Phillips SM. Treadmill training-induced adaptations in muscle phenotype in persons with incomplete spinal cord injury. Muscle Nerve 2004;30: 61-8.
[51] Zhou MY, Klitgaard H, Saltin B, Roy RR, Edgerton VR, Gollnick PD. Myosin heavy chain isoforms of human muscle after short-term spaceflight. J Appl Physiol 1995;78: 1740-4.
[52] Greeves JP, Cable NT, Reilly T, Kingsland C. Changes in muscle strength in women following the menopause: a longitudinal assessment of the efficacy of hormone replacement therapy. Clin Sci (Lond) 1999;97: 79-84.
[53] Lafage-Proust MH, Collet P, Dubost JM, Laroche N, Alexandre C, Vico L. Space-related bone mineral redistribution and lack of bone mass recovery after reambulation in young rats. Am J Physiol 1998;274: R324-34.
[54] Allen MR, Bloomfield SA. Hindlimb unloading has a greater effect on cortical compared with cancellous bone in mature female rats. J Appl Physiol 2003;94: 642-50.
[55] Bloomfield SA, Allen MR, Hogan HA, Delp MD. Site- and compartment-specific changes in bone with hindlimb unloading in mature adult rats. Bone 2002;31: 149-57.
[56] Sessions ND, Halloran BP, Bikle DD, Wronski TJ, Cone CM, Morey-Holton E. Bone response to normal weight bearing after a period of skeletal unloading. Am J Physiol 1989;257: E606-10.

[57] Vico L, Bourrin S, Very JM, Radziszowska M, Collet P, Alexandre C. Bone changes in 6-mo-old rats after head-down suspension and a reambulation period. J Appl Physiol 1995;79: 1426-33.
[58] Hefferan TE, Evans GL, Lotinun S, Zhang M, Morey-Holton E, Turner RT. Effect of gender on bone turnover in adult rats during simulated weightlessness. J Appl Physiol 2003;95: 1775-80.
[59] Fraysse B, Desaphy JF, Pierno S, De Luca A, Liantonio A, Mitolo CI, Camerino DC. Decrease in resting calcium and calcium entry associated with slow-to-fast transition in unloaded rat soleus muscle. Faseb J 2003;17: 1916-8.
[60] Wang XD, Kawano F, Matsuoka Y, Fukunaga K, Terada M, Sudoh M, Ishihara A, Ohira Y. Mechanical load-dependent regulation of satellite cell and fiber size in rat soleus muscle. Am J Physiol Cell Physiol 2006;290: C981-9.
[61] McCormick KM, Schultz E. Role of satellite cells in altering myosin expression during avian skeletal muscle hypertrophy. Dev Dyn 1994;199: 52-63.
[62] Schultz E, Darr KC, Macius A. Acute effects of hindlimb unweighting on satellite cells of growing skeletal muscle. J Appl Physiol 1994;76: 266-70.
[63] Siu PM, Pistilli EE, Alway SE. Apoptotic responses to hindlimb suspension in gastrocnemius muscles from young adult and aged rats. Am J Physiol Regul Integr Comp Physiol 2005;289: R1015-26.
[64] Winet H. A bone fluid flow hypothesis for muscle pump-driven capillary filtration: II. Proposed role for exercise in erodible scaffold implant incorporation. Eur Cell Mater 2003;6: 1-10; discussion 10-1.
[65] Qin YX, Kaplan T, Saldanha A, Rubin C. Fluid pressure gradients, arising from oscillations in intramedullary pressure, is correlated with the formation of bone and inhibition of intracortical porosity. J Biomech 2003;36: 1427-37.
[66] Rubin C, Xu G, Judex S. The anabolic activity of bone tissue, suppressed by disuse, is normalized by brief exposure to extremely low-magnitude mechanical stimuli. Faseb J 2001;15: 2225-9.
[67] Piekarski K, Munro M. Transport mechanism operating between blood supply and osteocytes in long bones. Nature 1977;269: 80-2.
[68] Qin YX, Rubin CT, McLeod KJ. Nonlinear dependence of loading intensity and cycle number in the maintenance of bone mass and morphology. J Orthop Res 1998;16: 482-9.
[69] Welch RD, Waldron MJ, Hulse DA, Johnston CE, 2nd, Hargis BM. Intraosseous infusion using the osteoport implant in the caprine tibia. J Orthop Res 1992;10: 789-99.
[70] Kiaer T. Bone perfusion and oxygenation. Animal experiments and clinical observations. Acta Orthop Scand Suppl 1994;257: 1-41.
[71] Tondevold E. Haemodynamics of long bones. An experimental study on dogs. Acta Orthop Scand Suppl 1983;205: 9-48.
[72] Radegran G, Saltin B. Muscle blood flow at onset of dynamic exercise in humans. Am J Physiol 1998;274: H314-22.
[73] Valic Z, Buckwalter JB, Clifford PS. Muscle blood flow response to contraction: influence of venous pressure. J Appl Physiol 2005;98: 72-6.
[74] Laughlin MH, Schrage WG. Effects of muscle contraction on skeletal muscle blood flow: when is there a muscle pump? Med Sci Sports Exerc 1999;31: 1027-35.

[75] South-Paul JE. Osteoporosis: part II. Nonpharmacologic and pharmacologic treatment. Am Fam Physician 2001;63: 1121-8.
[76] Burr DB. Muscle strength, bone mass, and age-related bone loss. J Bone Miner Res 1997;12: 1547-51.
[77] Hawkins SA, Schroeder ET, Wiswell RA, Jaque SV, Marcell TJ, Costa K. Eccentric muscle action increases site-specific osteogenic response. Med Sci Sports Exerc 1999;31: 1287-92.
[78] Fritton SP, McLeod KJ, Rubin CT. Quantifying the strain history of bone: spatial uniformity and self-similarity of low-magnitude strains. J Biomech 2000;33: 317-25.
[79] Rubin C, Turner AS, Bain S, Mallinckrodt C, McLeod K. Anabolism. Low mechanical signals strengthen long bones. Nature 2001;412: 603-4.
[80] Rubin CT. Skeletal strain and the functional significance of bone architecture. Calcif Tissue Int 1984;36 Suppl 1: S11-8.
[81] Rubin CT, Lanyon LE. Regulation of bone formation by applied dynamic loads. J Bone Joint Surg Am 1984;66: 397-402.
[82] Donahue HJ, McLeod KJ, Rubin CT, Andersen J, Grine EA, Hertzberg EL, Brink PR. Cell-to-cell communication in osteoblastic networks: cell line-dependent hormonal regulation of gap junction function. J Bone Miner Res 1995;10: 881-9.
[83] Gorza L, Gundersen K, Lomo T, Schiaffino S, Westgaard RH. Slow-to-fast transformation of denervated soleus muscles by chronic high-frequency stimulation in the rat. J Physiol 1988;402: 627-49.
[84] Westgaard RH, Lomo T. Control of contractile properties within adaptive ranges by patterns of impulse activity in the rat. J Neurosci 1988;8: 4415-26.
[85] Hudlicka O, Graciotti L, Fulgenzi G, Brown MD, Egginton S, Milkiewicz M, Granata AL. The effect of chronic skeletal muscle stimulation on capillary growth in the rat: are sensory nerve fibres involved? J Physiol 2003;546: 813-22.
[86] Mathieu-Costello O, Agey PJ, Wu L, Hang J, Adair TH. Capillary-to-fiber surface ratio in rat fast-twitch hindlimb muscles after chronic electrical stimulation. J Appl Physiol 1996;80: 904-9.
[87] Jarvis JC, Sutherland H, Mayne CN, Gilroy SJ, Salmons S. Induction of a fast-oxidative phenotype by chronic muscle stimulation: mechanical and biochemical studies. Am J Physiol 1996;270: C306-12.
[88] Kyparos A, Feeback DL, Layne CS, Martinez DA, Clarke MS. Mechanical stimulation of the plantar foot surface attenuates soleus muscle atrophy induced by hindlimb unloading in rats. J Appl Physiol 2005;99: 739-46.
[89] Hogan MC, Grassi B, Samaja M, Stary CM, Gladden LB. Effect of contraction frequency on the contractile and noncontractile phases of muscle venous blood flow. J Appl Physiol 2003;95: 1139-44.
[90] Naik JS, Valic Z, Buckwalter JB, Clifford PS. Rapid vasodilation in response to a brief tetanic muscle contraction. J Appl Physiol 1999;87: 1741-6.
[91] Zerath E, Canon F, Guezennec CY, Holy X, Renault S, Andre C. Electrical stimulation of leg muscles increases tibial trabecular bone formation in unloaded rats. J Appl Physiol 1995;79: 1889-94.

[92] Qin Y, Lam H. Intramedullary pressure and matrix strain induced by dynamic skeletal muscle contraction and its potential in adaptation. J Bone Miner Res 2008;Submitted:
[93] Perez M, Lucia A, Rivero JL, Serrano AL, Calbet JA, Delgado MA, Chicharro JL. Effects of transcutaneous short-term electrical stimulation on M. vastus lateralis characteristics of healthy young men. Pflugers Arch 2002;443: 866-74.
[94] Rodgers MM, Glaser RM, Figoni SF, Hooker SP, Ezenwa BN, Collins SR, Mathews T, Suryaprasad AG, Gupta SC. Musculoskeletal responses of spinal cord injured individuals to functional neuromuscular stimulation-induced knee extension exercise training. J Rehabil Res Dev 1991;28: 19-26.
[95] BeDell KK, Scremin AM, Perell KL, Kunkel CF. Effects of functional electrical stimulation-induced lower extremity cycling on bone density of spinal cord-injured patients. Am J Phys Med Rehabil 1996;75: 29-34.
[96] Belanger M, Stein RB, Wheeler GD, Gordon T, Leduc B. Electrical stimulation: can it increase muscle strength and reverse osteopenia in spinal cord injured individuals? Arch Phys Med Rehabil 2000;81: 1090-8.
[97] Mohr T, Podenphant J, Biering-Sorensen F, Galbo H, Thamsborg G, Kjaer M. Increased bone mineral density after prolonged electrically induced cycle training of paralyzed limbs in spinal cord injured man. Calcif Tissue Int 1997;61: 22-5.
[98] Dupont Salter AC, Richmond FJ, Loeb GE. Prevention of muscle disuse atrophy by low-frequency electrical stimulation in rats. IEEE Trans Neural Syst Rehabil Eng 2003;11: 218-26.
[99] Nemirovskaya TL, Shenkman BS. Effect of support stimulation on unloaded soleus in rat. Eur J Appl Physiol 2002;87: 120-6.
[100] Midura RJ, Dillman CJ, Grabiner MD. Low amplitude, high frequency strains imposed by electrically stimulated skeletal muscle retards the development of osteopenia in the tibiae of hindlimb suspended rats. Med Eng Phys 2005;27: 285-93.
[101] Kasten TP, Collin-Osdoby P, Patel N, Osdoby P, Krukowski M, Misko TP, Settle SL, Currie MG, Nickols GA. Potentiation of osteoclast bone-resorption activity by inhibition of nitric oxide synthase. Proc Natl Acad Sci U S A 1994;91: 3569-73.
[102] Rubin J, Rubin C, Jacobs CR. Molecular pathways mediating mechanical signaling in bone. Gene 2006;367: 1-16.
[103] Zhang P, Tanaka SM, Sun Q, Turner CH, Yokota H. Frequency-dependent enhancement of bone formation in murine tibiae and femora with knee loading. J Bone Miner Metab 2007;25: 383-91.
[104] Beck BR, Kent K, Holloway L, Marcus R. Novel, high-frequency, low-strain mechanical loading for premenopausal women with low bone mass: early findings. J Bone Miner Metab 2006;24: 505-7.
[105] Bacabac RG, Smit TH, Van Loon JJ, Doulabi BZ, Helder M, Klein-Nulend J. Bone cell responses to high-frequency vibration stress: does the nucleus oscillate within the cytoplasm? Faseb J 2006;20: 858-64.
[106] Ingram RR, Suman RK, Freeman PA. Lower limb fractures in the chronic spinal cord injured patient. Paraplegia 1989;27: 133-9.

[107] Judex S, Lei X, Han D, Rubin C. Low-magnitude mechanical signals that stimulate bone formation in the ovariectomized rat are dependent on the applied frequency but not on the strain magnitude. J Biomech 2007;40: 1333-9.
[108] Morey-Holton ER, Globus RK. Hindlimb unloading rodent model: technical aspects. J Appl Physiol 2002;92: 1367-77.
[109] Laib A, Kumer JL, Majumdar S, Lane NE. The temporal changes of trabecular architecture in ovariectomized rats assessed by MicroCT. Osteoporos Int 2001;12: 936-41.
[110] Parfitt AM, Drezner MK, Glorieux FH, Kanis JA, Malluche H, Meunier PJ, Ott SM, Recker RR. Bone histomorphometry: standardization of nomenclature, symbols, and units. Report of the ASBMR Histomorphometry Nomenclature Committee. J Bone Miner Res 1987;2: 595-610.
[111] Bloomfield SA. Cellular and molecular mechanisms for the bone response to mechanical loading. Int J Sport Nutr Exerc Metab 2001;11 Suppl: S128-36.
[112] Chow JW. Role of nitric oxide and prostaglandins in the bone formation response to mechanical loading. Exerc Sport Sci Rev 2000;28: 185-8.
[113] Robling AG, Castillo AB, Turner CH. Biomechanical and molecular regulation of bone remodeling. Annu Rev Biomed Eng 2006;8: 455-98.
[114] Dickerson DA, Sander EA, Nauman EA. Modeling the mechanical consequences of vibratory loading in the vertebral body: microscale effects. Biomech Model Mechanobiol 2007;
[115] Xie L, Jacobson JM, Choi ES, Busa B, Donahue LR, Miller LM, Rubin CT, Judex S. Low-level mechanical vibrations can influence bone resorption and bone formation in the growing skeleton. Bone 2006;39: 1059-66.
[116] Qin YX, Lin W, Rubin C. The pathway of bone fluid flow as defined by in vivo intramedullary pressure and streaming potential measurements. Ann Biomed Eng 2002;30: 693-702.
[117] Stevens HY, Meays DR, Frangos JA. Pressure gradients and transport in the murine femur upon hindlimb suspension. Bone 2006;39: 565-72.
[118] Rubin C, Turner AS, Muller R, Mittra E, McLeod K, Lin W, Qin YX. Quantity and quality of trabecular bone in the femur are enhanced by a strongly anabolic, noninvasive mechanical intervention. J Bone Miner Res 2002;17: 349-57.
[119] Johnson DL, McAllister TN, Frangos JA. Fluid flow stimulates rapid and continuous release of nitric oxide in osteoblasts. Am J Physiol 1996;271: E205-8.
[120] Pollack AA, Wood EH. Venous pressure in the saphenous vein at the ankle in man during exercise and changes in posture. J Appl Physiol 1949;1: 649-62.
[121] Sheriff DD, Van Bibber R. Flow-generating capability of the isolated skeletal muscle pump. Am J Physiol 1998;274: H1502-8.
[122] Garland DE, Adkins RH, Stewart CA, Ashford R, Vigil D. Regional osteoporosis in women who have a complete spinal cord injury. J Bone Joint Surg Am 2001;83-A: 1195-200.
[123] Slade JM, Bickel CS, Modlesky CM, Majumdar S, Dudley GA. Trabecular bone is more deteriorated in spinal cord injured versus estrogen-free postmenopausal women. Osteoporos Int 2005;16: 263-72.

[124] Vestergaard P, Krogh K, Rejnmark L, Mosekilde L. Fracture rates and risk factors for fractures in patients with spinal cord injury. Spinal Cord 1998;36: 790-6.
[125] Milgrom C, Finestone A, Levi Y, Simkin A, Ekenman I, Mendelson S, Millgram M, Nyska M, Benjuya N, Burr D. Do high impact exercises produce higher tibial strains than running? Br J Sports Med 2000;34: 195-9.
[126] Shields RK, Dudley-Javoroski S, Law LA. Electrically induced muscle contractions influence bone density decline after spinal cord injury. Spine 2006;31: 548-53.
[127] Hsieh YF, Turner CH. Effects of loading frequency on mechanically induced bone formation. J Bone Miner Res 2001;16: 918-24.
[128] Rubin CT, Lanyon LE. Regulation of bone mass by mechanical strain magnitude. Calcif Tissue Int 1985;37: 411-7.
[129] Rubin CT, Sommerfeldt DW, Judex S, Qin Y. Inhibition of osteopenia by low magnitude, high-frequency mechanical stimuli. Drug Discov Today 2001;6: 848-858.
[130] Srinivasan S, Weimer DA, Agans SC, Bain SD, Gross TS. Low-magnitude mechanical loading becomes osteogenic when rest is inserted between each load cycle. J Bone Miner Res 2002;17: 1613-20.
[131] LaMothe JM, Zernicke RF. Rest insertion combined with high-frequency loading enhances osteogenesis. J Appl Physiol 2004;96: 1788-93.
[132] Robling AG, Burr DB, Turner CH. Recovery periods restore mechanosensitivity to dynamically loaded bone. J Exp Biol 2001;204: 3389-99.
[133] Lam H, Qin Y. The Effects of Frequency-Specific Dynamic Muscle Stimulation on Inhibition of Trabecular Bone Loss in a Disuse Model. Bone 2008;Submitted:
[134] Hoelting BD, Scheuermann BW, Barstow TJ. Effect of contraction frequency on leg blood flow during knee extension exercise in humans. J Appl Physiol 2001;91: 671-9.
[135] Stainsby WN, Brechue WF, Ameredes BT. Muscle blood flow and distribution determine maximal VO2 of contracting muscle. Med Sci Sports Exerc 1995;27: 43-6.
[136] Judex S, Zernicke RF. High-impact exercise and growing bone: relation between high strain rates and enhanced bone formation. J Appl Physiol 2000;88: 2183-91.
[137] Rubin CT, Lanyon LE. Kappa Delta Award paper. Osteoregulatory nature of mechanical stimuli: function as a determinant for adaptive remodeling in bone. J Orthop Res 1987;5: 300-10.
[138] McLeod KJ, Rubin CT, Otter MW, Qin YX. Skeletal cell stresses and bone adaptation. Am J Med Sci 1998;316: 176-83.
[139] Garman R, Gaudette G, Donahue LR, Rubin C, Judex S. Low-level accelerations applied in the absence of weight bearing can enhance trabecular bone formation. J Orthop Res 2007;25: 732-40.
[140] Delp MD. Control of skeletal muscle perfusion at the onset of dynamic exercise. Med Sci Sports Exerc 1999;31: 1011-8.
[141] Laughlin MH, Armstrong RB. Muscular blood flow distribution patterns as a function of running speed in rats. Am J Physiol 1982;243: H296-306.
[142] Dodd SL, Powers SK, Crawford MP. Tension development and duty cycle affect Qpeak and VO2peak in contracting muscle. Med Sci Sports Exerc 1994;26: 997-1002.

[143] Kapur S, Baylink DJ, Lau KH. Fluid flow shear stress stimulates human osteoblast proliferation and differentiation through multiple interacting and competing signal transduction pathways. Bone 2003;32: 241-51.
[144] Kim CH, You L, Yellowley CE, Jacobs CR. Oscillatory fluid flow-induced shear stress decreases osteoclastogenesis through RANKL and OPG signaling. Bone 2006;39: 1043-7.
[145] McAllister TN, Du T, Frangos JA. Fluid shear stress stimulates prostaglandin and nitric oxide release in bone marrow-derived preosteoclast-like cells. Biochem Biophys Res Commun 2000;270: 643-8.
[146] Mullender MG, Dijcks SJ, Bacabac RG, Semeins CM, Van Loon JJ, Klein-Nulend J. Release of nitric oxide, but not prostaglandin E2, by bone cells depends on fluid flow frequency. J Orthop Res 2006;24: 1170-7.
[147] Knothe Tate ML, Steck R, Forwood MR, Niederer P. In vivo demonstration of load-induced fluid flow in the rat tibia and its potential implications for processes associated with functional adaptation. J Exp Biol 2000;203: 2737-45.
[148] Srinivasan S, Gross TS. Canalicular fluid flow induced by bending of a long bone. Med Eng Phys 2000;22: 127-33.
[149] Gregory CM, Vandenborne K, Castro MJ, Dudley GA. Human and rat skeletal muscle adaptations to spinal cord injury. Can J Appl Physiol 2003;28: 491-500.
[150] Narici M, Kayser B, Barattini P, Cerretelli P. Effects of 17-day spaceflight on electrically evoked torque and cross-sectional area of the human triceps surae. Eur J Appl Physiol 2003;90: 275-82.
[151] Trappe SW, Trappe TA, Lee GA, Widrick JJ, Costill DL, Fitts RH. Comparison of a space shuttle flight (STS-78) and bed rest on human muscle function. J Appl Physiol 2001;91: 57-64.
[152] Castro MJ, Apple DF, Jr., Staron RS, Campos GE, Dudley GA. Influence of complete spinal cord injury on skeletal muscle within 6 mo of injury. J Appl Physiol 1999;86: 350-8.
[153] Spungen AM, Adkins RH, Stewart CA, Wang J, Pierson RN, Jr., Waters RL, Bauman WA. Factors influencing body composition in persons with spinal cord injury: a cross-sectional study. J Appl Physiol 2003;95: 2398-407.
[154] Zehnder Y, Luthi M, Michel D, Knecht H, Perrelet R, Neto I, Kraenzlin M, Zach G, Lippuner K. Long-term changes in bone metabolism, bone mineral density, quantitative ultrasound parameters, and fracture incidence after spinal cord injury: a cross-sectional observational study in 100 paraplegic men. Osteoporos Int 2004;15: 180-9.
[155] Baldi JC, Jackson RD, Moraille R, Mysiw WJ. Muscle atrophy is prevented in patients with acute spinal cord injury using functional electrical stimulation. Spinal Cord 1998;36: 463-9.
[156] Gerrits HL, Hopman MT, Sargeant AJ, Jones DA, De Haan A. Effects of training on contractile properties of paralyzed quadriceps muscle. Muscle Nerve 2002;25: 559-67.
[157] Skold C, Lonn L, Harms-Ringdahl K, Hultling C, Levi R, Nash M, Seiger A. Effects of functional electrical stimulation training for six months on body composition and spasticity in motor complete tetraplegic spinal cord-injured individuals. J Rehabil Med 2002;34: 25-32.

[158] Hauschka EO, Roy RR, Edgerton VR. Periodic weight support effects on rat soleus fibers after hindlimb suspension. J Appl Physiol 1988;65: 1231-7.
[159] Morey-Holton ER, Globus RK. Hindlimb unloading of growing rats: a model for predicting skeletal changes during space flight. Bone 1998;22: 83S-88S.
[160] Boonyarom O, Inui K. Atrophy and hypertrophy of skeletal muscles: structural and functional aspects. Acta Physiol (Oxf) 2006;188: 77-89.
[161] Fisher JS, Hasser EM, Brown M. Effects of ovariectomy and hindlimb unloading on skeletal muscle. J Appl Physiol 1998;85: 1316-21.
[162] Hurst JE, Fitts RH. Hindlimb unloading-induced muscle atrophy and loss of function: protective effect of isometric exercise. J Appl Physiol 2003;95: 1405-17.
[163] McClung JM, Davis JM, Wilson MA, Goldsmith EC, Carson JA. Estrogen status and skeletal muscle recovery from disuse atrophy. J Appl Physiol 2006;100: 2012-23.
[164] Kernell D, Eerbeek O, Verhey BA, Donselaar Y. Effects of physiological amounts of high- and low-rate chronic stimulation on fast-twitch muscle of the cat hindlimb. I. Speed- and force-related properties. J Neurophysiol 1987;58: 598-613.
[165] Mabuchi K, Szvetko D, Pinter K, Sreter FA. Type IIB to IIA fiber transformation in intermittently stimulated rabbit muscles. Am J Physiol 1982;242: C373-81.
[166] Salmons S, Henriksson J. The adaptive response of skeletal muscle to increased use. Muscle Nerve 1981;4: 94-105.
[167] Eerbeek O, Kernell D, Verhey BA. Effects of fast and slow patterns of tonic long-term stimulation on contractile properties of fast muscle in the cat. J Physiol 1984;352: 73-90.
[168] Punkt K, Naupert A, Asmussen G. Differentiation of rat skeletal muscle fibres during development and ageing. Acta Histochem 2004;106: 145-54.
[169] Pette D, Sketelj J, Skorjanc D, Leisner E, Traub I, Bajrovic F. Partial fast-to-slow conversion of regenerating rat fast-twitch muscle by chronic low-frequency stimulation. J Muscle Res Cell Motil 2002;23: 215-21.
[170] Desaphy JF, Pierno S, Liantonio A, De Luca A, Didonna MP, Frigeri A, Nicchia GP, Svelto M, Camerino C, Zallone A, Camerino DC. Recovery of the soleus muscle after short- and long-term disuse induced by hindlimb unloading: effects on the electrical properties and myosin heavy chain profile. Neurobiol Dis 2005;18: 356-65.
[171] Marsh DR, Campbell CB, Spriet LL. Effect of hindlimb unweighting on anaerobic metabolism in rat skeletal muscle. J Appl Physiol 1992;72: 1304-10.
[172] Oishi Y, Ishihara A, Yamamoto H, Miyamoto E. Hindlimb suspension induces the expression of multiple myosin heavy chain isoforms in single fibres of the rat soleus muscle. Acta Physiol Scand 1998;162: 127-34.
[173] Caldwell CJ, Mattey DL, Weller RO. Role of the basement membrane in the regeneration of skeletal muscle. Neuropathol Appl Neurobiol 1990;16: 225-38.
[174] Hawke TJ, Garry DJ. Myogenic satellite cells: physiology to molecular biology. J Appl Physiol 2001;91: 534-51.
[175] Kadi F, Charifi N, Denis C, Lexell J. Satellite cells and myonuclei in young and elderly women and men. Muscle Nerve 2004;29: 120-7.
[176] Moss FP, Leblond CP. Satellite cells as the source of nuclei in muscles of growing rats. Anat Rec 1971;170: 421-35.

[177] Verdijk LB, Koopman R, Schaart G, Meijer K, Savelberg HH, van Loon LJ. Satellite cell content is specifically reduced in type II skeletal muscle fibers in the elderly. Am J Physiol Endocrinol Metab 2007;292: E151-7.
[178] Yoshida N, Sairyo K, Sasa T, Fukunaga M, Koga K, Ikata T, Yasui N. Electrical stimulation prevents deterioration of the oxidative capacity of disuse-atrophied muscles in rats. Aviat Space Environ Med 2003;74: 207-11.
[179] Petrofsky JS, Hendershot DM. The interrelationship between blood pressure, intramuscular pressure, and isometric endurance in fast and slow twitch skeletal muscle in the cat. Eur J Appl Physiol Occup Physiol 1984;53: 106-11.
[180] Valic Z, Naik JS, Ruble SB, Buckwalter JB, Clifford PS. Elevation in resting blood flow attenuates exercise hyperemia. J Appl Physiol 2002;93: 134-40.
[181] Buckwalter JB, Ruble SB, Mueller PJ, Clifford PS. Skeletal muscle vasodilation at the onset of exercise. J Appl Physiol 1998;85: 1649-54.
[182] Welsh DG, Segal SS. Coactivation of resistance vessels and muscle fibers with acetylcholine release from motor nerves. Am J Physiol 1997;273: H156-63.
[183] Hudlicka O. Blood flow and oxygen consumption in muscles after section of ventral roots. Circ Res 1967;20: 570-7.
[184] Schmidt-Nielsen K, Pennycuik P. Capillary density in mammals in relation to body size and oxygen consumption. Am J Physiol 1961;200: 746-50.
[185] Brown M. Change in fibre size, not number, in ageing skeletal muscle. Age Ageing 1987;16: 244-8.
[186] Davidson YS, Clague JE, Horan MA, Pendleton N. The effect of aging on skeletal muscle capillarization in a murine model. J Gerontol A Biol Sci Med Sci 1999;54: B448-51.
[187] Degens H, Ringnalda BE, Hoofd LJ. Capillarisation, fibre types and myoglobin content of the dog gracilis muscle. Adv Exp Med Biol 1994;361: 533-9.
[188] Tyml K, Mathieu-Costello O. Structural and functional changes in the microvasculature of disused skeletal muscle. Front Biosci 2001;6: D45-52.
[189] Tyml K, Mathieu-Costello O, Noble E. Microvascular response to ischemia, and endothelial ultrastructure, in disused skeletal muscle. Microvasc Res 1995;49: 17-32.
[190] Dawson JM, Hudlicka O. The effects of long term administration of prazosin on the microcirculation in skeletal muscles. Cardiovasc Res 1989;23: 913-20.
[191] Hather BM, Adams GR, Tesch PA, Dudley GA. Skeletal muscle responses to lower limb suspension in humans. J Appl Physiol 1992;72: 1493-8.
[192] Ebina T, Hoshi N, Kobayashi M, Kawamura K, Nanjo H, Sugita A, Sugiyama T, Masuda H, Xu C. Physiological angiogenesis in electrically stimulated skeletal muscle in rabbits: characterization of capillary sprouting by ultrastructural 3-D reconstruction study. Pathol Int 2002;52: 702-12.
[193] Egginton S, Hudlicka O, Brown MD, Walter H, Weiss JB, Bate A. Capillary growth in relation to blood flow and performance in overloaded rat skeletal muscle. J Appl Physiol 1998;85: 2025-32.
[194] Holly RG, Barnett JG, Ashmore CR, Taylor RG, Mole PA. Stretch-induced growth in chicken wing muscles: a new model of stretch hypertrophy. Am J Physiol 1980;238: C62-71.

[195] James NT. A stereological analysis of capillaries in normal and hypertrophic muscle. J Morphol 1981;168: 43-9.
[196] Fouces V, Torrella JR, Palomeque J, Viscor G. A histochemical ATPase method for the demonstration of the muscle capillary network. J Histochem Cytochem 1993;41: 283-9.
[197] Sillau AH, Banchero N. Visualization of capillaries in skeletal muscle by the ATPase reaction. Pflugers Arch 1977;369: 269-71.
[198] Sender S, Gros G, Waheed A, Hageman GS, Sly WS. Immunohistochemical localization of carbonic anhydrase IV in capillaries of rat and human skeletal muscle. J Histochem Cytochem 1994;42: 1229-36.
[199] Warhol MJ, Sweet JM. The ultrastructural localization of von Willebrand factor in endothelial cells. Am J Pathol 1984;117: 310-5.
[200] Stephenson TJ, Griffiths DW, Mills PM. Comparison of Ulex europaeus I lectin binding and factor VIII-related antigen as markers of vascular endothelium in follicular carcinoma of the thyroid. Histopathology 1986;10: 251-60.
[201] Sauter B, Foedinger D, Sterniczky B, Wolff K, Rappersberger K. Immunoelectron microscopic characterization of human dermal lymphatic microvascular endothelial cells. Differential expression of CD31, CD34, and type IV collagen with lymphatic endothelial cells vs blood capillary endothelial cells in normal human skin, lymphangioma, and hemangioma in situ. J Histochem Cytochem 1998;46: 165-76.
[202] Andersen P, Henriksson J. Capillary supply of the quadriceps femoris muscle of man: adaptive response to exercise. J Physiol 1977;270: 677-90.
[203] Kano Y, Shimegi S, Takahashi H, Masuda K, Katsuta S. Changes in capillary luminal diameter in rat soleus muscle after hind-limb suspension. Acta Physiol Scand 2000;169: 271-6.
[204] Fujino H, Kohzuki H, Takeda I, Kiyooka T, Miyasaka T, Mohri S, Shimizu J, Kajiya F. Regression of capillary network in atrophied soleus muscle induced by hindlimb unweighting. J Appl Physiol 2005;98: 1407-13.
[205] Dawson JM, Hudlicka O. Can changes in microcirculation explain capillary growth in skeletal muscle? Int J Exp Pathol 1993;74: 65-71.
[206] Henquell L, LaCelle PL, Honig CR. Capillary diameter in rat heart in situ: relation to erythrocyte deformability, O2 transport, and transmural O2 gradients. Microvasc Res 1976;12: 259-74.
[207] Brown MD, Hudlicka O. Modulation of physiological angiogenesis in skeletal muscle by mechanical forces: involvement of VEGF and metalloproteinases. Angiogenesis 2003;6: 1-14.
[208] Hansen-Smith F, Egginton S, Zhou AL, Hudlicka O. Growth of arterioles precedes that of capillaries in stretch-induced angiogenesis in skeletal muscle. Microvasc Res 2001;62: 1-14.
[209] Murfee WL, Hammett LA, Evans C, Xie L, Squire M, Rubin C, Judex S, Skalak TC. High-frequency, low-magnitude vibrations suppress the number of blood vessels per muscle fiber in mouse soleus muscle. J Appl Physiol 2005;98: 2376-80.
[210] Ferguson RA, Ball D, Krustrup P, Aagaard P, Kjaer M, Sargeant AJ, Hellsten Y, Bangsbo J. Muscle oxygen uptake and energy turnover during dynamic exercise at different contraction frequencies in humans. J Physiol 2001;536: 261-71.

[211] Folkow B, Haglund U, Jodal M, Lundgren O. Blood flow in the calf muscle of man during heavy rhythmic exercise. Acta Physiol Scand 1971;81: 157-63.
[212] Shoemaker JK, Tschakovsky ME, Hughson RL. Vasodilation contributes to the rapid hyperemia with rhythmic contractions in humans. Can J Physiol Pharmacol 1998;76: 418-27.
[213] Tschakovsky ME, Shoemaker JK, Hughson RL. Vasodilation and muscle pump contribution to immediate exercise hyperemia. Am J Physiol 1996;271: H1697-701.
[214] Laughlin MH. Skeletal muscle blood flow capacity: role of muscle pump in exercise hyperemia. Am J Physiol 1987;253: H993-1004.
[215] Hudlicka O. Is physiological angiogenesis in skeletal muscle regulated by changes in microcirculation? Microcirculation 1998;5: 5-23.
[216] Kano Y, Sampei K, Matsudo H. Time course of capillary structure changes in rat skeletal muscle following strenuous eccentric exercise. Acta Physiol Scand 2004;180: 291-9.
[217] Ellsworth ML, Pittman RN. Arterioles supply oxygen to capillaries by diffusion as well as by convection. Am J Physiol 1990;258: H1240-3.
[218] Han Y, Cowin SC, Schaffler MB, Weinbaum S. Mechanotransduction and strain amplification in osteocyte cell processes. Proc Natl Acad Sci U S A 2004;101: 16689-94.
[219] Lean JM, Mackay AG, Chow JW, Chambers TJ. Osteocytic expression of mRNA for c-fos and IGF-I: an immediate early gene response to an osteogenic stimulus. Am J Physiol 1996;270: E937-45.
[220] MacIntyre I, Zaidi M, Alam AS, Datta HK, Moonga BS, Lidbury PS, Hecker M, Vane JR. Osteoclastic inhibition: an action of nitric oxide not mediated by cyclic GMP. Proc Natl Acad Sci U S A 1991;88: 2936-40.
[221] van't Hof RJ, Ralston SH. Cytokine-induced nitric oxide inhibits bone resorption by inducing apoptosis of osteoclast progenitors and suppressing osteoclast activity. J Bone Miner Res 1997;12: 1797-804.
[222] Parfitt AM. The mechanism of coupling: a role for the vasculature. Bone 2000;26: 319-23.